THE GEOLOGY OF POTASH DEPOSITS AT PCS CORY MINE, SASKATCHEWAN.

A Thesis

Submitted to the Faculty of Graduate Studies

and Research

in Partial Fulfilment of the Requirements

for the Degree of

Master of Science

in the Department of Geological Sciences

University of Saskatchewan

by

Christopher Boys

Saskatoon, Saskatchewan

February, 1990

The author has agreed that the Library, University of Saskatchewan, shall make this thesis freely available for inspection. Moreover, the author has agreed that permission for extensive copying of this thesis for scholarly purposes may be granted by the professor or professors who supervised the thesis work recorded herein or, in their absence by the Head of the Department or the Dean of the college in which the thesis work has been done. It is understood that due recognition will be given to the author of this thesis and to the University of Saskatchewan in any use of material in this thesis. Copying or publication or any other use of the thesis for financial gain without approval by the University of Saskatchewan and the author's written permission is prohibited.

Requests for permission to copy or to make other use of material in this thesis in whole or in part should be addressed to:

Head of the Department of Geological Sciences
University of Saskatchewan
Saskatoon, Saskatchewan, Canada
S7N 0W0

TABLE OF CONTENTS

PART 3. DISCUSSION

LIST OF TABLES

LIST OF FIGURES

LIST OF PLATES

ACKNOWLEDGEMENTS

There are many people without whom I would not have been able to complete this thesis. I thank Doctors Robin Renaut and Fred Langford of the Department of Geological Sciences, University of Saskatchewan, who helped in the mine, and provided advice and encouragement. Doctor Langford also prepared the first drafts of figures 5.2-5.4. Other faculty, especially Dr. W. Braun, Dr. Malcolm Reeves, Dr. Don Gendzwill, and staff of the Department were helpful and encouraging. Terry Danyluk, of the Potash Corporation of Saskatchewan, provided advice, computer assistance, and access to PCS files. I am also grateful to the staff of PCS Mining Limited, Cory Division. Ken Florizeau, of PCS, helped draft figures 4.3 and 5.5. Conversations and mine trips with George McVittie and David Mackintosh of Cominco, Alan Coode of Central Canada Potash, Gordon Phillips of PCS, and other members of the Saskatchewan potash industry gave me access to untold amounts of experience and knowledge on Saskatchewan potash deposits. I received help in the form of advice, discussion, encouragement, and analysis of samples from friends and peers, notably: Cherdsak Uthaaroon, Don Chipley, Patrick Cashman, and Kelly Edwards. Dr Parviz Mottahed, formerly of PCS, was instrumental in arranging for the Potash Corporation of Saskatchewan to provide a two-year research grant to finance this project.

ABSTRACT

Salt anomalies are a common problem to potash mining in Saskatchewan. The geology of the PCS Cory potash mine in the Patience Lake Member of the Prairie Evaporite Formation was studied to attempt to find indicators of proximity to anomalies. Initially, a basic understanding of normal potash ore was needed to provide a foundation of data for the study. The ore zone was divided into six units, based on potash rock-types and clay seams. The units may be correlated throughout the mine with varying degrees of success and are mappable.

The potash deposition appears to have been cyclic, expressed in the repetitive distribution of hematite and other insoluble minerals. Four potash cycles, each about 1 m thick, make up the lower Patience Lake Member. In the upper Patience Lake Member there are 3 complete potash cycles, and 3 or 4 incomplete potash cycles. The cyclic distribution of disseminated insolubles was possibly due to a combination of source proximity and the strength of winds. The potash salts and associated iron oxides probably formed just beneath the sediment surface. Possible disconformities, created by the dissolution of overlying potash-bearing beds, may be indicated by an abundance of residual hematite in clay seams. Desiccation polygons, desiccation cracks, microkarst pits, and chevron halite crystals indicate that the Patience Lake Member was deposited in a shallow-brine, salt-pan environment. The insoluble minerals found in the PCS Cory samples are, in approximate order of decreasing abundance: dolomite, clays [illite, chlorite (including swelling-chlorite/chlorite), and septechlorite], quartz, anhydrite, hematite, and goethite. Detrital minerals include dolomite, illite (or mica precursors), chlorite, quartz, and fossil fragments. The septechlorite and swelling-chlorite/chlorite are probably authigenic. X-ray peaks and heating data indicate that the chlorites are rich in magnesium. Except in collapse features, the secondary redistribution of insolubles, other than iron oxides, is insignificant.

Up to five post-burial facies, including carbonate-mud collapse breccias and bedded sylvinite, may result from post-burial leaching. The effects of the leaching that produced the anomalies, range from weak to strong, from selectively preserving delicate laminae and chevron textures, to deforming and destroying salt beds. Good preservation of iron oxides in halite may indicate that the leaching was weak or of short duration. In leach anomalies, salinities increase downward possibly because fluids exited downward. NaCl-saturated fluids tend to follow the chemical gradient provided by potash beds. Common indicators may exist equally for two different types of anomalies. Large blebs (eg. >200 cm^2) of sylvite-poor potash

cross-cutting units of an incomplete potash cycle near the top of the ore zone, were found about 5 m from a salt anomaly. Anhydrite was more common in an anomaly than in ore. Once into an anomaly, indicators of a major collapse feature may include: stretched clay seams, folded beds, small collapse features (1-20 m), split clay seams with injected salt, and drops in topography >10 m of the marker seams. Any number, or none, of these indicators may be found close to a major collapse feature. The local abundance of anhydrite in ore may indicate the proximity of a salt anomaly.

PART 1: INTRODUCTION AND METHODS

Chapter 1. INTRODUCTION

Despite many years of study of the Middle Devonian potash deposits of Saskatchewan there has been little attempt to gather information systematically on the detailed stratigraphy of the main potash ore zones. This thesis describes the detailed stratigraphy, sedimentology, and the mineralogy of the water-insoluble fraction at PCS Mining Limited, Cory Division potash mine, which is about 8 km west of Saskatoon, Saskatchewan (Fig. 1.1). The rocks of the mine level were the main target of investigation. These lie within the upper Patience Lake Member of the Prairie Evaporite Formation of the Elk Point Group (Fig. 1.2). Samples from the Central Canada Potash mine (Fig. 1.1) at Colonsay were also collected for analysis of the water-insoluble minerals. Observations were also made at the PCS Lanigan and Cominco potash mines (Fuzesy, 1982).

The Patience Lake Member is the uppermost of four potash-bearing members in the Prairie Evaporite Formation (Fig. 1.2). Sylvinite and halite are the main rock types. Sylvinite is a mixture of halite (NaCl) and sylvite (KCl); minor carnallite ($KCl \cdot MgCl_2 \cdot 6H_2O$) is present locally. Additionally, there may be up to 20 wt.% water-insoluble

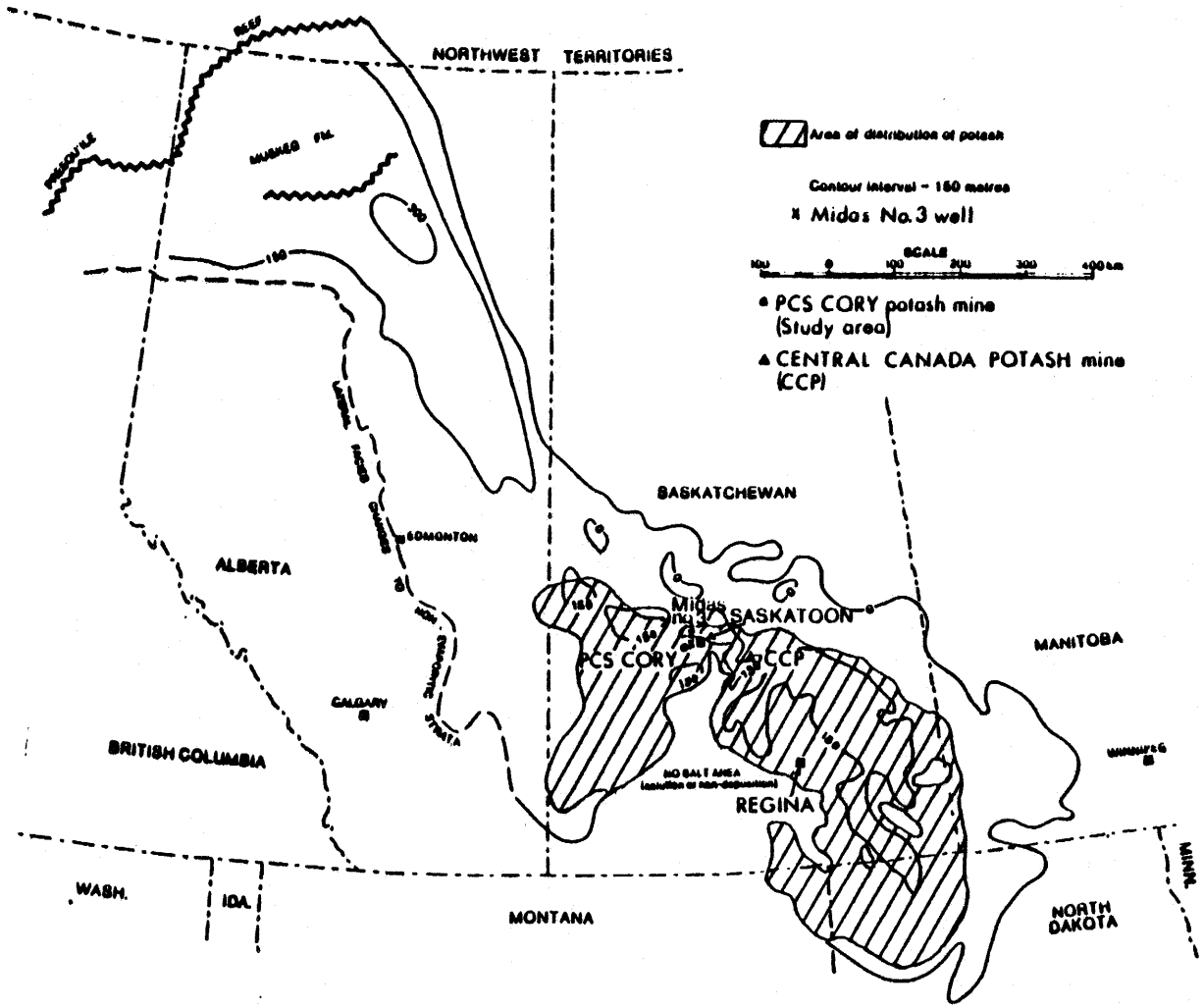

Fig. 1.1 An isopach map of the Prairie Evaporite in the Elk Point Basin showing locations of the PCS Ltd. Cory Division potash mine (Fig. 2.1), the Midas No. 3 well (Fig. 1.2), and the Central Canada Potash mine. Modified from Fuzesy (1982).

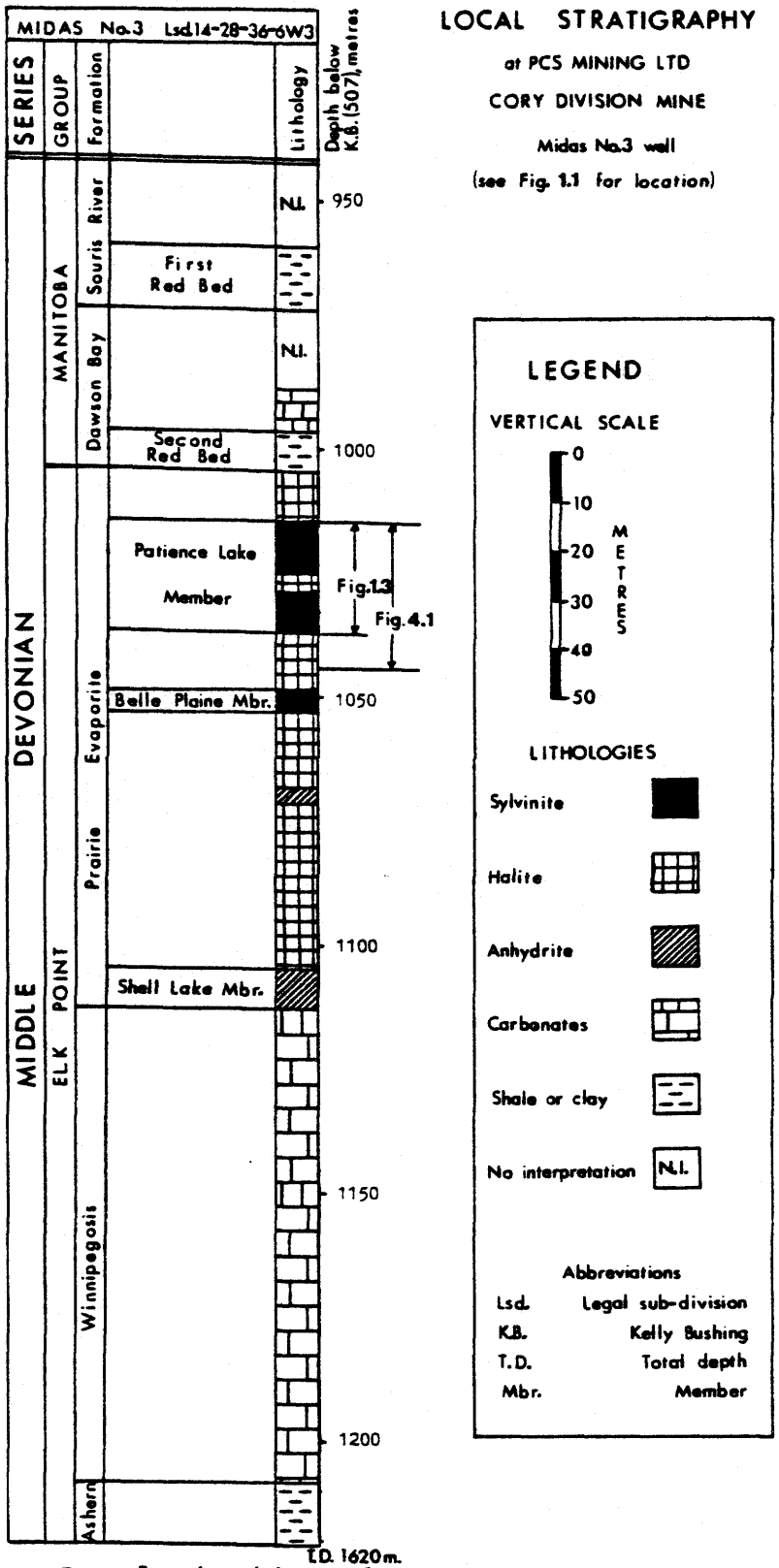

Fig. 1.2 Local stratigraphy at PCS Ltd. Cory Division mine, Midas No.3 well. Compiled from Holter (1969) and PCS well logs.

minerals ("insolubles") present. Overlying the evaporites of the studied section is 12 m of bedded halite capped by the dolomitic mudstones of the Second Red Beds of the Dawson Bay Formation (Dunn, 1983). Below the Patience Lake Member are the salt and potash of the lower members of the Prairie Evaporite Formation, and the Winnipegosis Formation carbonates (Fig. 1.2).

Within the potash-bearing members, there are commonly brecciated or leached areas which are called "anomalous". If the anomalous area is comprised mostly of halite then it is termed a salt anomaly. The anomalies have been divided into three types by Mackintosh and McVittie (1983) - washout, leach, and collapse anomalies.

The term "insolubles" includes all those minerals that do not dissolve in room-temperature water. In the Prairie Evaporite Formation, these include dolomite, gypsum, anhydrite (which can dissolve in hot water, eg. >60°C), magnesite, micas, several clay minerals, quartz, hematite, goethite, pyrite, feldspars, calcite, hydrocarbons, and other organic material. "Mud seam, clay parting, clay seam, insoluble seam" are terms used in previous studies that refer to a layer within the evaporite that has a relatively high amount of insolubles. In this report "clay seam" and "insoluble seam" are used interchangeably. "Clay" is also used specifically to

refer to clay minerals, such as chlorite and illite. As well as occurring as distinct seams, insolubles occur as disseminated interstitial minerals within crystalline salts.

1.1 OBJECTIVES

The two main aims of this thesis are: 1) to identify the structure and distribution of salt anomalies and to seek indicators of their proximity, and 2) to understand the origin of the potash deposits and salt anomalies. The detailed stratigraphy, sedimentology, and the mineralogy of the water-insoluble fraction are studied with these aims in mind. Not only are the salt anomalies uneconomic due to insufficient sylvinite, but they can be unsafe for mining, and some can serve as conduits for groundwaters that may flood the mine. This thesis lays the groundwork for more research into potash and salt anomalies.

To predict the proximity of anomalies it is necessary to understand the nature of the potash and its normal range of variability. If significant variations can be noticed in advance of the mining machine, they may be indicators of anomalous ground (salt anomalies). Therefore, a major emphasis of this thesis has been to provide a geological definition for "normal" of the normal potash ore zone. The mine definition of suitable ore grade, 10-50% K_2O (16-79% KCl)

with an average of about 25% K_2O (40% KCl), in the ore zone (Fig. 1.3) has indicated the norm for potash in Saskatchewan.

1.2 REGIONAL GEOLOGICAL SETTING

The Saskatchewan potash deposits are of Middle Devonian age, and occur near the top of the Elk Point Group (Fig. 1.1). They are part of the thickest, most widespread salt deposits in North America, and were laid down in the Elk Point Basin (Fuzesy, 1982, Zharkov, 1984). The portion of the Elk Point Basin that includes the potash deposits has been referred to as the Saskatchewan Sub-basin (Fig. 1.1; Holter, 1969).

During deposition, the highest salinities were attained in the Saskatchewan Sub-basin, which was the farthest portion of the Elk Point Basin from the open ocean. The main source of marine water was probably to the northwest beyond the Presqu'ile Reefs, but with possible influxes from the east (Fig. 1.1; Williams, 1984). The salts grade vertically, and laterally toward the northwest and west depositional edges into sulphates, carbonates, and clastics. For example, the Muskeg Formation, composed chiefly of anhydrite beds, lies between the Prairie

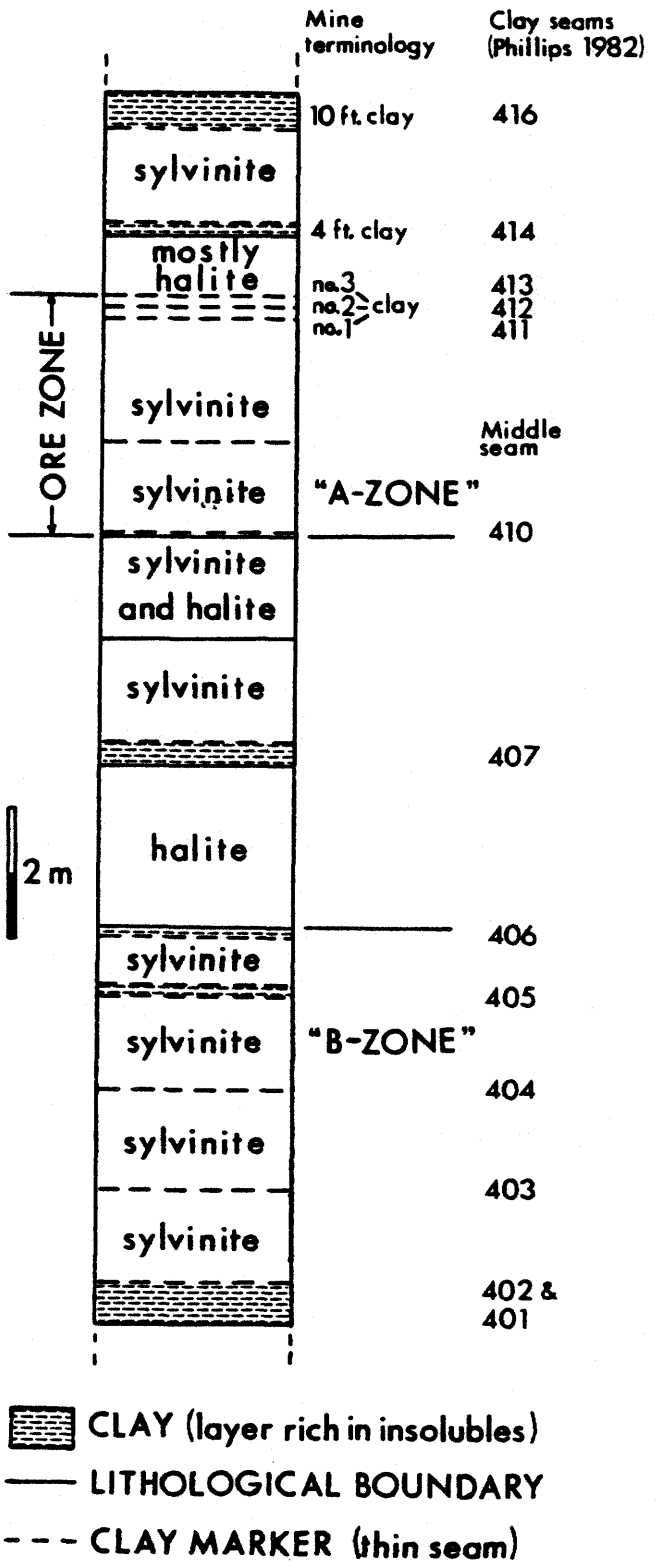

Fig. 1.3 Generalized stratigraphy of the Patience Lake Member, showing the ore zone and the position of the main clay seams using local mine terminology and that of Phillips (1982). Compiled from PCS internal reports.

Evaporite Formation and the carbonates of the Presqu'ile Formation (Fig. 1.1; Holter, 1969). To the south, in Montana and North Dakota, the Lower Salt of the Prairie Evaporite Formation grades into anhydrite, carbonates, and shale (Holter, 1969). The Prairie Evaporite Formation most likely extended farther northeast than its present erosional edge (Fig. 1.1).

There are five evaporite cycles in the Elk Point and overlying Manitoba Groups of Western Canada (Holter, 1969). An evaporite cycle, as defined by Holter (1969) and Fuzesy (1982), comprises a depositional sequence from bottom to top of:
red-beds, carbonates, sulphates, salts, and potash salts. The Prairie Evaporite Formation of the Elk Point Group is part of the third cycle from the bottom, which is the largest and the most complete of the five. The first two evaporite cycles of the Lower Elk Point Group are found only in Alberta (Grayston et al., 1964, Meijer Drees, 1986).

The third cycle starts with the Ashern Formation at the base of the Elk Point Group (Fig. 1.2). This is a series of red and grey argillaceous dolostones, 12-50 m thick, that, in Saskatchewan, rest unconformably on the Silurian Interlake Formation (Lobdell, 1984). According to Wilson (1985), the overlying Winnipegosis Formation (Fig. 1.2) has a lower unit

of dolomitized fossiliferous carbonates from 6-15.5 m thick. The upper unit of the Winnipegosis Formation consists of flat-topped, broadly circular, mud-mound carbonate banks from 30-100 m thick, and from 0.5 to 6 km across the top (Wilson, 1985). The mounds are disconformably overlain by anhydrites and salts of the upper Prairie Evaporite Formation (Reinson and Wardlaw, 1971). Between the mounds are bituminous carbonate and anhydrite laminites from 0.6-16 m thick (Wilson, 1985), which are conformably capped by the anhydrites and halite of the lower Prairie Evaporite (Reinson and Wardlaw, 1971). The maximum thickness of the Prairie Evaporite Formation is about 220 m (Holter, 1969).

The fourth evaporite cycle begins with a disconformity and the Second Red Beds, which are part of the Dawson Bay Formation, and comprise 3-8 m of red and green dolomitic mudstones (Fig. 1.2). The rest of the Dawson Bay Formation consists of fine grained carbonates which, east of the third meridian, are capped by halite of the Hubbard Evaporite. The total thickness of this cycle is from 35-40 m (Dunn, 1983). The fifth cycle is in the Souris River Formation - from the First Red Bed at the base to the Davidson Evaporite at the top (Holter, 1969).

The Patience Lake Member is the upper and westernmost of the potash members in the Prairie Evaporite

Formation. It is thickest (>20 m) southeast of Saskatoon (Fuzesy, 1982), and has two potash-bearing zones separated by about 2 m of halite (Fig. 1.3). In the study area, the Patience Lake Member is about 22 m thick from the top of the upper (A) potash zone (being mined) to the bottom of the lower (B) potash zone (Fig. 1.3). The halite overlying the Patience Lake Member varies in thickness from 3 to 12 m (Holter, 1969). The Patience Lake Member is richer in insolubles than the three lower members of the Prairie Evaporite Formation (Holter, 1969).

1.3 **PREVIOUS WORK**

According to Fuzesy (1982), salt springs and seepages in Saskatchewan and Manitoba were associated with Devonian formations as early as 1858. Exploration wells drilled for oil and gas in the early 1940's led to the incidental discovery of potash in Saskatchewan. McGehee (1949) was probably the earliest author to recognize a shale-carbonate-evaporite sequence, which he called the Elk Point Formation, in eastern Alberta and western Saskatchewan. Baillie (1953) introduced the terms "Ashern", "Winnipegosis", and "Prairie Evaporite". The effects of salt dissolution in Saskatchewan were first described in the 1950's by Bishop (1954), Milner (1957), and Walker (1957). The mining of potash began in 1958 with the Potash Corporation of America's

Patience Lake mine, and the Duval Sulphur & Potash Company opened what is now the PCS Cory mine in 1968 (Fuzesy, 1982). Reports specifically on the geology of potash deposits were published by the industry in 1966 (Keyes, 1966, Klingspor, 1966). Studies on the stratigraphy, geochemistry, and petrology of the potash deposits were made at the University of Saskatchewan in the 1960's (Wardlaw and Hartzell, 1963, Schwerdtner, 1964, Wardlaw and Schwerdtner, 1966, McIntosh and Wardlaw, 1968, Wardlaw, 1968).

Since 1957, five different names for each of the potash members of the Prairie Evaporite Formation have been suggested (Goudie, 1957, Klingspor, 1966, Harding and Gorrell, 1967, Holter, 1969, Meijer Drees, 1986). Holter's (1969) nomenclature is the most commonly used and is adopted in this thesis.

Holter's report (1969) is still the most inclusive study on the Prairie Evaporite Formation in Saskatchewan. Maps and sections for the Prairie Evaporite Formation in the United States are presented in Anderson and Swinehart (1979), and for southeastern Saskatchewan, in Worsley and Fuzesy (1979).

The studies most closely related to this one on the geology of Cory potash mine, were by Keyes (1966) and McIntosh and Wardlaw (1968) on the geology of the Esterhazy IMC potash

mine and the Esterhazy mining zone, respectively. McIntosh and Wardlaw (1968) also studied the bromine chemistry of barren halite bodies in the Esterhazy zone. They concluded that bromine could not be used to predict the salt anomalies, and that the salts of normal and anomalous ground were mostly recrystallized. Keyes (1966) and Baar (1974) identified several types of anomalies, including post-ore channels. Mackintosh and McVittie (1983) classified, interpreted, and gave the most successful methods of predicting, salt anomalies.

Several authors (Schwerdtner, 1964; Wardlaw and Schwerdtner, 1966; McIntosh and Wardlaw, 1968; Wardlaw, 1968; and Fuzesy, 1983), using the bromine chemistry and petrographic analyses of the Prairie Evaporite Formation, have concluded that most of the salts have been recrystallized from the originally deposited halite or halite and carnallite. This has been supported recently by Baadsgaard (1987) who found ages from Cretaceous to Recent, for sylvite and carnallite. In contrast, Wardlaw (1968) obtained older ages of Permian to Mississippian for the formation of sylvite and concluded that the sylvite may have been primary; ie. it was not recrystallized. Baadsgaard (1987) suggests this was due to a re-introduction of argon into the sylvite after it was recrystallized in the Cretaceous. Chipley and Kyser (1989) also concluded the salts are not primary by using

homogenization temperature and stable isotope data of fluid inclusions.

Although recrystallization has taken place, there are, nevertheless, numerous potentially primary features, such as chevron halite and desiccation polygons, that indicate what the depositional environment of the Prairie Evaporite Formation was like (Klingspor, 1966; Wardlaw and Schwerdtner, 1966; Baar, 1973; Meijer Drees, 1986; and Mackintosh and McVittie, 1987). Most authors agree that the potash beds formed in shallow brines that were periodically desiccated (Klingspor, 1966; Wardlaw and Schwerdtner, 1966; Holter, 1969; Baar, 1973; Meijer Drees, 1986; Mackintosh and McVittie, 1987). However, opinions are divided as to whether the lower Prairie Evaporite Formation formed in deep water (Wardlaw and Schwerdtner, 1966; Holter, 1969) or shallow water (Shearman and Fuller, 1969; Utha-aroon, pers. comm. 1989). Wardlaw and Schwerdtner (1966, p. 341) note that since the Prairie Evaporite Formation formed very quickly (modern analogues indicate 4,000 years as the minimum required time), subsidence must have been negligible and, barring any drastic changes in world-wide sea level, "the initial water depth must have been equal to, or in excess of, the total thickness of salt" (i.e. 200 m). The Presqu'ile Reefs in north Alberta were assumed to have formed a barrier between the open ocean and the Elk Point Basin (Grayston et al., 1964). Shearman and Fuller (1969) and

C. Utha-aroon (pers. comm., 1989) point out that algal mats, nodular anhydrite, and desiccation features are present in the lower Prairie Evaporite Formation which indicate that there was a profound fall in relative water-level after the formation of the Winnipegosis mounds. Wardlaw and Reinson (1971) found exposure disconformities within the Winnipegosis mounds.

There have been several studies on different aspects of the distribution and mineralogy of insolubles in the Prairie Evaporite Formation. The amount of insolubles increases in successively higher potash members of the Prairie Evaporite Formation and is greater than in all halite beds except those above the Patience Lake Member (Wardlaw, 1968, Holter, 1969). The insolubles in the lower Prairie Evaporite Formation, which does not contain potash, are mostly anhydrite, with minor dolomite and traces of calcite (Wardlaw and Schwerdtner, 1966, Wardlaw, 1968, Holter, 1969). In the upper Prairie Evaporite Formation, which has received more attention, the insolubles include dolomite, clays, quartz, anhydrite, gypsum, hematite, goethite and potassium feldspar (Droste, 1963, McIntosh and Wardlaw, 1968, Wardlaw, 1968, Holter, 1969, Mossman et al., 1982, Fuzesy, 1983). Mossman et al. (1982) identified the insoluble minerals of clay seams in the ore zones of several potash mines, and were able to distinguish detrital from authigenic clays. Hematite is common

in sylvite, carnallite, and in brown clay seams (Wardlaw, 1968, Holter, 1969). Goethite was found in carnallite, and in sylvite adjacent to carnallite (Wardlaw, 1968). Oriented goethite fibers in carnallite suggest that the two minerals grew together while a lack of orientation of hematite in sylvite suggests the sylvite was recrystallized (Wardlaw, 1968, McIntosh and Wardlaw, 1968). Clay minerals include: illite, chlorite (Droste, 1963, Wardlaw, 1968, Mossman et al., 1982), septechlorite, minor sepiolite, smectite, mixed layer chlorite/smectite, traces of vermiculite (Mossman et al., 1982) and minor corrensite (Droste, 1963). Mossman et al. (1982) also found potassium feldspar, traces of hydrocarbons, and palynomorphs. Acritarchs and chitinous fragments that were found in some clay seams are of marine origin; large spores indicate terrestrial influence (Nautiyal, 1975, Cashman, pers. comm., 1987).

Two interim papers using some of the material in this thesis have been published. In Langford et al. (1987) the potash rock types, and a type stratigraphic section of the ore zone were presented. A method for classifying the clay-rich rocks was given in Boys et al. (1986).

Chapter 2. FIELD METHODS AND ROCK CLASSIFICATIONS

2.1 General Methods

At the PCS Cory mine the first objective was to develop a classification system of potash, clay, and halite rock types, in order to subdivide the ore zone and the Patience Lake Member into small mappable, stratigraphic units. A type section of the ore zone, based on these units, was established and then correlated with other sections throughout the mine. Despite some lateral variation in the thickness and lithology, individual units or groups of units maintain their identity within the ore zone of the mine.

Primary and secondary (secondary includes both post-burial and late diagenetic) features of the evaporites, such as fluid inclusions, mineral assemblages, textures, fabrics, or structures, have been used to help interpret the geological history. Many features are ambiguous and their origins remain speculative.

The methods of this study included stratigraphic descriptions, photography and sampling in the mine, and the analyses of the samples in the laboratory. Correlating stratigraphic sections was undertaken both in the mine and in the laboratory. Samples were analysed for percentage of

insolubles and the percentage KCl. Petrographic observations were made on hand samples, rock slices and thin sections. These helped in developing the classification of rock types and in the identification of: primary features, secondary features, and textural relationships. Twenty-six samples from Cory were analysed for their insoluble minerals, as were a suite of samples from the Central Canada Potash mine. A table providing analytical and sampling data is included in Appendix 1.

In the PCS Cory potash mine, walls were cleaned, photographed, described, and sampled. After loose pieces of potash were scaled, the walls were cleaned using a broom, and sprayed with water from a pump-action fire extinguisher. Enough water was used to remove surface grime without significantly dissolving the potash. Sections were measured on mine walls with respect to a datum at the base of the #1 (411) clay seam (Fig. 1.3). Short core samples (3 cm length X 2.5-5 cm diameter) were collected at vertical intervals ranging from <5 to ~50 cm using a portable drill equipped with a coring bit. Other samples were collected using conventional hammer-and-chisel methods, where appropriate.

There was no existing method to describe hand specimens of the potash rock-types. Thus, it was necessary to devise a scheme whereby the rocks could be identified

adequately in hand specimen and *in situ*. Three criteria - colour, texture, and the amount of sylvite present, were used to classify cores and hand samples of the potash and clay rocks (Langford *et al.*, 1987, Boys *et al.*, 1986). The rocks with >10% insolubles were classified as clay rocks.

Ten thin sections were made of samples 1-3 m from a leach salt anomaly in the vicinity of the #2 shaft (Fig. 2.1). To make rock slices (2 mm) an oil-cooled saw was used. These were then sanded to a suitable thickness (1-3 mm) and wax-mounted on glass. Other samples were examined after smooth-sanding only one surface. A magnesium dipicrylamine solution (Clark, 1964) was used to distinguish sylvite from halite in rock slices.

The percentages of insolubles and sylvite (KCl) were determined routinely for many samples. The powder produced during drilling for the core samples was collected and later analyzed. The hand samples needed to be broken to about 0.25 mm (60 mesh) before separating a representative portion for analysis. In all cases, a sample divider was used to ensure an unbiased separation. The powder was then dissolved in about 100 ml of deionized water.

The potassium content of the water soluble fraction was analyzed by an Orion ion specific electrode,

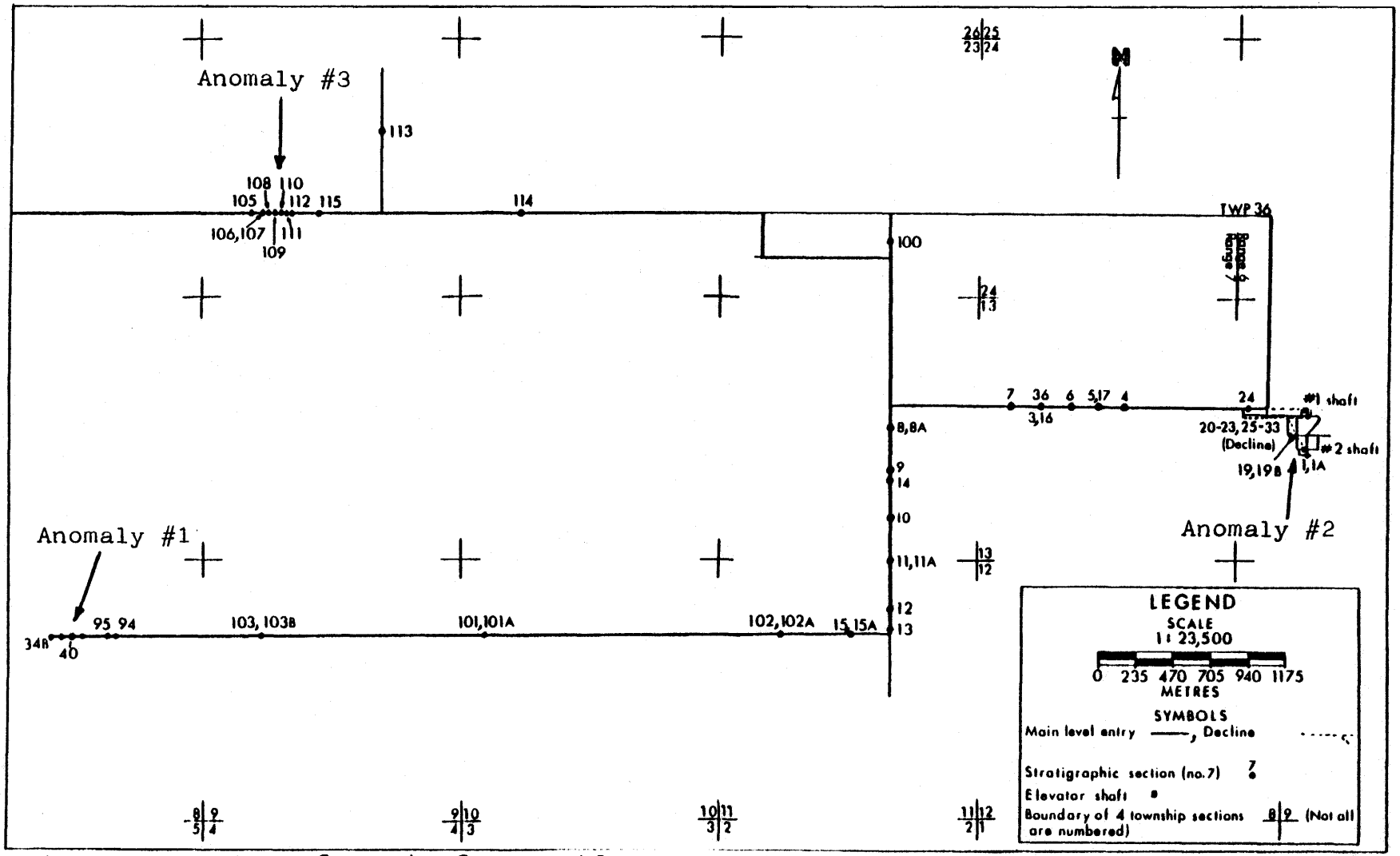

Fig. 2.1 A map of part of PCS Ltd. Cory potash mine showing location of the major stratigraphic sections. See Appendix 1 for entry and breakthrough no's. for all sections. See Fig. 1.1 for location.

using the method outlined by Ellwood (1983) and Chipley (1986). To check the accuracy of the results, the same solutions from two sets of samples (section 3 and 15) were also analysed by atomic absorption spectrophotometry (Appendix 2a). The percentage of insolubles was determined as the weight difference after dissolution of the sylvite and halite in deionized water at room temperature.

Some sample splits were analyzed semi-quantitatively for salt mineralogy by X-ray diffraction with reference to prepared standards. The ratio of the heights of the most intense peaks of sylvite (3.17 Å) and halite (2.82 Å) was directly related to their relative percentages (as determined using the prepared standards). This gave an estimate of the amount of KCl in the sample, which provided a further check on the results obtained using the ion specific electrodes (Appendix 2b). The samples were prepared by grinding to 200 mesh and slurry mounting on glass with ethanol. They were then analyzed from 31 to 27° 2theta, to include the most intense peaks of halite and sylvite, on a Rigaku Rotaflex X-ray diffractometer using Cu K alpha radiation set at 40 kV and 80 mA.

2.2 Potash, halite, and clay rock-types.

A classification into lithological types was developed in this study as a preliminary attempt to standardize descriptive terminology. Although emphasis has been given to utility rather than to genetic connotations, the differences between the main potash rock-types relate to how they formed.

Klingspor (1966) attempted a classification of sylvinite ore on the basis of ore grade. McIntosh and Wardlaw (1968) subdivided rocks from the ore beds and salt anomalies of the Esterhazy mining zone based on colour and composition. A formal classification of halite rock types for the Prairie Evaporite Formation has not been developed. However, Hovorka (1987) developed a textural classification with genetic significance for nine different types of halite in the Permian San Andres Formation of Texas.

The rocks were classified on the basis of composition, colour, translucency, grain or crystal size, texture, and the amount and form of insolubles. There are three major kinds of rocks in the Patience Lake Member: sylvinite (potash), halite, and clay rocks. A fourth type, carnallitite, is very minor in the Cory potash mine. Sylvinite encompasses variable mixtures of halite and sylvite. Halite,

as a rock term ('rock salt' is equivalent), designates those rocks that are made up almost exclusively of halite. If the amount of sylvite is 5% or greater, then the rock is considered to be sylvinite; if less, then it is halite. The clay rocks have more than 10% insolubles, and almost all the clay seams, a centimetre or more in thickness, meet this requirement. However, some sylvinite and halite samples may contain more than 10% disseminated insolubles without being classified as clay rocks because they lack lateral continuity.

'Granoblastic' refers here to evaporite rocks that are generally equigranular with interlocking crystals, whether the texture was produced as a primary crystal accumulation or by subsequent overgrowth or recrystallization. 'Porphyroblastic' is used where larger, generally euhedral to subhedral crystals are present within a matrix of smaller crystals.

Sylvinite (Potash) Rock Types

Sylvinite is a rock composed of a mixture of halite (NaCl) and sylvite (KCl), with variable minor amounts of insolubles. The sylvinite of the Patience Lake Member is typically red, coarse grained (1-15 mm), and has from 5-80% sylvite. Only minor carnallite ($KCl \cdot MgCl_2 \cdot 6H_2O$) has been found

in the sections examined at Cory Division, although it is common elsewhere (Wardlaw, 1968; Holter, 1969; Fuzesy, 1983).

Four broadly defined potash rock types have been recognized from more than 300 samples examined, informally labelled 'A', 'B', 'D', and 'G'. Colour, governed mainly by the iron oxides, and the amount of sylvite, are the main criteria used, as in similar systems by Klingspor (1966) and McIntosh and Wardlaw (1968). Wherever the sylvite is red the rock has higher amounts of greenish-grey insolubles than where it is pale orange. The characteristics of the four types of sylvinite are summarized in Table 2.1, and illustrated in Plates 1-3. Types 'C', 'E', and 'F' were discontinued when they were found to be too rare or inadequate. No formal lithological names have yet been applied. Detailed descriptions of each of the potash rock types are included in Appendix 4 and in Langford et al. (1987).

Variations of the sylvinite rock types are common, and they may grade into one another, varying with distribution and the amount of sylvite and red insolubles (mostly hematite). For example, given an A-type, a decrease in the amount of hematite, which is usually accompanied by a

	ROCK TYPE	A	B	D	G
DIAGNOSTIC	FEATURES	Orangey-red thick rims on many evenly distributed sylvite crystals.	Pale orange. Low in insolubles.	Majority thin red rimmed sylvite.	Patchy reddish sylvite.
	TRANS-LUCENCE	Opaque	Low to high	Opaq.to low	Low-med. Patchy
	TEXTURE	Granoblastic Porphyroblastic	Granoblastic Porphyroblastic	Granoblastic	Granoblastic
	OCCURRENCE	Most common	Common	Common	Common
SYLVITE	Crystal size	1-8 Gbl. 1.5-12 Pbl.	0.5-8 Gbl. 1-18 Pbl.	1-12, avg.6	0.5-8
	Crystal shape	Subhedral, most anhedral	Anhedral	Anhedral equant	Anhedral
	Colour	Orangey-red red thick fringes. Clear to cloudy centre	Whispy orange. Clear, cloudy	Red rims Clear to cloudy centre	Orangey-red to red
	Amount	15-85% avg. 54±13	15-85% avg. 51±17	24-56% avg. 42±12	5-45% avg. 17±11
	Other	Hematite and goethite inclusions	Halite inclusions		Remnant crystals
HALITE	Crystal size	1-9 Gbl. 2-15 Pbl.	1-9 Gbl. 1-18 Pbl.	1.5-12 most 4-10	1-12 max 20
	Crystal shape	Anhedral & subhedral	Anhedral &subhedral	Anhedral subhedral	Most anhedral
	Colour	Clear & small cloudy	Clear & cloudy	Most clear	Clear & cloudy
	Amount	Low to moderate	Moderate to low	Moderate	Moderate to high
	Other	Thin films Inclusions			Thin films
INSOLUBLES	Amount	<1-25% avg. 4±3	<1-3% avg. 0.7±0.5	1-19% avg. 8±6	<1-15% avg. 3±3
	Colour	Mostly green-grey	Green-grey	Green-grey some brown	Mostly green-grey
	Distr-ibution	Mostly interstitial Inclusions Especially with halite	Inclusions & interstitial Especially with halite	Seamlets inclusions & interstitial	Inclusions are abundant Interstitial

Table 2.1: Properties of four sylvinite rock types from the ore zone. See appendix for fuller descriptions. Abbreviations: Gbl. = granoblastic, Pbl.= porphyroblastic. Crystal sizes in millimetres. Mineral amounts in weight percent, range given then average ±1 standard deviation, see Figs. A1-A3. Revised from Langford et al. (1987).

decrease in total insolubles, would give B-type sylvinite. Concentrating the hematite in thin margins to the sylvite crystal boundaries would give D-type. Decreasing the amount of sylvite would give G-type. Gradations between the rock types are observed, eg A(G)-type. Mixed rock types arise when two or more rock types occur within close proximity, for example, lenses of B-type in A-type (Plate 3c).

Halite Rock Types

The halite rock types are differentiated by colour: red, orange, pink, brown, grey, white, and mixed (Plate 4a). Their origins, whether from an anomaly or from the normal bedded halite, can be determined from the colour and presence of sylvite. Normal halite, which may be any colour except red, includes all that outside of anomalies, such as the halite between the upper and lower parts of the Patience Lake Member. Red halite (Plate 4a,b) has only been found in salt anomalies. There are two varieties of orange halite: 1) with sylvite in normal salt beds, and 2) without sylvite in salt anomalies (Plate 4a). Pink halite is a paler variety of orange halite, having less hematite. Brown and grey halite (Plate 4a) are the most common. The brown and grey halite derive their colour from disseminated insolubles. Mixed colours of brown, orange, grey, and white, are most common in halite from salt anomalies. White or clear halite is usually very low in

insoluble content (<2%, Plate 4a). Fluid inclusions give the milky white colour, and a lack of any inclusions gives it the clear appearance. Detailed descriptions of the type samples of red, orange, brown, grey, and white halite are included in Appendix 4. A textural classification, similar to that of Hovorka (1987), was not made because of the limited textural varieties.

Granoblastic and porphyroblastic varieties are found in all the halite rock types. In general, crystal size ranges from <1 to 18 mm in granoblastic rocks, and 1 to 25 mm in porphyroblastic varieties. Rocks from washout and collapse anomalies may have salt crystals up to several tens of centimetres across. Crystal shapes are commonly anhedral to subhedral. Generally, crystals tend to be larger and more euhedral in rocks from anomalies than in rocks from the normal bedded halite.

Insoluble Rock Types

Insolubles occur as seams or layers variously separating beds of halite and sylvinite, as patches within potash ore, interstitially dispersed between crystals of various salts, and in minor amounts as dark colour bands in bedded halite. They also fill collapse structures,

depressions, and joints such as polygon cracks, microkarsts, channel beds, and portions of collapse anomalies.

The clay rock classification is summarized in Table 2.2 (from Boys et al., 1986). To be considered a clay seam, the rock should have more than 10% measured insolubles in adequate continuity (eg. >5 m long). In the clay seams, the amount of insolubles averages 26±11 percent (Fig. 2.2a). The clay rock-types, and the variables of thickness and continuity are used to characterize the clay seams. A given clay seam may have more than one clay rock type. The criteria used to classify the clay rock types are colour, texture, and a threshold amount of sylvite.

Colour is the most commonly and easily observed criterion. Greenish-grey to green is the most common colour of clay seams in the potash-bearing beds, while mottled greenish-grey-and-brown is most common overall. Clear, beige and brown halite are common in all types of clay seams. Cloudy, white, chevron halite crystals are common in the clay seams. Red salt crystals were usually sylvite. In this study only one sample, a deep purplish-red clay, was found that was convincingly red, CCP sample #15 from below the ore zone (Table 7.4, see **Insoluble Mineralogy**). So, red insolubles were considered rare enough that they were included in brown.

Table 2.2

CLASSIFICATION OF CLAY ROCKS (Boys et al., 1986)

D = disseminated
M = massive
S = sylvite visible

The colour is green or greenish grey

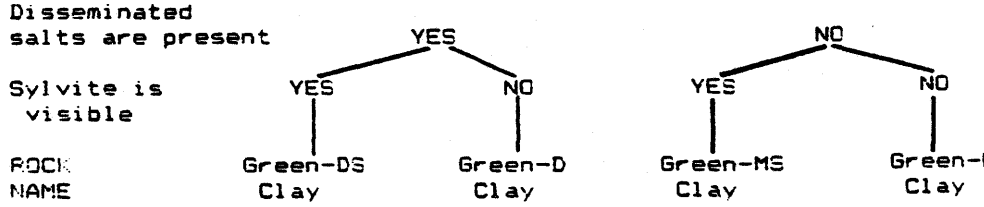

The colour is brown

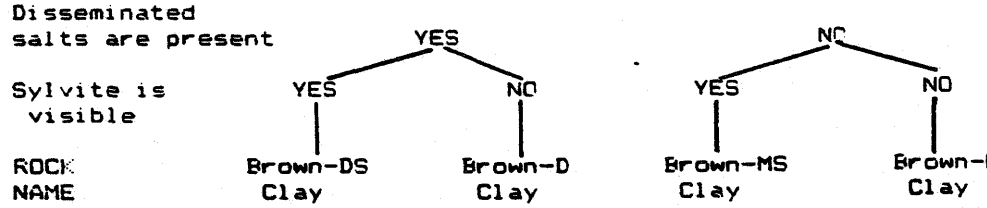

The colour is mottled green and brown

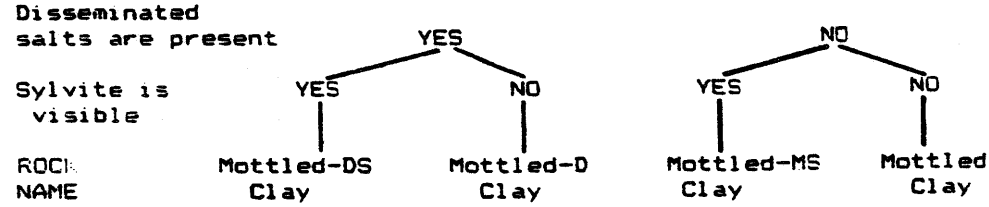

Note: if the rock contains patches of one kind in another, the secondary feature may be put in brackets. Eg Brown-D(M) for a disseminated rock with subsidiary massive areas.

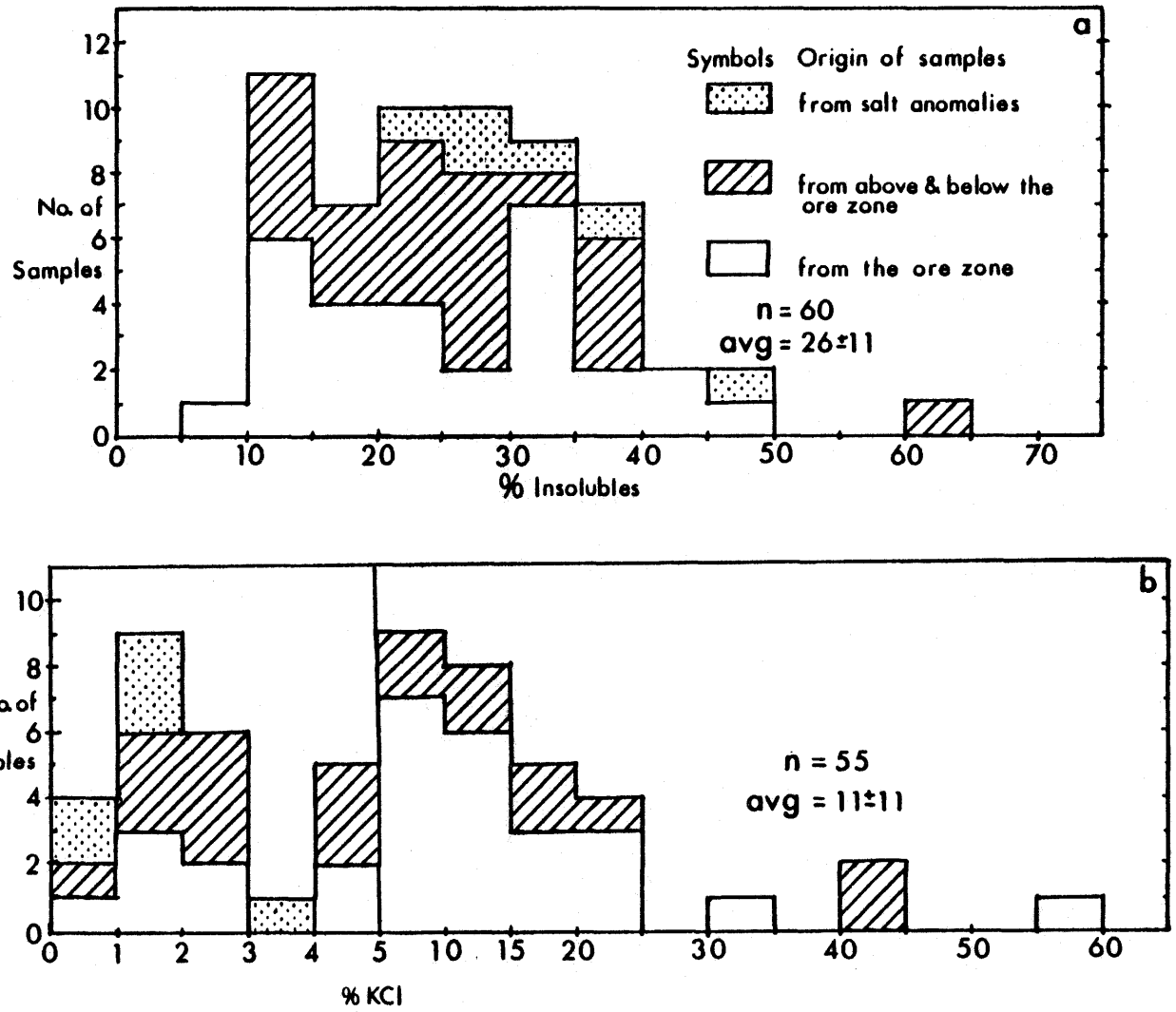

Fig. 2.2 Histograms of a) % insolubles, and b) % KCl for clay rocks. The meaning of the symbols is the same for a) and b). The average (avg) is given ∓1 standard deviation.

The presence of visible sylvite (>5%) is considered to be important in using the clay-seam composition as an indicator of anomalous mining ground. Figure 2.2b shows that most of the seams have less than 25% sylvite and that, of those that that have >5% KCl, most are from the ore zone. Samples from salt anomalies have less than 5% sylvite. Sylvite is most common in the greenish-grey clay seam samples (Plate 4c).

There appears to be a continuous variation in the ratio of salts to insolubles. Where the rock appears to be dominantly insolubles, the texture is called massive. Where the insolubles appear to be 40% or less the texture is called disseminated (Plate 4c). Analyses indicate that the maximum content of insolubles is about 40% (Fig. 2.2a), which is about half of what the appearance suggests. Some seams of disseminated clay are comprised of salts with interwoven clays giving the rock an irregular honeycomb texture (Plate 4c). ("Disseminated" also refers to insolubles that occur in the sylvinite and halite beds, but in insufficient quantity and competency to be called a clay seam.) Seams with disseminated salts are much more common than massive seams.

Chapter 3. THE INSOLUBLES: METHODS

The insoluble minerals were examined for 26 samples from PCS Cory Division Potash mine, and 23 samples from the Central Canada Potash mine (Fig. 3.1). Both clay seams and the intervening salt beds at Cory were sampled, but only clay seams at Central Canada Potash were sampled. In both mines ore-grade potash and one anomaly were sampled. At Cory the stratigraphic interval sampled for a normal section from the bottom of the ore zone up to the 416 clay seam, was taken from sections 16, 3, 36 (Fig. 2.1). The anomalous salt section, #40 (Fig. 2.1), was sampled from top to bottom of the ore zone. In the Central Canada mine samples were taken from three sections: from the bottom of the ore zone to the 416 clay seam above, from the middle of the ore zone to 6.7m below, and from the top three seams of the ore zone to the 416 seam above in a salt anomaly (Fig. 3.1).

For all samples rock type, percent insolubles, minerals detected in the untreated insoluble portion, and the percent anhydrite + dolomite (soluble in weak HCl) were evaluated. The amount of KCl was determined only for the samples from sections 16, 3, 36. The "insolubles colour" (Table 7.2) is the colour of the dry powder on the slides prior to being X-rayed, and was noted for the Cory samples

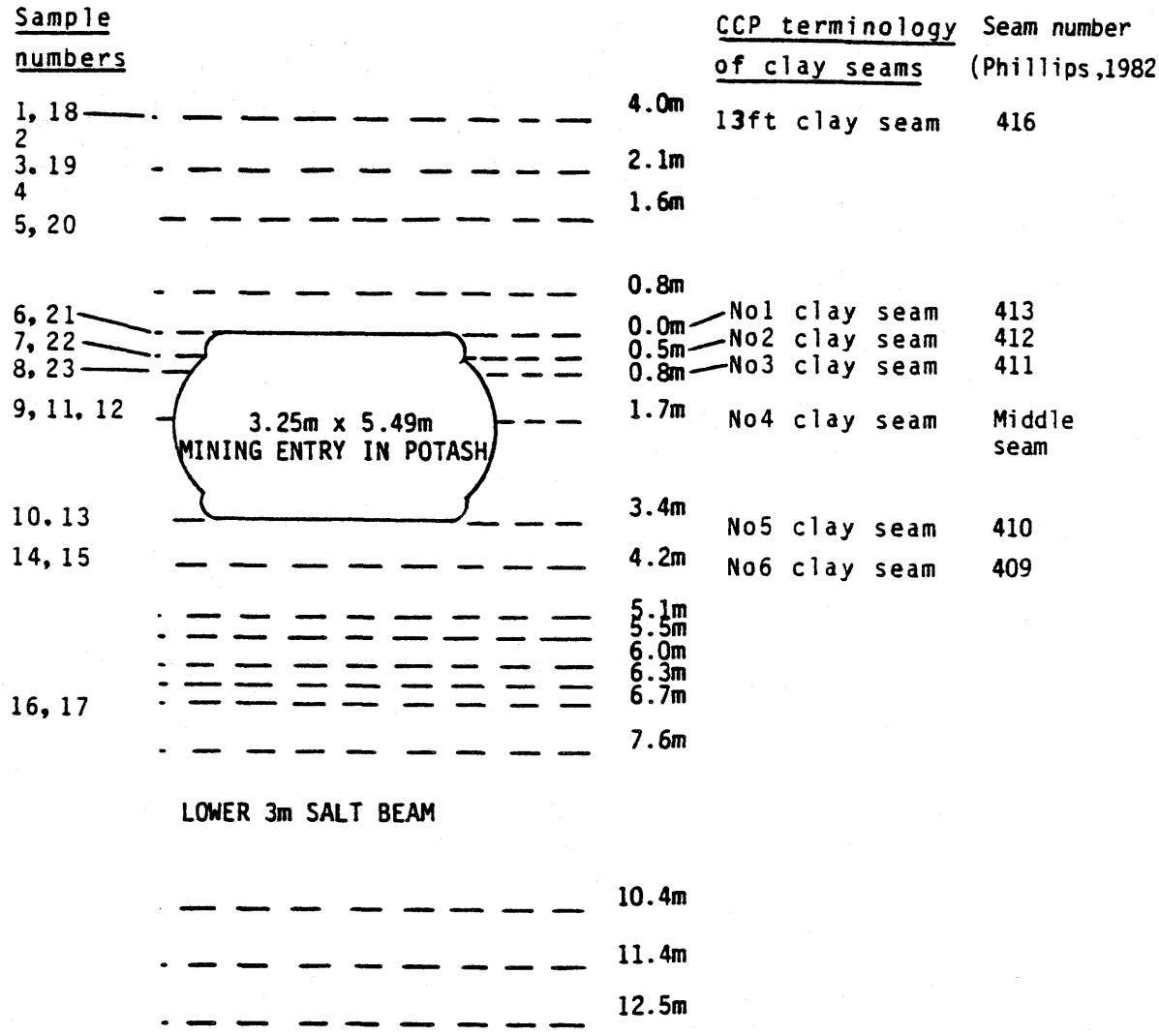

Fig. 3.1 Stratigraphic column of the Patience Lake Member at the Central Canada Potash mine. Sample locations and clay seams (dashed lines) are indicated (Coode, pers. comm., 1988).

only. For all samples, the combined weight percentage of dolomite and anhydrite was determined as the weight difference after digesting the water-insoluble fraction in 3N hydrochloric acid. Barium chloride ($BaCl_2$), applied to the filtrate to produce a white precipitate upon reacting with sulphate (Kinghorn, 1983, p.45), was used to detect anhydrite. "Spiking" Cory sample #40.4 with 5 and 10 % anhydrite, and extrapolating from the increased peak heights at d-spacings of 3.54 and 1.75 Å gave estimates of the anhydrite content for the other samples. The percentages quoted are intended to give a semi-quantitative indication of the amount of anhydrite present.

The residue from the HCl treatment of the Cory samples was then centrifuged to obtain the <2 micron fraction. From this fraction were determined the illite:chlorite:septechlorite ratios, and the amounts of hematite and goethite relative to the other samples. The relative amounts of iron oxides were estimated qualitatively by comparing the most intense peaks of the mineral concerned from sample to sample. The samples were then glycolated to determine the presence of swelling clay minerals: smectites, mixed-layer clays, and swelling chlorite. The flow chart in Table D (Appendix 3) summarizes the analytical procedures. All samples were X-rayed using a Rigaku Rotaflex X-ray

diffractometer with Cu K alpha radiation, set at 40 kV and 80 mA.

The illite:chlorite:septechlorite ratios were determined using the method of Mossman et al. (1982, p. 2130). They provided the only data on clay mineralogy for the Patience Lake Member that is available for comparison. The method involves measuring the net peak heights (peak height minus background, Fig. 3.2) of 001 diffraction lines, which for air-dried mounts of chlorite, illite, and septechlorite (001) + chlorite (002) are at 6.2, 8.8, and 12.4° 2 theta, respectively. To obtain the amount of septechlorite (001), the combined peak of septechlorite (001) + chlorite (002) was reduced by an amount equal to the chlorite (001) peak. As Mossman et al. (1982) point out, there are problems with assigning equal intensities to the chlorite (001) and (002) peaks. Chlorite (002) is commonly larger than, or the same size as, chlorite (001). Chlorites with a higher iron content have even larger (002) peaks while increasing the aluminum content favours a larger (001) peak. Also, the chlorite (002) and the septechlorite (001) peaks do not perfectly coincide.

Further complications arise when other minerals are present, such as kaolinite, smectite, mixed-layer clays, and swelling chlorite. Glycolated samples (Figs. 3.2 and

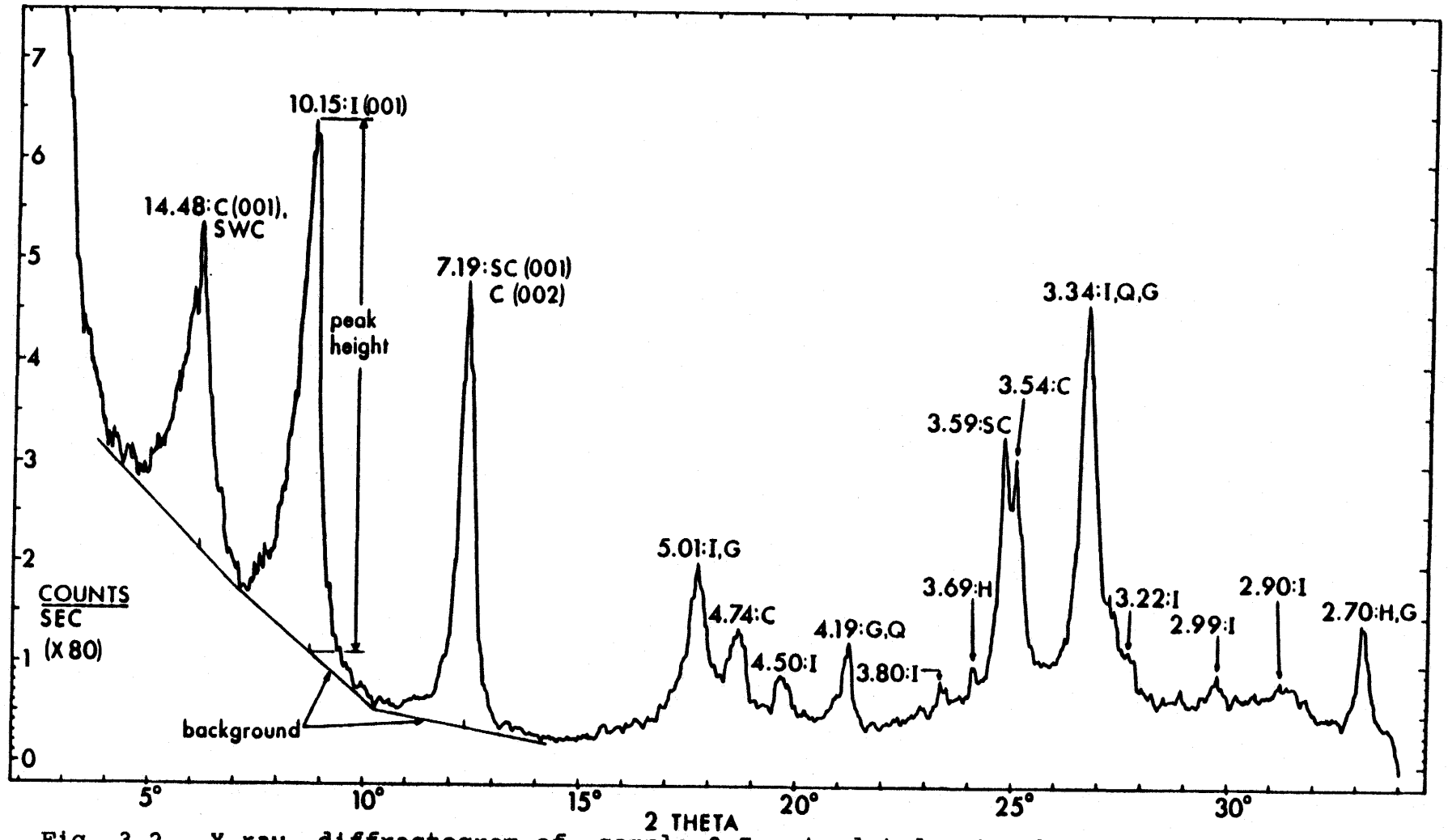

Fig. 3.2 X-ray diffractogram of sample 3.7 air dried: insolubles, HCl treated, <2 micron fraction. Scanned at 40kV, 80mA, and 2°/min. Minerals: C = chlorite, G = goethite, H = hematite, I = illite, Q = quartz, SC = septechlorite, and SWC = swelling chlorite. D spacings in angstroms (Å). Background and a sample peak height for determining clay mineral ratios are shown.

3.3), give an extra broad, asymmetrical peak at about 16 Å (5.5° 2theta) that could be due to smectite or swelling chlorite, or both (Brown and Brindley, 1980). Glycolation was used on all the <2 micron-fraction slides of the Cory samples and on all the Central Canada samples. The method used was to soak a sheet of filter paper in a petri dish with ethylene glycol and overlay a dry sheet of filter paper. The slides were inverted on top, covered with a plastic lid, allowed to equilibrate for 24 hours, and then analysed. The extra peak at 16.3 degrees 2theta meant that further tests were required to discern, if possible, which of the swelling minerals were responsible.

Hot HCl destroys chlorite and saponite, a species of smectite, but not other smectites nor kaolinite. Thus, a 12-17 angstrom peak that survives this treatment indicates the presence of one of the latter two minerals. As it turned out, there were no peaks within this range of d-spacing after the hot HCl treatment of three samples. Furthermore, from experimental work in the system $MgO-Al_2O_3-SiO_2-H_2O$, Velde (1973) concluded that the expandable phase swelling-chlorite/chlorite was more likely to form authigenically than montmorillonite/chlorite. Saponite (Mg-smectite) was found in salt (Fisher, 1988), but is not considered to be present in this study because of the absence of large saponite peaks at 9.1, 8.5, and 5.7 Å (JCPDS, 1983, p.1001). Therefore, swelling

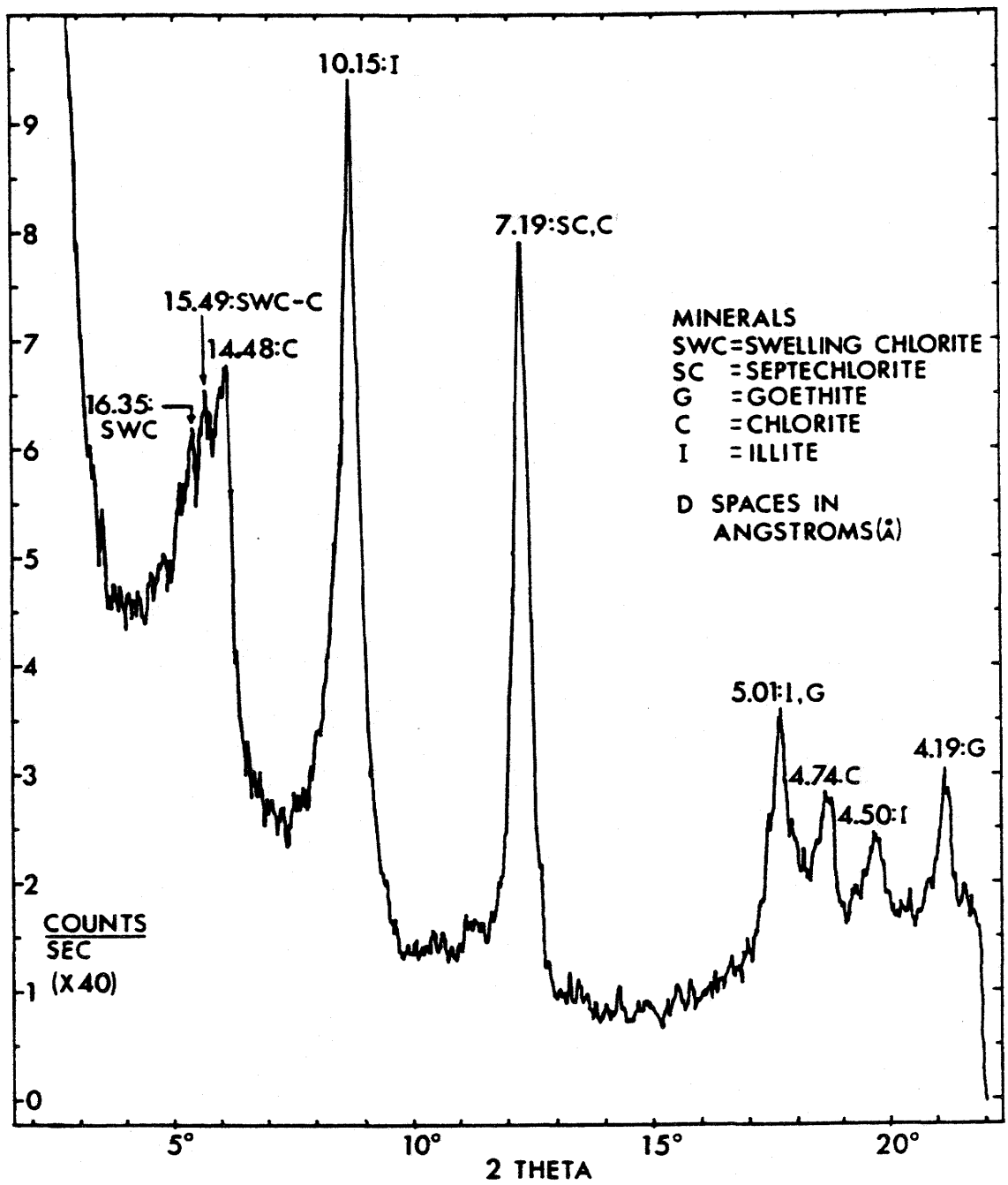

Fig. 3.3 X-ray diffractogram of sample 3.7 glycolated: insolubles, HCl treated, <2 micron fraction. Scanned at 40kV, 80mA, and 2°/min. Minerals: C = chlorite, G = goethite, I = illite, SC = septechlorite, and SWC = swelling chlorite. D spacings in angstroms (Å).

chlorites, not smectites, are most likely causing the expansion. Furthermore, because the peaks are broad and asymmetrical, which are typical of mixed-layer clays (Brown and Brindley, 1980), they indicate the presence of mixed-layer swelling-chlorite/chlorite, as found by Droste (1963). Hence, the illite:chlorite:septechlorite ratios presented are those determined from air-dried (unglycolated) samples and 'chlorite' includes swelling-chlorite/chlorite.

If the glycolated samples were used to determine the ratios of the three clay minerals, the expanded peak due to the swelling chlorite (Fig. 3.3) would detract some of the intensity from the regular (14 angstrom) chlorite. As a result, the amount of septechlorite would increase slightly with respect to 14 angstrom chlorite and, to a lesser degree, illite.

X-ray diffractograms were also obtained for three heat-treated samples at 300, 450, 560, 650, and 725°C. The results of the clay mineral data should be interpreted by keeping in mind that the hot HCl and heat-treatment tests were applied to only a few samples, and that other tests, such as soaking in cation-saturated solutions (Brown and Brindley, 1980), were not used.

For estimates of the percent anhydrite and the clay mineral ratios, the accuracy of the X-ray instrument and sample repeatability are well within the margin of error of sample reproducibility. As Mossman et al. (1982) discovered, the sampling problem is considerable. The clay mineral ratios for different portions of the same sample, as well as different samples from the same stratigraphic level, may differ by as much as 20%. For example, the <2 micron fraction of sample 3.17 was split into 5 portions, each of which were analysed separately. The average illite:chlorite:septechlorite ratio was 50:30:20 with one standard deviation of 3:5:9.

The estimates of the percent dolomite + anhydrite, insolubles dissolved in HCl, are considerably more reliable than the X-ray diffraction data. Again, reproducibility is about 5 to 10%. Given the proven heterogeneity of the samples (Mossman et al., 1982), precise determinations of the analyses of individual samples would not add significantly to the interpretations to be made.

PART 2. RESULTS

Chapter 4. STRATIGRAPHY

The Patience Lake Member has two main beds of sylvinite separated by halite (Figs. 1.2, 1.3). Seams 1-30 cm thick and abundant in water-insoluble material (clay seams or insoluble seams) separate salt beds. The ore zones of PCS Cory, PCS Allan, Central Canada, and Cominco potash mines are each about 3 m thick and lie in the middle of the upper Patience Lake Member (Phillips, 1982). Generally there are 3 insoluble seams in the upper 1 m of the ore zone, one seam in the middle, and an insoluble seam at the base of the ore zone. The rest of the ore zone is made up of moderate to high-grade sylvinite. Within the mining zone, the clay seams and the insoluble mineralogy help to characterize stratigraphic levels in both normal and anomalous ground. For example, the 411 clay seam (Fig. 1.3) is green in the normal ore zone and mottled green-and-brown near and within salt anomalies.

4.1 THE PATIENCE LAKE MEMBER: A detailed stratigraphic section

A detailed stratigraphic section, 26 m thick, from the top of the Patience Lake Member to below the Allan Marker

bed is presented in Fig. 4.1. It was compiled from stratigraphic sections #20-33 down a decline to the base of the #2 shaft at the PCS Cory mine (Fig. 2.1). The results of analyses for weight percent insolubles and sylvite are included. Six potash cycles (described below) are indicated. The Patience Lake Member includes all sediments from the top of seam 416 to the bottom of seam 401 (Phillips, 1982). It is 18 m thick in this section. The clay seam designations of Phillips (1982) were based on neutron density logs from wells in the Lanigan area (Fig. 4.2). Only at the top of the ore zone, seams 411 to 413, was the rock record taken into account. The Allan Marker bed is a prominent potash bed between the Patience Lake and Belle Plaine Members of the Prairie Evaporite Formation (Phillips, 1982).

The top 3 m of Fig. 4.1 is correlated with three other sections to give an idea of the "normal" salts above the ore zone (Fig. 4.4), because at this section there is anomalous halite from the 416 seam to 75 cm below the 411 seam. Below this anomaly, the entire section in Fig. 4.1 is considered representative of the normal rock sequence. The brown halite beneath the Allan Marker bed may be a possible exception because the poor bedding may be due to recrystallized halite. A gamma-ray log is sensitive to sylvinite and clearly shows up the salt anomaly (Fig. 4.2). The neutron density log in Fig. 4.2 also shows the clay seams

STRATIGRAPHIC SECTION OF THE PATIENCE LAKE MEMBER
AND THE ALLAN MARKER BED
IN PCS CORY POTASH MINE

Fig 4.1

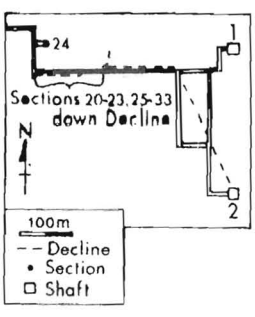

LEGEND

Scale given below

Clay seam <3cm thick

Clay seam ≥3cm thick

Hb Colour bands in halite (H), (b,g,p,w-brown, grey, pink, white)

Abrupt contact

Gradational contact

B A Mixed potash rock types layers, lenses, and blebs (A > B) Rock types (A,B,D,G,H) described in text

CLAY SEAMS

Gn Greenish-grey
Bn Brown
Mot Mottled Gn & Bn

M Massive texture
D Disseminated salts
S Sylvite visible

413 Seam no (Phillips, 1982)

1-6 Potash cycles

SALT TYPE

% Insolubles 0 5 10 20 40

% Sylvite 0 8 16 32 64

416 Mot M
Hw
Mot D
Hg
Bn D
Hw
415 Mot D
Hb
Mot D
Hg
414 Bn D(M)
Hb
413 Mot D
412 "
Hb
411 Bn D
Hb
leach salt anomaly
1m
B A
Middle seam
Gn DS
A
G(A)
6
G(B)
A
Gn D
A
410 Bn D
D
"
D
Mot D
G(B)
409
Hb
Hg
Hb
Mot D
G
Bn D
G
408 Mot D
Gn DS
Hb
A
B
5
A
Gn DS
A
Gn DS
"
A
407 Bn DS
Gn D
Hp
Hw
406 Mot DS
Mot D
A
B
4
Gn DS
405 Mot DS
A
A
3
G(B)
A
404 Mot D
A
2
G(B)
Mot DS
G
403 Gn D
A
B
A
402 & 401 Bn DS
Hb
Hb
Hg
Mot D
Hb
Bn D
Hb
1m
Hw
Bn D
Hb
Bn D
Hb
Hw
A ALLAN
B MARKER
BED
D
Bn D
Hb

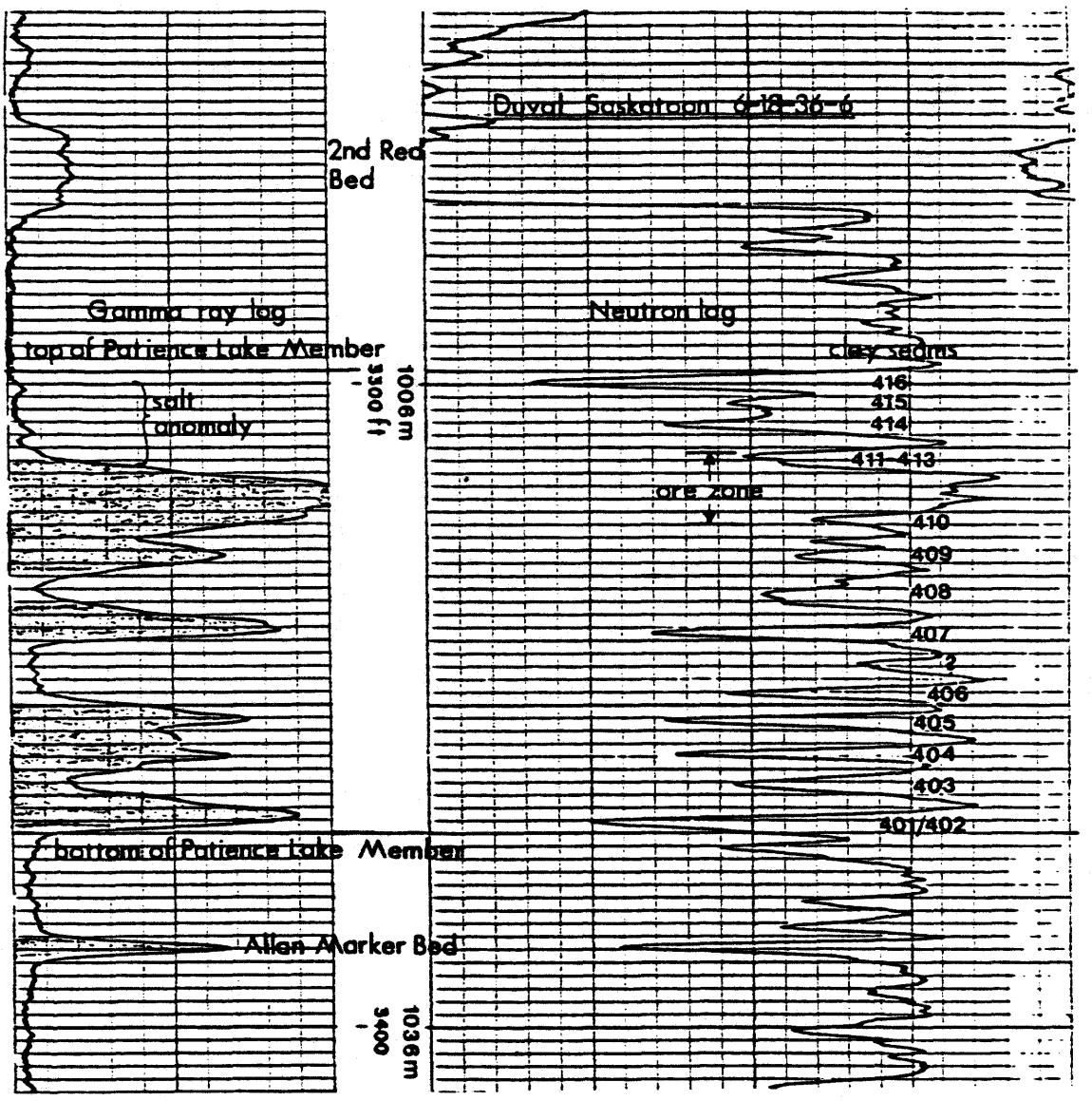

Fig. 4.2 Gamma ray and neutron logs of Duval Saskatoon 6-18-36-6. This is essentially from the #2 shaft (Fig. 2.1). Clay seam numbers are from Phillips (1982). Shaded areas in the gamma ray log indicate abundant potash.

and clay-rich salts well. An extra neutron density peak in the middle of the banded halite, between clay seams 406 and 407, cannot be accounted for in the stratigraphic section (Fig. 4.1). The peak indicates that insolubles may become abundant in this interval toward the #2 shaft, about 200 m away, from where the well log was taken.

Potash beds in the lower, and most of the upper, Patience Lake Member show a sequence of repetitive cycles. The main feature of the "potash cycle" is that pale orange, insoluble-poor B- or G-type sylvinite rarely contacts a clay seam. From bottom to top, one complete cycle passes from clay seam to red A- or D-type potash to pale orange B- or G-type potash, then back into red A- or D-type potash and, finally, ends with another clay seam (Fig. 4.3). The potash cycle is from 1 to 2 m thick. Four of these cycles make up the lower Patience Lake Member: cycle one is from the 401/402 seam to the 403 seam, cycle two from the 403 to the 404 seam, cycle three from the 404 to the 405 seam, and cycle four is from the 405 to the 406 clay seam (Fig. 4.1). Cycles three and four are illustrated in Plate 5 and Figure 4.3.

In the upper Patience Lake Member there are 3 complete potash cycles, and 3 or 4 incomplete potash cycles. For example, a fifth cycle is from clay seam 407 to the halite just below seam 408 (Fig. 4.1). The first complete cycle is

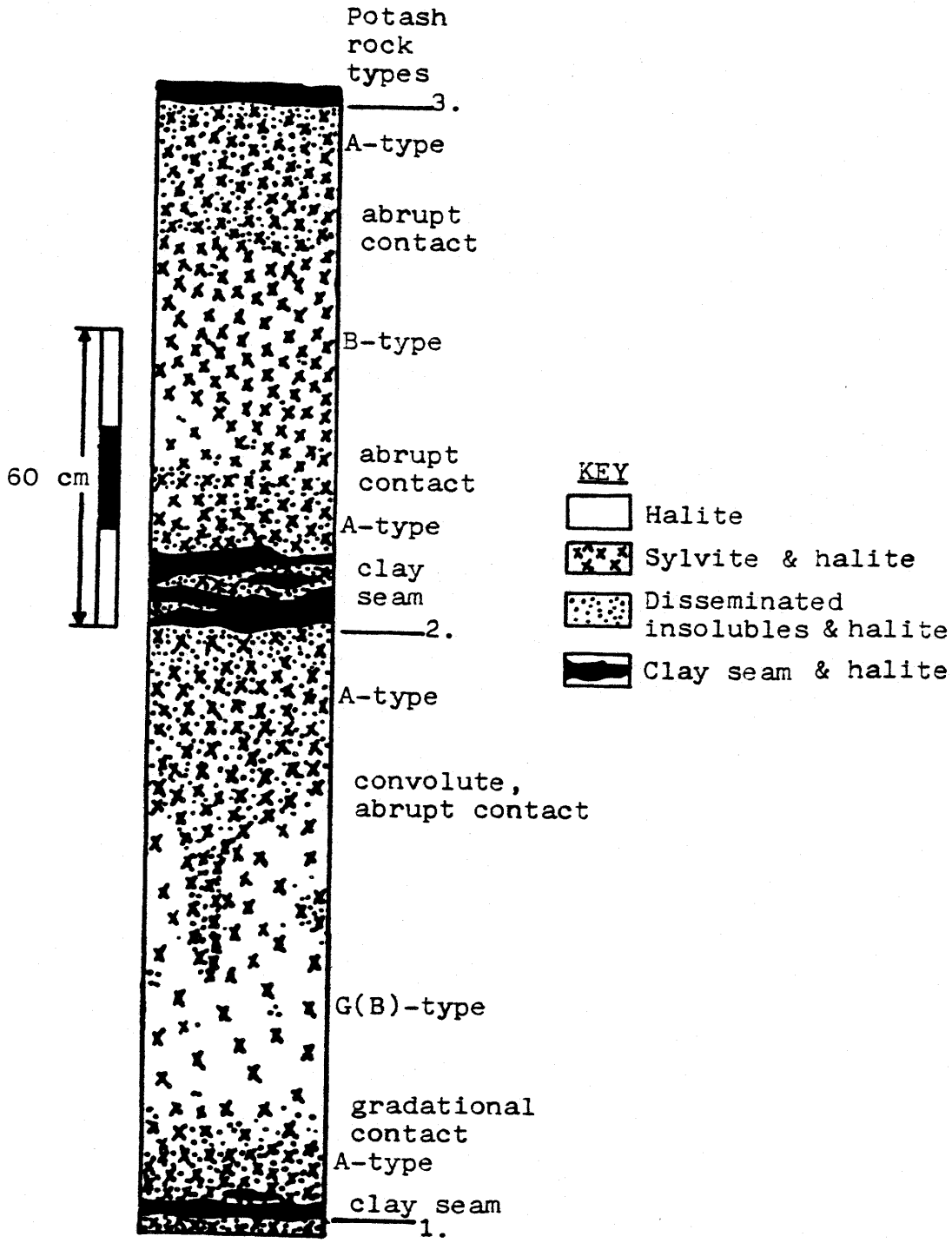

Fig. 4.3 Sketch of two potash cycles; from 1. to 2. is one cycle, and from 2. to 3. is another. Derived from Plate 5, potash cycles 3 and 4. Refer to Fig. 4.1 for % insolubles and % KCl.

from seam 410 to the Middle clay seam of the ore zone. As will be shown, the normal ore zone from the Middle seam up to seam 411 deviates from the potash cycle in that B-type sylvinite is found close to both clay seams. Above the ore zone, the potash cycle repeats itself between seam 414 and the bottom of seam 415, and between seam 415 and 416 (Fig. 4.4).

The cycle of rock types is reflected in a parallel cycle in the amounts of insolubles, hematite, and sylvite. The amount of insolubles is highest in the clay seams, fairly abundant in A-or D-type potash, but negligible in the B-type potash. Wherever the sylvite is red the rock has higher amounts of greenish-grey insolubles than where it is pale orange. In fact, as may be seen in the insoluble profile (eg. cycle 4 in Fig. 4.1), it is the distribution of the insolubles that is cyclic. Though the term "potash cycle" is retained, perhaps "cyclic insolubles in potash" would be more apt from a genetic viewpoint. The amounts of hematite are largest in the red sylvinite, moderate to low in the B-type potash and mottled clay seams, and negligible in greenish-grey insolubles. The amount of sylvite is lowest in the clay seams, and moderate to low in G-type potash.

The Allan Marker bed seems to imitate part of a potash cycle, except that the layered B-type sylvinite grades up into halite (Fig. 4.1). Halite truncates the top of cycle

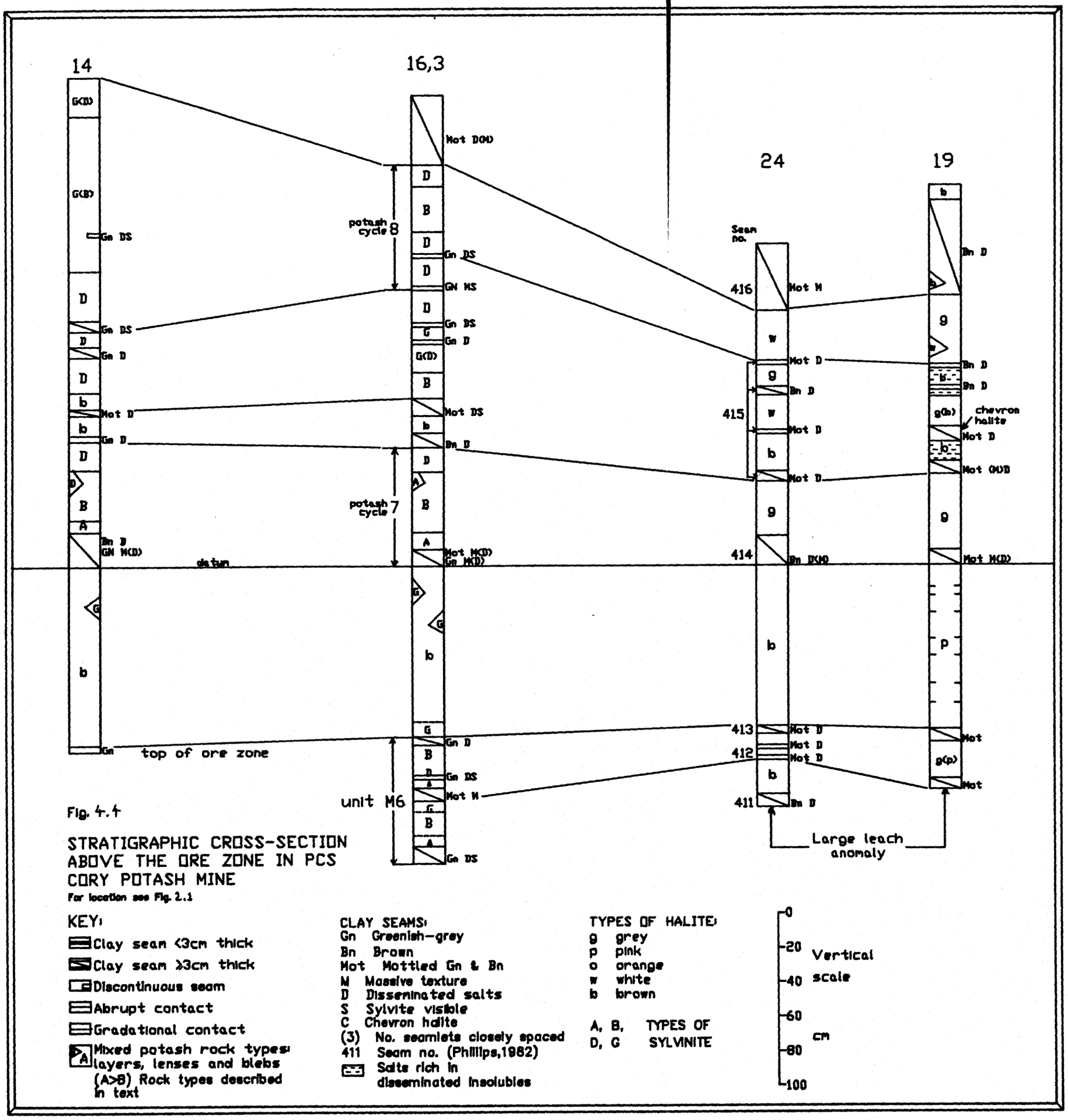

Fig. 4.4

STRATIGRAPHIC CROSS-SECTION ABOVE THE ORE ZONE IN PCS CORY POTASH MINE

For location see Fig. 2.1

KEY:

- Clay seam <3cm thick
- Clay seam >3cm thick
- Discontinuous seam
- Abrupt contact
- Gradational contact
- Mixed potash rock types: layers, lenses and blebs (A>B) Rock types described in text

CLAY SEAMS:
Gn Greenish-grey
Bn Brown
Mot Mottled Gn & Bn
M Massive texture
D Disseminated salts
S Sylvite visible
C Chevron halite
(3) No. seamlets closely spaced
411 Seam no. (Phillips,1982)
Salts rich in disseminated insolubles

TYPES OF HALITE:
g grey
p pink
o orange
w white
b brown

A, B, D, G TYPES OF SYLVINITE

five below clay seam 408. Thick intervals rich in insolubles separate the tops of major halite beds from potash beds (seams 401/402, 407, and 414, Figs. 4.1, 4.2). Clay seams are also at the bottoms of major salt beds contacting potash beds (seams 416, 414, and 406, Figs. 4.2, 4.1).

Of the 16 major clay seams identified in the Patience Lake Member by Phillips (1982), seven are made up of 2 to 6 separate and distinct clay seams (compare Figs. 4.1 and 4.2, Phillips, pers. comm., 1987). These clay seams are, with the number of separate seams in parentheses: #415 (4-6), #412 (1-2), #411 (1-4), #410 (4-6), #408 (4), #407 (3), and #403 (2). Seam 402 of the Lanigan potash mine is missing at Cory mine (Phillips and Danyluk, pers. comm., 1987). Instead, it may be included with seam 401, which is a 40-60 cm thick clay-rich zone of brown insolubles with disseminated salts and visible sylvite in desiccation cracks (Fig. 4.1). Seams 401/402, 405, 407, 415, and 416 are insoluble-rich layers thicker than 10 cm (Fig. 4.1, Plate 5). The other seams commonly range from 1 to 10 cm thick.

Mottled greenish-grey-and-brown seams are the most common, overall, in the Patience Lake Member (Fig. 4.1). Mottled seams occur in sylvinite, salt anomalies, and at the contacts between halite and sylvinite. Mottled seams may be brown in the middle with green upper and lower contacts or

vice versa. Laterally they may change abruptly from green to brown, have intermixed green and brown parts or be a mixed light brown to green throughout. Brown seams occur in the halite below the Patience Lake Member, and brown is the dominant colour of the seams in the leach anomaly a section through which is at the top 4 m of Fig. 4.1. In general, brown insolubles, whether of a mottled or brown seam, are associated with halite, very low-grade patchy sylvinite, and at the contacts of halite and sylvinite. Red or reddish-brown may be the colour of the unleached 416 clay seam, and red clay may also be present in the top part of the 414 clay, in thin beds above the 416 clay, and in many thin beds below the ore section (McVittie, pers. comm., 1987). Greenish-grey insoluble seams, especially those containing sylvite, rarely occur in halite or at the contacts of halite and sylvinite (Fig. 4.1). Greenish-grey seams are most common in potash beds.

The clay seams have fairly abrupt but wavy contacts with adjacent salts, and commonly have either or both massive insolubles and disseminated salts. Seams with disseminated salts are much more common than massive seams. The tops or bottoms, or both, of some seams may be disseminated or break up into anastomosing thin seams (seamlets) while being more massive to the middle or to one contact. Where there is a clay seam in the potash there is at least 1-2 cm of red potash, A- or D-type, above and below it.

Two green clay seams from the Patience Lake Member were investigated and found to contain a very low density of fossils. Provisionally, the fossils include acritarchs, eg. Navifusa (Nautiyal, 1971), large spores (50-140 microns) with or without spines, and chitinous fragments (chitinozoans and hydrozoan fragments, Cashman, pers. comm., 1988).

Salts within clay seams are most commonly without inclusion patterns, and anhedral. Other halite crystals may have chevron or hopper fluid inclusion textures. Some halite crystals are euhedral.

Fractures in clay seams, commonly filled with pale sylvinite or orange halite fibers perpendicular to the walls, are 0.2 to 6 mm thick and thought to be desiccation cracks. On the surface of the bedding plane they have a polygonal pattern. They have been found mostly in brown and mottled greenish-grey-and-brown clay seams; these include the 416, 414, 412, 407, 405, and 401 seams (Figs. 1.3, 4.1, and 4.2). These are also the thickest and most massive seams of the Patience Lake Member. Other features seen in or below the Patience Lake Member include bedded halite, microkarsts, and chevron halite. The descriptions and origins of these features are discussed later.

4.2 THE REFERENCE SECTION OF THE ORE ZONE

The reference section of the ore zone of the Patience Lake Member, #3&36, is located 1800 m west of the Number 1 shaft at the Cory Mine (Fig. 2.1). Two measured sections within 5 m of each other were combined to produce the reference section. The section is 4.9 m thick and is divided into 6 units according to the main potash rock type(s) present, and the positions of clay seams. These units differ from those used in Langford et al. (1987), and are illustrated in Fig. 4.5 and Plate 6. Plates 6 and 7 show the subtle differences in rock type that were used to subdivide the ore zone into different units. The thicknesses of the units in the reference and other sections are listed in Table 4.1. The reference section of the ore zone extends from the clay seams that define the top of the mining unit, to a 5 cm thick, mottled clay seam that is 4.9 m below it.

Normally, the thickness of the mined zone is 3.3 m, which is governed by the height of the mining machine, and extends down from the top of the 413 seam. Unit M1 is included in the mined units because it is exposed in enough areas to facilitate correlation (Fig. 4.5, Plates 6 and 7).

Units M1, M2, and M6 were determined by the positions of clay seams (Fig. 4.5). The top and bottom units,

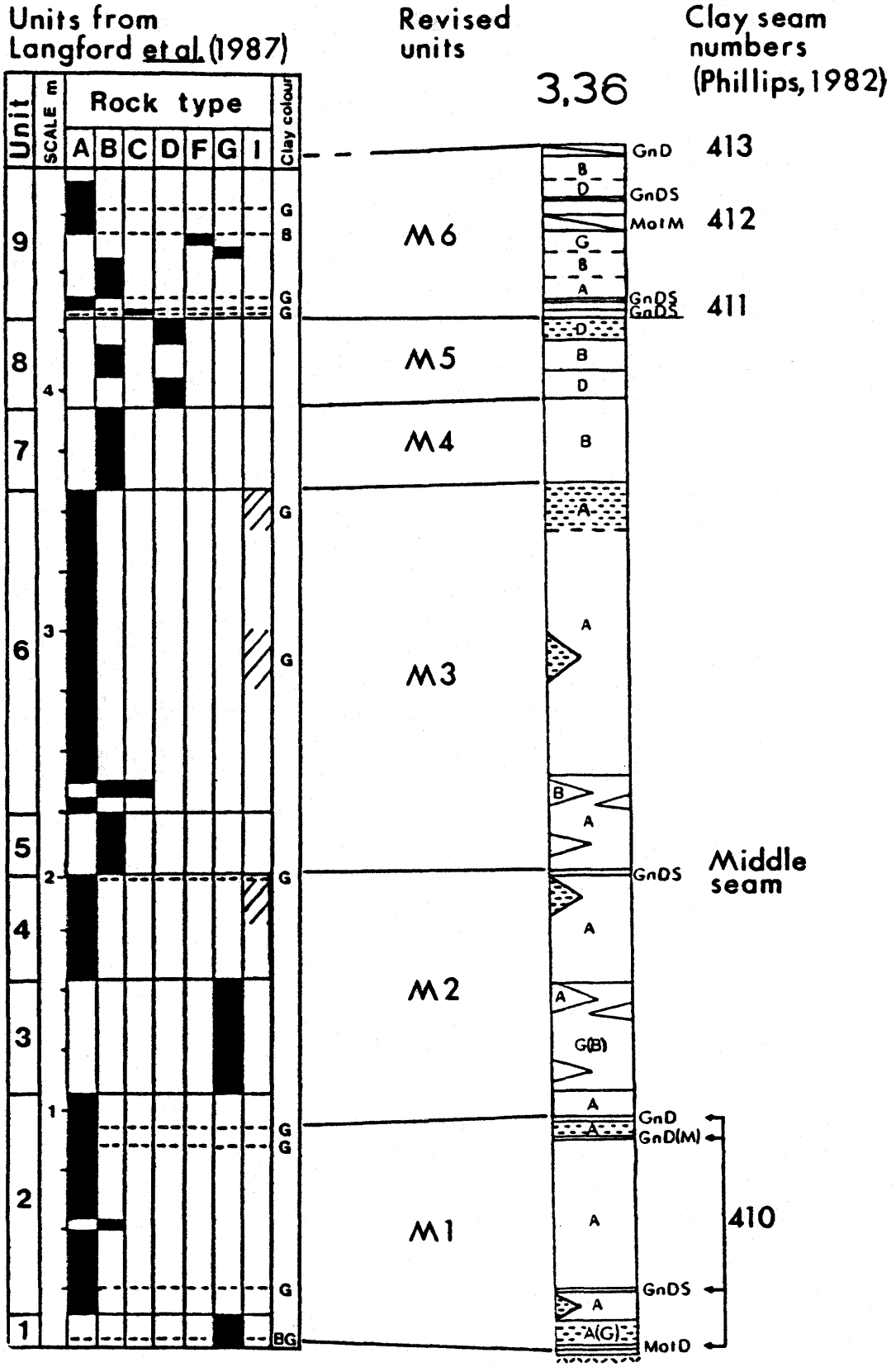

Fig. 4.5 The reference section of the ore zone in PCS Cory showing the units revised from Langford et al. (1987).

UNIT THICKNESSES (cm)

Section number	Unit M1	Unit M2	Unit M3	Unit M4	Unit M5	Unit M6	Sub-unit 1	Sub-unit 2
105			141	34	35	73	21	25
115	84	95	122	23	44	64	22	23
113			167	44	16	64	23	14
114			148	69	27	85	26	24
100	85	99	120	38	21	80	24	26
8		94	131	37	30	59	16	19
3,36	94	100	160	34	33	72	28	24
9			138	45	31			
10			132	56	12	65	17	29
11		90	128	40	48	74	27	19
12		61	128	40	30	78	21	32
13		69	128	30	33			
15		70	143	32	44	66	22	22
102	86	93	140	59	14	54	15	16
101	96	100	145	26	14	68	13	27
103	91	104	156	36	23	73	33	20
94			153	64	17	57	21	11
95			155	70	10	57	17	21
decline	63	103						
Avg.	86	90	141	43	27	68	22	22
Std.	10	14	13	14	11	9	5	5
n=	7	12	18	18	18	16	16	16

Table 4.1. The thicknesses of all the units in the 18 sections in the stratigraphic cross-sections (Figs. 4.5-4.7 in pocket). Sub-unit 1 is between seams 411 and 412, and sub-unit 2 is between seams 412 and 413.

M1 and M6, have a high amount of insolubles and clay seams, and variable but generally low amounts of sylvite. The other units are relatively potash-rich and insoluble-poor. A-type sylvinite is the main rock type in units M1 and M3. A complete potash cycle, of A-type to G(B)-type up into A-type and the Middle clay seam, forms unit M2 (Fig. 4.5). The insoluble profile and the rock types indicate units M3 to M5 may be 3 incomplete potash cycles. Unit M4 is made up of B-type potash, and unit M5 is a mixture of D- and B-types.

4.3 CORRELATION AND VARIABILITY OF THE ORE ZONE

The units defined can be correlated with other sections with variable degrees of success. Three cross sections (Figs. 4.6-4.8 in pocket) of the north, centre, and south of PCS Cory potash mine, show the lithological correlation between the designated reference section and eighteen other sections. The base of the lowest clay seam (#411) of Unit M6 is used as the datum because it is present throughout the mine. The thicknesses for each of the units in these sections are included in Table 4.1. Although there is some variation in the thickness of the units and also in the rock types, the majority of the units can be recognized within a given section and are mappable. Each of the units is

described separately - first giving the general features, then the details of correlation.

Contacts between units are either abrupt over distances of <3 cm, or gradational over distances of 3 to 5 cm. Where they are marked by clay seams, they may be sharp.

The potash cycle, present in unit M2 of the ore zone and several times in the lower Patience Lake Member (Fig. 4.1), is not apparent in units M3-M5 of the ore zone. The top of unit M3 in most of the sections throughout the mine is rich in disseminated insolubles (Figs. 4.6-4.8 in pocket). Had it formed a clay seam, then a potash cycle would be evident from its base to the base of the 411 seam above (see 9.1 SYNDEPOSITIONAL HISTORY).

Disseminated insolubles may also be locally abundant as blebs elsewhere in unit M3 (Fig. 4.7 in pocket, insoluble analyses). The disseminated insolubles are more commonly associated with halite, eg. as 'skins' or inclusions, than with sylvite. A red "sub-clay" unit with fairly abundant insolubles is common beneath the 411 and Middle clay seams of the ore zone. Brown insoluble-rich halite is common 1-2 cm beneath the 412 clay seam.

Wherever the sylvite is red, the rock has higher amounts of greenish-grey insolubles than where it is pale orange. The pale orange to white sylvinite (B type) has less than 3% insolubles. Where there is a clay seam in the potash there is a sub-clay unit of deep red A- or D-type potash. Insoluble seams in the potash, especially greenish-grey seams, commonly have these coronas of red sylvinite both above and below (see previous section on the Patience Lake Member). Blebs of the red sylvinite commonly extend down into paler B type sylvinite (Plate 5). In cross-section these blebs take on a variety of shapes, but the most common are like triangular roots or tornado twisters (Plate 5). The insolubles in the sylvinite are almost always greenish-grey, which is thought to be due to the absence of hematite or to less oxidized iron than in the red or brown insolubles (see Chapter 8).

Unit M1

Part or all of unit M1 has been exposed in 13 of the 18 stratigraphic sections depicted in Figs. 4.6-4.8 (in pocket), and in sections 21, and 22 (Figs. 2.1, 4.1). It includes the clay seams that comprise the 410 seam of Phillips (1982), and all the potash in between (Plate 7). The average thickness of unit M1 in 7 sections is 86 cm (Table 4.1). It may be subdivided into three sub-units: the top set of clay

seams, the middle potash sub-unit, and the bottom set of clay seams (Plate 7, Figs. 4.6-4.8 in pocket).

In the top 30 cm there are 1-3 greenish-grey seams with disseminated salts and visible sylvite. The bottom 2 seams may be thick and mottled greenish-grey-and-brown in some areas. The seams are commonly 1-3 cm thick but may vary up to 8 cm thick. The salts in between are commonly insoluble-rich.

Below the top set of clay seams there is 25-30 cm of primarily A-type sylvinite. In the south of the mine (Fig. 4.7 in pocket), lenses of B-type potash suggest this may have developed into a potash cycle if the insoluble deposition had not been so high.

In the bottom 30-40 cm of unit M1 there are several clay seams closely spaced. The top seam in most sections is greenish-grey. Below this, insoluble-rich A- or D-type potash is followed by 15-25 cm of clay seams. These bottom seams are brown or mottled with disseminated salts. In the north and central parts of the mine (Figs. 4.6, 4.7), there are fewer insolubles in the bottom interval than in the south of the mine (Fig. 4.8).

Unit M2

Unit M2 includes the top of the Middle seam down to the top of the 410 seam (Fig. 4.5). Unit M2 is totally or partially exposed in all the sections studied. It has an average thickness of 90 cm (Table 4.1). This unit represents an entire potash cycle with 10 to 30 cm of A-type potash at the base overlain by 30 to 70 cm of B- or G(B)-type potash up into 10 to 40 cm of A-type again, and finally a clay seam at the top. The Middle clay seam is commonly greenish-grey, with disseminated salts and visible sylvite. It occurs in the middle of the ore zone, and is 2 to 4 cm thick and laterally discontinuous.

Generally, the middle of unit M2 has <1% insolubles, minor iron oxides, and only moderate amounts of sylvite [G(B)-type potash]. The middle of unit M2 may have an unusual layered appearance as in section 100 (Fig. 4.6 in pocket). Above this the amount of insolubles, including iron oxides, increases upwards to the base of the Middle clay seam (Figs. 4.6, 4.8). Unit M2 is unusually thin (60-70 cm) in the south-centre of the mine (sections 12,13,15, Fig. 4.7 in pocket).

Unit M3

Unit M3 is the thickest unit, and the major ore-bearing portion, of the mine zone. The top is marked by insoluble-rich A-type sylvinite, and the base is defined by the top of the Middle clay seam. It is exposed in all the sections measured in the mine. The average thickness of unit M3 is 141 cm (Table 4.1). The thickness is more variable in the north (Fig. 4.6 in pocket) than in the south (Fig. 4.8 in pocket).

In unit M3, the main rock type is A-type sylvinite, with lesser amounts of B- or G-type. The amount of sylvite is generally high, but the amount of insolubles is variable. In some sections, subdivisions of the unit were based on the abundance of B-type sylvinite, and on the modal amount of insolubles. For example in sections 10 and 11 (Fig. 4.7 in pocket) there are large (120X35 cm) blebs of B-type potash. Smaller streaks and blebs of B-type potash are very common. There tend to be sharp contacts between B-type and insoluble-rich A-type sylvinites. Homogeneous A-type potash throughout the entire unit is unusual. Equally uncommon are discontinuous streaks of white sylvinite. Section 101 is unusual because the top of unit M3 is so rich in insolubles that there is a discontinuous greenish-grey clay seam.

Colour-banding, which is a subtle alternation of thin bands (<1-3 cm) of red and pale orange potash (Plate 7), is not an uncommon variation, especially 5 to 40 cm above the Middle clay seam. However, as seen in Plate 7, it is discontinuous, and of ambiguous origin. In some areas the colour-banding may be defined by insolubles that are distributed in parallel lenses and layers.

Unit M3 may represent what were originally 2 incomplete potash cycles. It is generally comprised of 20-40 cm of insoluble-rich A-type potash at the top. About 5 cm above the Middle clay seam at the bottom, there is about 30 cm where B-type potash is abundant. In the middle 60-80 cm of unit M3 there are roughly equal amounts of: insoluble-rich A-type, A-type, and B-type potash. These appear to be evenly spaced in sections 3/36, 10, and 11, indicating a possible primary distribution pattern akin to that of the potash cycle, but with insufficient insolubles to form clay seams (Fig. 4.7 in pocket).

Unit M4

Pale orange, fairly translucent B-type potash defines unit M4. However, the rock types range from A-type with lenses and blebs of B-type (eg. sections 10, 100, 101) to discontinuous B-type and white sylvinite (eg. sections 8, 9,

102). The unit commonly has an abrupt, relatively straight lower contact with unit M3, and a convolute upper contact with unit M5. The average thickness is 43 cm (Table 4.1). Insoluble are typically <2 wt% and the amount of sylvite is high to very high (Figs. 4.7, 4.8 in pocket).

Unit M4 is topographically low in sections 11 and 15 compared to other sections (Fig. 4.7 in pocket). Colour-banding is locally present. The unit is very thin with only minor streaks and lenses of B-type sylvinite in section 101, which is at the bottom of a topographic low.

In some areas (eg. section 113), the salt crystals in parts of unit M4 appear to be elongated parallel to bedding. Samples from unit M4 of section 8 show foliation in shear zones about 2 cm thick. The sylvite is preferentially mylonitized while the halite crystals are considerably larger and randomly oriented.

Unit M5

The red, insoluble-rich, potash below the 411 seam defines unit M5. It is present in all the sections in Figs. 4.6-4.8 (in pocket). The sylvinite rock types are typically a mixture of red A, G, or D-types. The lower contact is commonly convolute; hence the unit thickness is quite variable,

averaging 27 cm (Table 4.1). Blebs or "roots" of the unit commonly extend down into unit M4 (as in Plate 5). Assay values indicate that there is a general decrease in the amount of sylvite, and an increase in the amount of insolubles upward within the unit (Figs. 4.7, 4.8 in pocket). It represents the top of an incomplete potash cycle.

The sylvinite of unit M5 is commonly very distinct; the sylvite crystals are small, dark red, and act as a matrix for large (about 1 cm) halite crystals that commonly have "skins" of greenish-grey insolubles.

In section 95 unit M5 is very thin and its lower contact with sylvite-poor G-type is very irregular and gradational, probably due to partial leaching of sylvite.

Unit M6

Unit M6 is the interval from the top of the 413 seam to the bottom of the 411 seam (Plate 8b). It is partially or completely exposed in all the sections in Figs. 4.6-4.8 (in pocket). The base of the unit is the stratigraphic datum for the sections of the ore zone. The average thickness is 68 cm (Table 4.1).

The 411 clay seam typically consists of a 3-4 cm thick basal seamlet (a "seamlet" is a thin seam <5 cm thick) with 1 to 4 cm of fine-grained A-type sylvinite above, and then one or two thin (0.4-2 cm) seamlets at the top. Seamlets may anastamose, and they vary in thickness. Thick clots of insolubles may join to form the top seamlet(s). The seam is bent up over a horizontal distance of about 40 cm at section 13 (Fig. 4.7 in pocket). The most common rock type consists of greenish-grey disseminated insolubles, with subsidiary massive areas, and visible sylvite. Desiccation cracks were seen in section 114 (Fig. 4.6 in pocket, Plate 8b). Most of the other clay seams contain less sylvite than the 411 seam. Sylvite comes more from layers, lenses and streaks between seamlets, than from the salts disseminated within the seamlets.

Short discontinuities (4-10 cm across) in the seam may have thick disseminated insolubles below that indicate some sort of a dissolving-collapse mechanism, eg. in sections 95 and 101. The colour change from greenish-grey to mottled greenish-grey-and-brown at sections 94 and 95 (Fig. 4.8 in pocket) is an obvious indicator of anomalous ground. There is more brown in the 411 seam of section 95, which is closer to the salt anomaly than in the seam of section 94.

The sub-unit between the 411 and 412 seams is an average of 22 cm thick (Table 4.1). In colouration it

represents a thin potash cycle yet the potash grade decreases upward. Above the B-type sylvinite, between A- or D-types, may be so pale as to be white, and it tends to be discontinuous.

The 412 seam generally has mottled greenish-grey-and-brown insolubles, a massive clay-rich texture, desiccation cracks, and <5% sylvite. Local colour changes to greenish-grey or brown can be very abrupt (within 2 cm). The 412 seam is generally comprised of one uninterrupted thickness of massive insolubles that are more disseminated at the contacts. Halite is dominant within the 1-2 cm contact zones, especially in the lower contact. Desiccation cracks are most common where the seam is thick, mostly brown, and massive (sections 105, 114, 100, 8, 10, 15, and 95). Very fine-grained, red sylvinite commonly fills the cracks; the disseminated salts are mostly halite.

The average thickness of the sub-unit between seams 412 and 413 is 22 cm (Table 4.1). With some exceptions, the ore grade tends to decrease upward. About 5 cm above the 412 seam there is commonly a thin (<1cm) discontinuous Gn DS seamlet. Red sylvinite, A- or G-type, is associated with the insolubles. Lenses of pale B or G-types of sylvinite are common above the thin seamlet. In almost all sections there is a 1-3 cm thick red fringe below the 413 seam.

The 413 seam is generally greenish-grey to grey, somewhat discontinuous, variable in thickness, and has abundant disseminated halite. It is used to guide the upper limit of the mining machine. Brown insolubles are present in the seam at sections 12 and 15 but do not persist for more than 10 m west of section 15 (Fig. 4.6 in pocket). A somewhat peculiar yellow halite is found within the 413 seam at sections 102, and 94.

Chapter 5. THE ANOMALIES

5.1 ANOMALY CLASSIFICATION

Salt anomalies are areas of unusually low ore grade, comprised mostly of halite. They are also known as salt horses, anomalous ground, and barren halite zones. There are three main types of anomalies, which Mackintosh and McVittie (1983) called washouts, leached zones, and collapse zones (Fig. 5.1). Those which can be shown to have resulted from processes operating in the depositional environment, such as washouts, may be termed primary or syngenetic anomalies. Those anomalies which may be linked to much later events, such as most collapse zones, may be called secondary or epigenetic. Unfortunately, because the mining machine is withdrawn rapidly when most anomalies are encountered, exposure is commonly poor, and the origin of many remains ambiguous. Furthermore, some anomalies may be composite, having started to form in the depositional environment, and possibly reactivated in the post-burial environment.

"Washouts are salt-filled V-or U-shaped structures which transect the normal bedded sequence and obliterate the stratigraphy" (Fig. 5.1a, Mackintosh and McVittie, 1983, p. 60). They are commonly several metres across. Baar (1973)

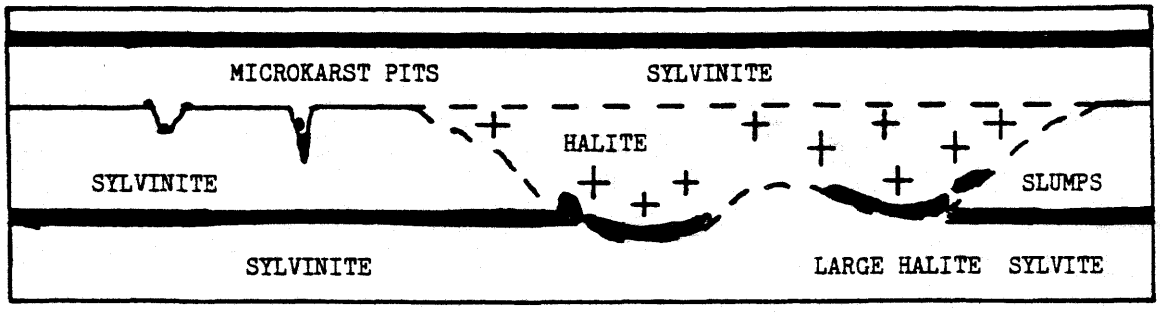

A) WASHOUT ANOMALY

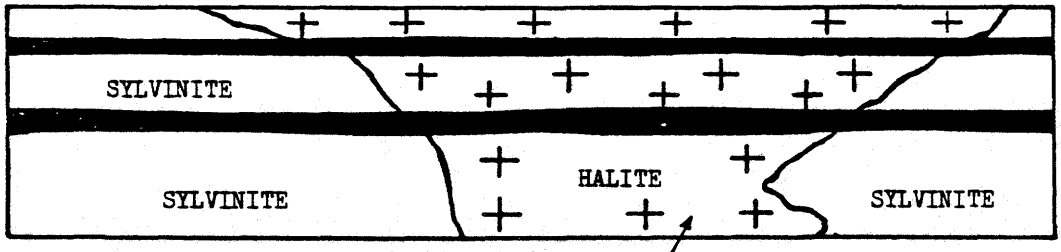

B) LEACH ANOMALY

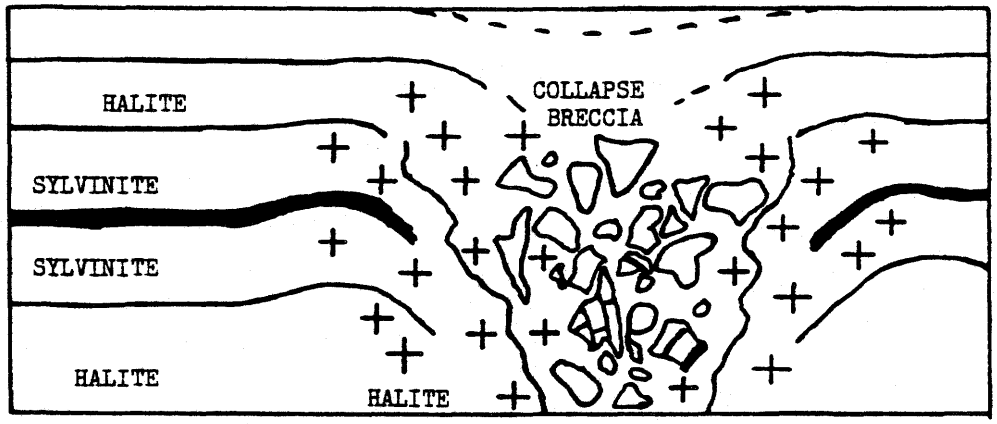

C) COLLAPSE ANOMALY

Fig.5.1 The three main types of salt anomalies (Mackintosh and McVittie, 1983).

noted that these washouts or channels can lead into sinks, and postulated that dissolution by occasional rain storms may have caused these local anomalies.

In leach zones (Fig. 5.1b) the sylvite has been partially or completely replaced without significantly disturbing the normal stratigraphic sequence. Some loss of volume is common. They therefore formed either contemporaneously due to depressions in the ore beds, or by later low-energy percolation of Na-saturated, K-undersaturated brines (Mackintosh and McVittie, 1983; McIntosh and Wardlaw, 1968). The latter method of formation is also likely where they occur on the margins of collapse zones (leach-collapse anomaly).

Collapse zones (Fig. 5.1c) are characterized by a loss of recognizable strata which are replaced by brecciated, recemented, or recrystallized material. In extreme cases, all the salt has been removed and the overlying strata, including the Dawson Bay Formation, have collapsed into the cavity (solution collapse feature). Leached zones commonly separate the collapse zones from normal bedded potash. Collapse structures are commonly found over the edges of Winnipegosis Formation mud-mounds (Gendzwill, 1978, Mackintosh and McVittie, 1983, Wilson, 1985), and are commonly in topographical lows. Some collapse features seem to be related

to faults (Gendzwill, 1987, pers. comm.). The leaching fluids may have come from below or above to form collapse structures anytime after initial deposition.

Of 19 anomalous areas (excluding washout channels) in PCS Cory potash mine, only seven were readily accessible, of which three were studied. Only one washout channel, 6m wide and 2m deep, was observed in PCS Cory (Plate 9f). It includes some of the coarsest sylvite crystals (20 cm^2) observed in the mine. Anomalies in the Central Canada Potash and PCS Lanigan mines were visited, but not examined in detail.

5.2 ANOMALY #1: LARGE LEACH-COLLAPSE ANOMALY

A large leach-collapse anomaly (Anomaly #1) in the southwest of the mine (Section 94 to west of 34B, Fig. 2.1), has received the most attention. It is >300 m from the edge of the anomaly to the major collapse portion west of section 34B (Fig. 5.2 in pocket), but the extent of the anomaly beyond the collapse is unknown. At depth, it is underlain by the margin of a Winnipegosis Formation carbonate mound identified by seismic survey (Danyluk, pers. comm., 1987).

The contact between the ore and leach-collapse anomaly is irregular in plan view (Fig. 5.3), as are the contacts of most other salt anomalies in PCS Cory and

elsewhere (Keyes, 1966, Linn and Adams, 1966, McIntosh and Wardlaw, 1968, Borchert, 1972, Baar, 1974). The contact has an hyperbola-shaped profile that starts off with a shallow dip then drops off rapidly, from a 30 cm drop over 150 m, to 200 cm over 50-100 m, as the centre of the anomaly is approached (Fig. 5.2 in pocket, Fig. 5.3). The sylvinite shows partial dissolution of sylvite where the contact is steep, layered A- and G-type potash in unit M2 of section 44 (Fig. 5.2 in pocket), and pods of G-type potash at the contact (Fig. 5.4 in pocket). It is common to find brown or grey insoluble-rich halite, orange or pink insoluble-poor halite, but not white halite, directly on the anomalous side of the contact (Plate 12b, Figs. 5.2, 5.4 in pocket).

In the leached areas of the leach-collapse anomaly sylvite was removed and partially or completely replaced by halite without significantly disrupting the clay seams (Plate 12b,d). The average thickness between the 411 and Middle clay seams (units M3-M5) is 200 cm in ore and 150 cm in the anomaly, representing a 25% loss of volume (Fig. 5.2 in pocket). However, in unit M2, between the Middle and 410 seams, almost all the sylvite must have been replaced, because there is only a 5% loss of volume when compared to

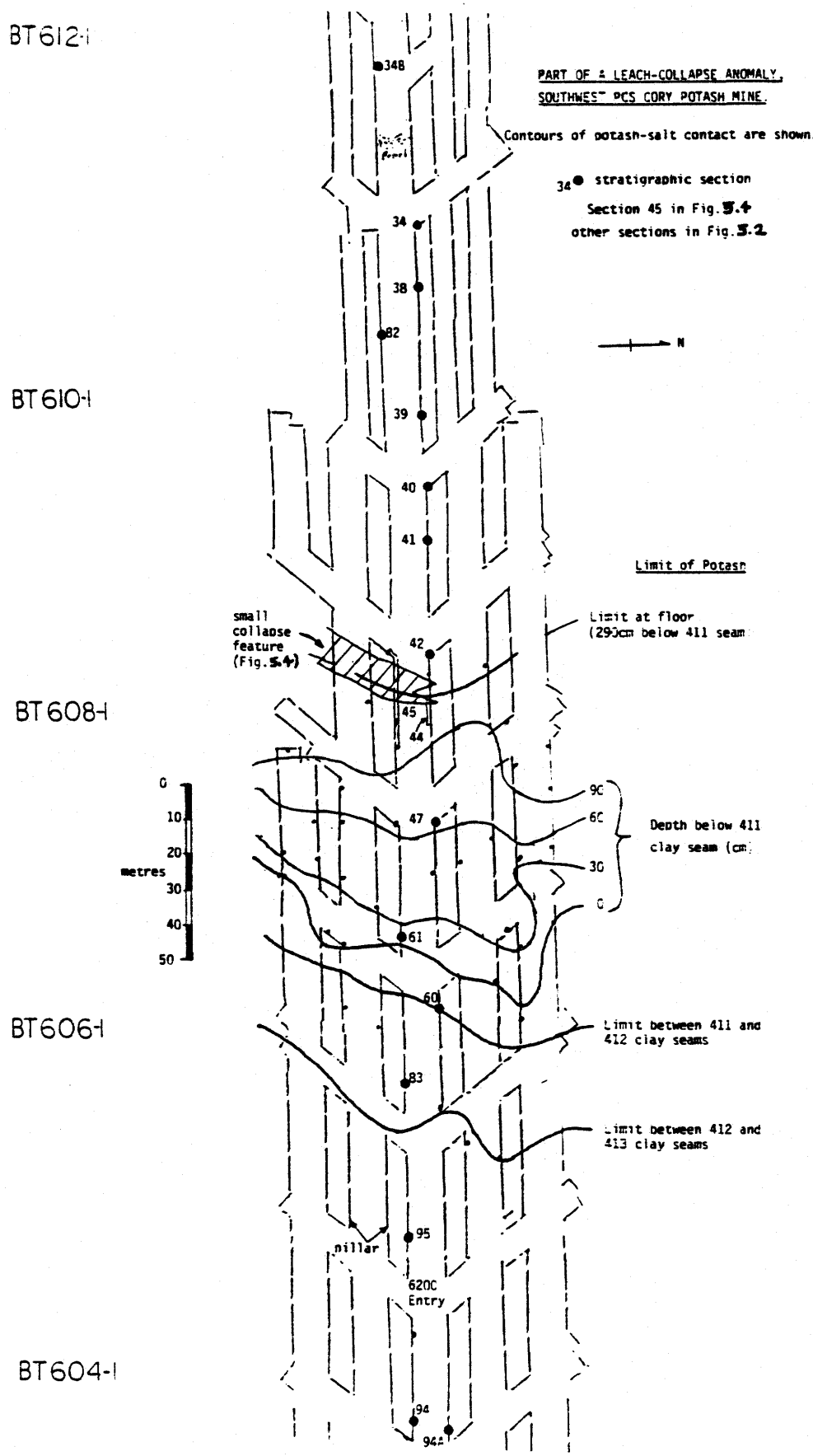

Fig. 5.3 A map of the edge of the leach-collapse salt anomaly in the southwest of PCS Cory (Fig. 2.1). The contours of the potash-salt contact, the locations of the sections in Fig. 5.2, and the location of section 45 the small collapse feature in Fig. 5.4 are shown.

the same unit in local ore, and a 10% gain when compared to the mine average thickness of unit M2. There was also some loss of volume due to sylvite removed from unit M6 between the top three clay seams (Fig. 5.2 in pocket).

The removal of sylvite in units M3-M5 led to local concentration of the insolubles. Generally, bedding is preserved beyond the collapse portions of the anomaly (Fig. 5.3). The top of unit M3 may still be recognized in the anomaly by a high concentration of insolubles in the salt (Fig. 5.2 in pocket). An apparent loss of distinction between units M4 and M5 and the reconcentration of insolubles suggests that insolubles were transported short distances (eg. <10 cm). Insoluble-poor halite above unit M3 suggests that insolubles were not transported upwards.

Within 100 m of the anomaly, the clay rock types changed from greenish-grey to mottled brown-and-green (Plate 12b,d), perhaps by the addition of hematite pigment from dissolved sylvite (Chapter 8, p. 138). Hematite pigment is also present in orange and pink halite, and in brown disseminated insolubles. Orange, pink, and white halite, low in insolubles, remain where there was insoluble-poor pale orange B-type potash in the equivalent ore (Fig. 5.2 in pocket). Grey, and brown halite with abundant disseminated insolubles are the remnants of the more insoluble-rich

sylvinites, A-, D-, and G-types (Fig. 5.2 in pocket, Plate 12d). In some places, local redistribution of insolubles appears to have created fine bedding (Plate 12c,d).

Fine beds of halite are flexed downward in a collapse feature on the inside edge of the leach-collapse anomaly (Figs. 5.2, 5.4 in pocket, Plate 12c). The main collapse portion of the anomaly, west of section 34B (Fig. 2.1), was inaccessible. Small collapsed portions were also observed to have disrupted one or more clay seams (eg. sections 39 and 41, Fig. 5.2 in pocket). As may be seen in Fig. 5.4 (in pocket), collapse features destroy clay seams, salt beds, and redistribute the insolubles. A small bleb or xenolith of red A-type sylvinite with gradational margins survives in the midst of the halite (Fig. 5.4 in pocket, Plate 12c). In other anomalies (e.g. the Colonsay CCP mine), sylvite may locally recrystallize in pods up to several metres across.

Coarse, white, recrystallized halite is common in collapse features. Salt beds within the anomaly may be severelly deformed, stretched and folded, as in a PCS Lanigan leach-collapse anomaly (Plate 13b,c). Stretched clay seams, folded beds, small collapse features (1-20 m), split clay seams with injected salt, and drops in topography (eg.>10 m)

may indicate an impending major collapse portion to a salt anomaly.

The 412 and 411 seams change colour from greenish-grey to mottled greenish-grey-and-brown more than 100 m from the large leach-collapse anomaly in the southwest of the mine (Figs. 4.8, 5.2 in pocket). However, the colour of the Middle seam remains constant (Fig. 5.2 in pocket). In section 95 unit M5 is very thin and its lower contact with sylvite-poor (G-type) potash is very irregular and gradational. These are likely to be the effects of partial leaching of sylvite.

5.3 ANOMALY #2: LARGE LEACH ANOMALY

A large leach anomaly (Anomaly #2) stretches from the #2 shaft to 800 m west of it (Fig. 2.1). An inaccessible collapse portion lies about 700 m west of the shaft. From the #2 shaft to the collapse there is a drop in topography of 28 m. However, the lowest point in the area, another 2 m deeper, lies within normal potash. Other than some stratiform coarse, white, recrystallized halite there are no other indicators of a collapse feature. The halite beds are fairly straight and uninterrupted for tens to hundreds of metres. Therefore, it is uncertain whether the large leach anomaly and the collapse formed at the same time. The collapse breccia includes fragments from the Second Red Bed (Danyluk, pers. comm.,

1988), and therefore, must have formed in the post-burial environment.

The contact between the ore and the leach anomaly is lobate in plan view. The dip of the contact is virtually unchanged to within 150 m of the small, but profound collapse, where exposure is limited. The ore-anomaly contact ranges from 20 to 80 cm below the 411 clay seam; potash is beneath halite (Fig. 4.1). The contact is most commonly sharp, and may be insoluble-rich on the potash side. In some places it is gradational over 20-40 cm, where A- or B-type potash merges with low-grade G-type, adjacent to anomalous halite.

The thickness of halite between the 413 and 414 clay seams does not change significantly from a normal section to the anomaly (Fig. 4.4). Therefore, halite was not removed by the anomaly-producing fluids. The colour-banded halite in this interval of section 19 (Fig. 4.4) is very similar to that in the middle of the Patience Lake Member (Fig. 4.1, Plate 9a) except that minor sylvite has been removed. The colour-bands may be surviving primary features (cf. Dellwig, 1972), even though the two normal sections are not colour-banded in this interval (Fig. 4.4). This, and the survival of chevron halite in section 19 (Fig. 4.4), indicate that the leaching was selective and very delicate. Comparison of sections 24 and 19 to 16 (Fig. 4.4) indicates that the dissolution of sylvite has

removed about 35% of the volume between clay seams 414 and 416. The insolubles have been concentrated primarily in the region of the 415 seam. Brown, rather than greenish-grey, has become the dominant colour of the insolubles.

About 5 m beyond the eastern edge of the anomaly there are large blebs (>200 cm^2) of low-grade G(B)-type potash cross-cutting units M4 and M5 that may have resulted from partial dissolution of sylvite. The 411 clay seam is brown. In the same vicinity, there is secondary halite growth around primary fluid inclusion patterns (Plate 11b), although complete chevrons exist in the anomaly (Fig. 4.4).

5.4 ANOMALY #3: LEACH ANOMALY

In the north of the mine, there is a leach anomaly (Anomaly #3), >300 m in length, between sections 105 and 115 (Fig. 2.1). Several aspects distinguish this leach anomaly from the other two. It is smaller and has no associated collapse feature. In the west, the ore-anomaly contact may be seen above and below the potash (Fig. 5.5). There is red halite (Plate 4a,b) above the contact (section 112, Fig.

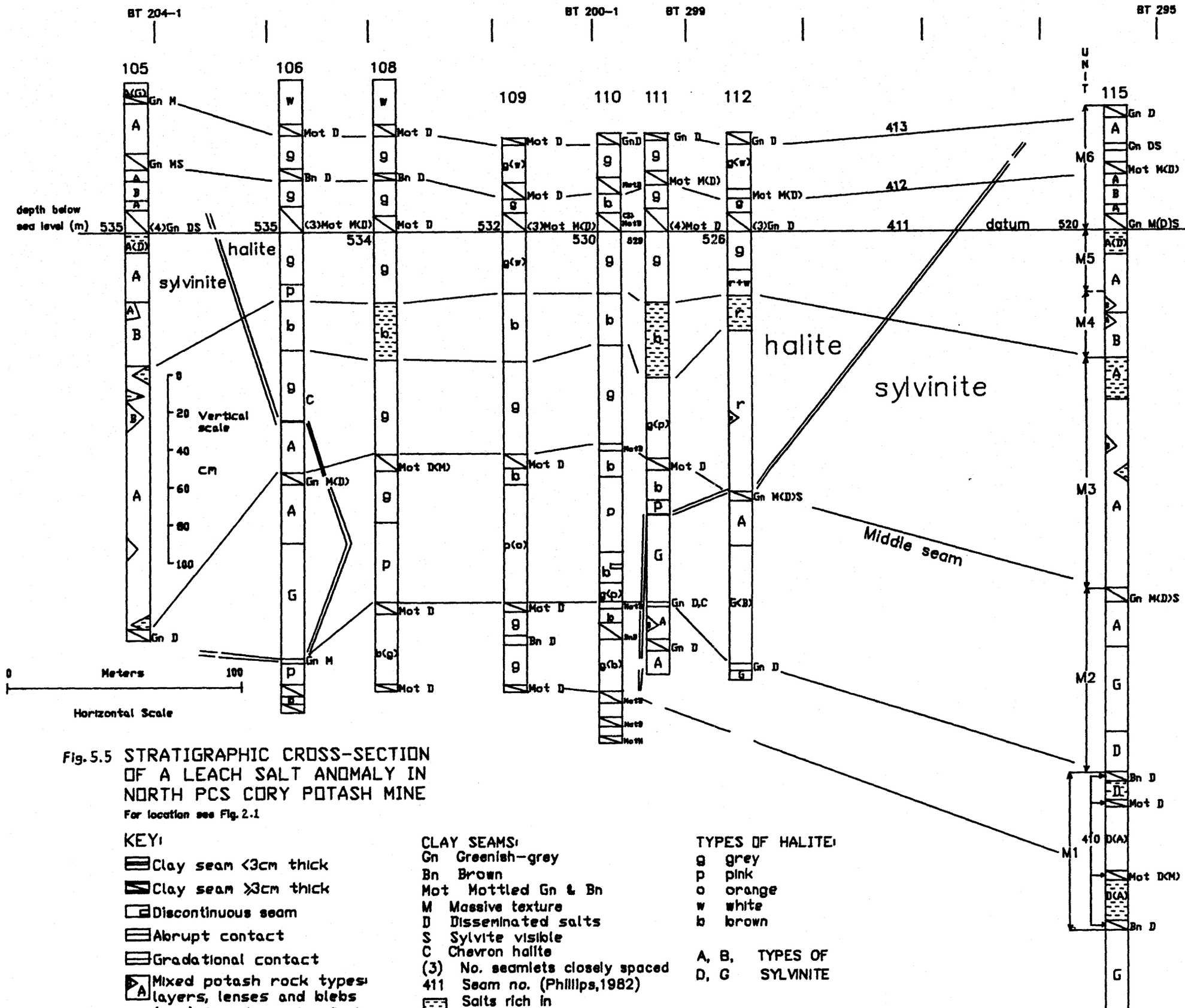

Fig. 5.5 STRATIGRAPHIC CROSS-SECTION OF A LEACH SALT ANOMALY IN NORTH PCS CORY POTASH MINE

For location see Fig. 2.1

KEY:

- Clay seam <3cm thick
- Clay seam >3cm thick
- Discontinuous seam
- Abrupt contact
- Gradational contact
- Mixed potash rock types: layers, lenses and blebs (A>B) Rock types described in text

CLAY SEAMS:
Gn Greenish-grey
Bn Brown
Mot Mottled Gn & Bn
M Massive texture
D Disseminated salts
S Sylvite visible
C Chevron halite
(3) No. seamlets closely spaced
411 Seam no. (Phillips, 1982)
Salts rich in disseminated insolubles

TYPES OF HALITE:
g grey
p pink
o orange
w white
b brown

A, B, D, G TYPES OF SYLVINITE

5.5), and no apparent colour change in the clay seams close to the anomaly.

The contact between the ore and the anomaly may be gradational or abrupt. In section 106 (Fig. 5.5), the top contact is abrupt, the bottom gradational. From section 106 to where the potash is totally removed, the G-type sylvinite has a finely-layered appearance similar to that in unit M2 of section 44 in the leach-collapse anomaly (Fig. 5.2 in pocket). G-type (low grade) sylvinite is also on the ore side of the contact in section 111 (Fig. 5.5).

An average thickness from the Middle seam to the 411 seam (units M3-M5) of 120 cm compared to 200 cm in ore, indicates a 40% net loss of volume. In unit M2 of the anomaly there is only a 10% loss in volume due to more complete replacement of dissolved sylvite by halite. As in the other anomalies, the insolubles have been concentrated locally in thin lenses and blebs that may reflect the original bedding. For example, brown insoluble-rich halite marks the top of unit M3 (Fig. 5.5). Insoluble-poor pink or orange halite in the middle of unit M2 remains after the dissolution of B- or pale orange G-type potash. Chevron halites, just above the ore-anomaly contact in section 106 (Fig. 5.5), have survived leaching.

As in other anomalies, hematite pigment may have been transfered from dissolved sylvite to insolubles rendering most clay seams brown or mottled greenish-grey-and-brown. The beds of red halite (section 112, Fig. 5.5) strongly resemble sylvinite, and the disseminated insolubles remain greenish-grey. The hematite is concentrated in the outer parts of small anhedral, interstitial halite crystals (Plate 4b). White and grey halite are virtually hematite-free. Brown halite derives its colour from the insolubles that were likely enriched by hematite.

5.5 SUMMARY OF OBSERVATIONS

The three salt anomalies studied in PCS Cory have several features in common. Sylvite was dissolved and, in leached areas, the remaining salt beds reflect the ore bedding. Hematite pigment from red sylvite has changed the colour of insolubles from greenish-grey to brown or mottled greenish-grey-and-brown. These colour changes may also occur in clay seams in ore close to the anomaly. The halite colour changed from white and clear to red, orange, or pink. Halite in salt anomalies tends to be less cloudy and coarser than halite from the ore zone. The effects of leaching decrease from the interior of the anomalies to their edges, where chevron halite is more apt to be preserved (Chipley, pers. comm., 1988) and less hematite has been removed. The effects

of leaching range from weak to strong, from selectively preserving delicate laminae and chevron textures to destroying and, indirectly, deforming salt beds. Close to anomalies #1 and #2 unusual blebs of sylvite-poor G-type potash were found to have replaced or cross-cut normal ore units.

The amount of volume reduction, due to incomplete replacement of dissolved sylvite by halite, changes significantly from one anomaly to another, and even from one unit to another. In the ore-level anomalies, #1 and #2, the maximum volume reductions of 35 and 40% are in units that overlie unit M2, which has only 10% or less volume reduction. Stratigraphically lower units show a higher degree of replacement of sylvite by halite than do overlying units. It is poorly understood how the overlying beds were prevented from collapsing. Perhaps the removal of sylvite was slow enough to allow for constant, slow readjustment of overlying beds to changes in volume.

The contacts between ore and anomaly are abrupt in the large leach-collapse anomaly, mostly abrupt in the leach anomaly, and mostly gradational in the small leach anomaly. Three contact profiles - hyperbolic, flat, and tapering - were observed. Red halite was found only in the small leach anomaly. Collapse features are abundant and of varied sizes in the leach-collapse anomaly. There was only one, deep collapse

feature, small in area, in the large leach anomaly. Stretched clay seams, folded beds, small collapse features (1-20 m), split clay seams with injected salt, and drops in topography (eg.>10 m) indicate an impending major collapse portion to a salt anomaly (Coode, pers. comm., 1988).

Chapter 6. PRIMARY AND SECONDARY FEATURES OF THE PRAIRIE EVAPORITE FORMATION

6.1 PRIMARY SEDIMENTARY FEATURES

Primary (or syndepositional) features are those that formed in the depositional environment and include penecontemporaneous features. By depositional Hardie et al. (1985, p.12) mean "formed at the time of deposition of a sedimentation unit or deposited in its existing form" and by penecontemporaneous they mean "post-depositional but pre-burial, i.e. formed diagenetically soon after deposition by processes controlled by the existing depositional environment". "Feature" may include a mineral, mineral assemblage, texture, fabric, fluid inclusion or structure (Hardie et al., 1985).

Many of the sedimentary features preserved in the Prairie Evaporite Formation, including desiccation polygons and chevron halite crystals, can be explained within the framework of the saline pan cycle of Lowenstein and Hardie (1985). The saline pan cycle relates primary depositional features to three stages of sedimentation in a closed evaporite basin: flooding, evaporative concentration, and desiccation (Fig. 6.1). During the flooding stage, there is dissolution of the pre-existing saline crust followed by

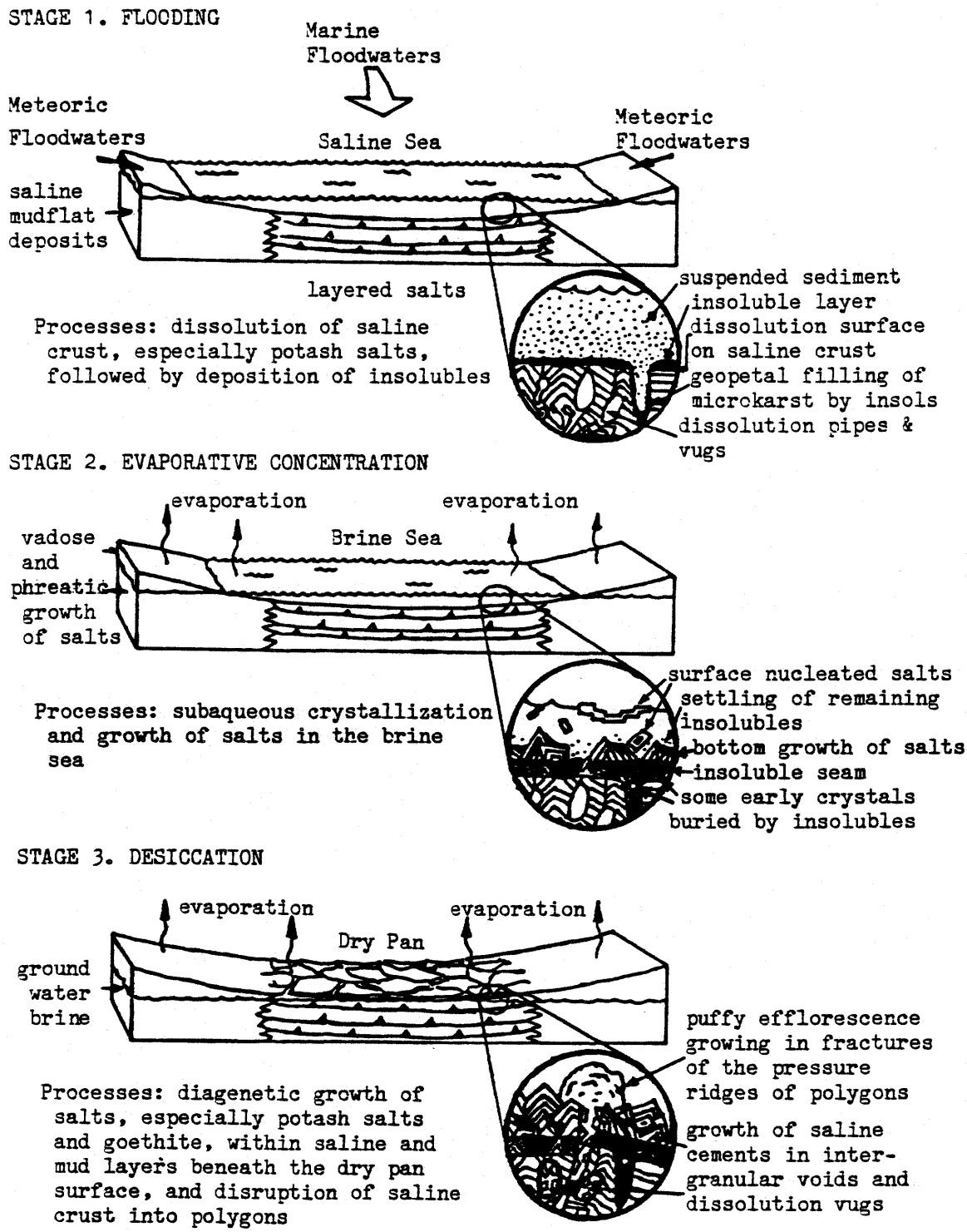

Fig.6.1 The basic elements of the saline pan cycle (modified after Lowenstein and Hardie, 1985).

deposition of insolubles. During the second stage, evaporative concentration leads to subaqueous crystallization and growth of salts. Continued evaporation leads to subaerial exposure of the salt surface in the third stage. During exposure, salt crystallization continues in the residual brine beneath the newly formed crust, which is broken into polygons (Fig. 6.1).

Bedding

The largest depositional feature in the Patience Lake Member is bedding. Clay seams and individual potash units have
been traced for up to a hundred or more kilometres (Phillips, 1982). However, because the potash itself may have formed or recrystallized in the post-burial environment, the bedding as seen in exposure and core, may be a reconstituted primary feature.

Clay seams are present at most of the potash-halite contacts in the Patience Lake Member (seams 401/402, 406, 407, 409, 413, and 414, Figs. 4.1, 4.2 in pocket). In the Patience Lake Member (Fig. 4.1) thicker, denser clay seams are more commonly found beneath potash beds than beneath halite beds (compare seams 401/402, 407, 414, to seams 406, 413, Fig. 4.1). Two exceptions to this are seams 416, which is very thick and overlies potash beds (Fig. 4.4), and seam 409, which

is thin and marks the beginning of a gradual increase in salinity from halite to G-type sylvinite (Fig. 4.1). In two occurences halite overlies sylvinite without significant intervening insolubles (below clay seam 408, and above the Allan Marker Bed, Fig. 4.1).

Very fine (0.3-5 cm), straight bedding, similar to that in the Retsof salt mine in New York (Dellwig, 1972), is present about 5 m below the ore zone in PCS Cory potash mine (Plate 9a.). The sample shown in Plate 9b is from the section shown in Plate 9a. It shows what seems to be a layer of cloudy (inclusion-rich) halites with minor sylvite underlain by a layer of clear, inclusion-poor, halite also with minor sylvite. The colour-banded halite is a combination of layers that are variously: insoluble-rich (anhydrite partings); cloudy and white, due to abundant fluid inclusions; relatively clear of fluid inclusions; and, relatively rich in red sylvite (<5%).

Bedding within sylvinite is rarely as clearly defined as in colour-banded halite. Although the beds in the potash cycle probably reflect primary conditions, their origin is ambiguous because no modern analogues exist for comparison.

Desiccation polygons

Desiccation polygons are metre-scale disruptions in bedding that are polygonally shaped in plan view (Hardie et al., 1985, Lowenstein and Hardie, 1985). The cracks which separate the polygons are commonly downward tapering in section. In the PCS Cory mine, some were recognized above the ore zone in the large leach anomaly by the disruption of clay seams, in the form of small (10 cm wide) but, in places, deep (eg. 1 m) V-shaped cracks. The cracks began (about 6 cm wide) at the clay seam and continued down through several insoluble-rich layers, terminating in insoluble-rich halite. However, nowhere are they so obvious as in the orange halite about 2.5 m above the 416 clay seam at the Cominco mine (Plate 9c, Mackintosh, person. commun., 1986; and Meijer Drees, 1986). At this site, the margins between the polygons (4-10 cm wide) contain red sylvite, and tend to be more insoluble-rich than the rest of the salt. At Cominco, they have also been found in the ore zone, about one metre above the ore zone, about 50 m below the ore zone, and they seem to be of different varieties or different states of preservation (Mackintosh, pers. comm., 1989). They most commonly originate from a clay seam.

Desiccation cracks

Desiccation cracks form an interconnecting mosaic in clay seams as seen in Plate 9d (photographed in the CCP Colonsay, Saskatchewan potash mine). Although they are shaped like irregular polygons in plan view, they are much smaller than desiccation polygons, and they are confined to clay seams. The size of the cracks ranges from 0.4 mm to 10 mm or more in width, and up to 10 cm or more in length (Plate 9d). Their orientation is sub-vertical. These cracks are common in clay seams of most of the potash mines. In PCS Cory, they have been found mostly in brown and mottled greenish-grey-and-brown clay seams (Figs. 1.3, and 4.4). These are the thickest and most massive seams of the Patience Lake Member. Desiccation cracks are generally filled with pink salts that, except in salt anomalies, tend to be sylvite-rich.

Microkarst pits and washout channels

A channel-shaped feature (Plate 9d), approximately 1X3 m, just 1 m north of section 12 (Fig. 4.7 in pocket) appears to be a washout channel. Disseminated insolubles are thickly concentrated between, and below, two very coarse, white salt bodies which are flat-topped and convex on the bottom (Plate 9d). Beds are not disturbed over 2 m above the white salts (Plate 9d).

Microkarst pits were described by Hovorka (1987) as being "vertical dissolution features" that cut across anhydrite partings and primary fabrics in halite. They are shaped like an irregular cylinder, circular in plan view, and are 1-10 cm wide and up to 2 m in length (Hovorka, 1987). Similar features are present in the colour-banded halite above the Allan Marker bed (Plate 9e.). They are microkarst pits up to 40 cm long and 10 cm wide, with a characteristic enrichement of insolubles. Root-like blebs of red sylvinite that extend down into pale orange sylvinite (Plate 5) have a similar appearance to the microkarst pits in the colour-banded halite, without the cross-cut anhydrite parting. These have been found in the potash of the lower Patience Lake Member, and in units M5-M4 of the ore zone.

Chevron texture and primary fluid inclusions

Fluid inclusions concentrated in growth zones of halite crystals, form a chevron texture (Roedder, 1984, Lowenstein and Hardie, 1985). Plate 10 a and c shows chevron-textured halite crystals from the Patience Lake Member. Although chevron-textured halite is not uncommon in the potash ore zone (Chipley, pers. comm., 1988), it is rarely as large and well-preserved as the sample in Plate 10a, which comes from between the upper and lower sets in the 410 clay seam (Fig. 4.7 in pocket). Chevron-textured halite has been

observed in cores of the Patience Lake Member and tends to be common in the disseminated parts of some insoluble seams (Utha-aroon, pers. comm., 1987). Plate 10c shows the relationship between insolubles and chevron halites. Chevron-textured halite is more common in ore than in anomalies, and more common at the margins of anomalies than towards their centres (Chipley, pers. comm., 1988). In most cases, the chevrons point upward. Wardlaw and Schwerdtner (1966) found abundant "chevron crystals conspicuously elongated perpendicular to bedding" in the lower half of the Prairie Evaporite Formation.

Plate 11b shows fluid inclusions along cubic growth zones (hopper texture) in the centre of a halite crystal. The rest of the crystal is made up of relatively clear halite. The sample was taken from near the top of the ore zone. Similar overgrowths around primary fluid inclusion patterns were observed in samples from anomalies. Growth zones in sylvite are suggested by the pattern of hematite inclusions in Plate 11a.

Ripple marks in anhydrite interbeds were observed above the White Bear Member of the Prairie Evaporite Formation at Cominco's Vanscoy potash mine (Meijer Drees, 1986), but were not observed at either the PCS or CCP mines.

6.2 SECONDARY FEATURES

The criteria that identify post-burial features are textures and structures that record the disruption, deformation, and destruction of primary features, along with mineral assemblages and fluid inclusion data that indicate elevated temperatures and pressures. Hardie et al. (1985) prefer the term "post-burial" to "secondary" because these features are "formed by late diagenetic or metamorphic-metasomatic processes controlled by the subsurface burial environment". However, "secondary" is a more widely accepted term.

Secondary features in the Prairie Evaporite Formation range in size from the large "no-salt" area in southeastern Saskatchewan (Fig. 1.1) to the mineralogy of the insolubles. There is abundant structural, petrographic, and geochemical evidence for the secondary dissolution, recrystallization, and deformation of much of the salts of the Prairie Evaporite Formation (Clark, 1964; Schwerdtner, 1964; Wardlaw and Schwerdtner, 1966; McIntosh and Wardlaw, 1968; Wardlaw, 1968; Holter, 1969; Fuzesy, 1983; and Baadsgaard, 1986; Chipley and Kyser, 1989).

Many features associated with salt anomalies are secondary. Collapsed and deformed beds are the most obvious

examples. Elongated salt beds are manifested in a stretched clay seam near the edge of a PCS Lanigan leach-collapse anomaly (Plate 13b). Large folds in the salt strata may be found on the approach to the collapse portion of a leach-collapse salt anomaly. Close to the collapsed centre of a PCS Lanigan salt anomaly, the beds develop higher angles of dip (Plate 13c.). Other secondary features associated with salt anomalies include: small collapse features (1-20m, Plate 12a,c, Figs. 5.2-5.4 in pocket), split clay seams with injected salt, and drops in elevation of bedding planes greater than 10 m (Coode, pers. comm., 1988). Commonly associated with collapse features are large crystals of recrystallized halite that transect bedding. The hematite from dissolved sylvite causes halite to become orange or red (Plate 4a,b), and may also occur in leach anomalies of unknown origin. Secondary anhydrite was found in the halite of a secondary leach-collapse salt anomaly (p. 122).

Mylonitized sylvinite is most common along clay seams of the ore zone. It is also common in areas of high stress where salts have moved to fill in old mine openings (Mackintosh, pers. comm., 1987). Most of the mylonites have formed within the last 10 to 20 years.

6.3 AMBIGUOUS FEATURES

Features that may be either syndepositional (primary) or post-burial (secondary) are termed "ambiguous" (Hardie et al., 1985). A common and unique feature of the Patience Lake Member, the abundant sylvite, is the most ambiguous in origin. Very little is known of the form of primary natural sylvite, or even if it is primary and not derived from carnallite as suggested by Wardlaw (1968). The only modern natural potash deposit, in northern China, is still only poorly understood (Yuan et al., 1985).

In the Patience Lake Member, the potash beds are not as fine as colour-banded halite (tens of cm vs. 0.3-10 cm, Figs. 4.1, 4.6-4.8 in pocket, Plates 5-7). The beds in the ore zone and the potash cycles are defined by significant changes in the different types of sylvinite (where not defined by the clay seams). Units M3-M5 in the main part of the ore zone are distinguishable throughout the mine, yet they change significantly in thickness and in the distribution of their main rock types. For example, blebs of A-type potash extend down from unit M5 into unit M4 (Fig. 4.6 in pocket), and the same features are seen in the potash cycles below the ore zone (Plate 5). The main differences between the four potash rock types (Table 2.1) are in the amounts of insolubles, sylvite, and iron oxides, and in the distribution of the iron oxides.

The amount of sylvite in G-type is lower than in the other potash types. G-type potash is found in the regular bedded sequence, such as above seam 409, in seam 408 (Fig. 4.1), and in halite beds that have some sylvite (below the Patience Lake Member, Fig. 4.1, and below seam 414, Fig. 4.4). It is also associated with anomalies, such as at a salt anomaly contact (centre of Fig. 5.4). The red hematite-rich A-type sylvinite is associated with higher amounts of insolubles than B-type sylvinite. The iron oxides are concentrated to thin outer margins of sylvite crystals in D-type potash as opposed to thick margins in A-type. D-type sylvinite is associated within, underneath, and close to insoluble seams.

The thin halite films that interconnect separate halite crystals form a matrix for the sylvite crystals (Plates 1a, 10a,b, 11c,d). They are very common in A-type sylvinite, but harder to see in B- and D-types. There are other features that indicate sylvite grew after halite. Fluid inclusion patterns in halite (Plate 11c) are cross-cut by an extension of sylvite. Most insolubles seem to have been pushed aside by growing sylvites (Plates 10a, 11d). Hematite sutures mark where sylvites would have joined, in some cases trapping other insolubles (Plate 11c,d). Hematite inclusions could have bridged the halite between growing sylvite crystals (Plate 11c). Although these features may indicate a relative timing,

their origin in the primary or secondary environments is ambiguous.

Other features, such as halite overgrowths and euhedral anhydrite laths (Plates 11b and 13a respectively), may have formed equally in the primary or secondary environments. Some leach anomalies, and the leach portion of the large anomaly in the vicinity of the #2 shaft, PCS Cory are ambiguous. Even the causes of collapse features, features which are obviously secondary, may have had origins, perhaps fault-controlled, in the primary environment.

Chapter 7. INSOLUBLE MINERALOGY

7.1 THE INSOLUBLE MINERALS

The insoluble minerals found in the PCS Cory samples of this study are, in approximate order of decreasing abundance: dolomite, clays [illite, chlorite (including swelling-chlorite/chlorite), and septechlorite], quartz, anhydrite, hematite, and goethite. This is similar to the findings of Mossman et al. (1982). The minerals not found in this study, but common in other studies of salt deposits (Table 7.1), include: magnesite, euhedral quartz, feldspar, smectite or mixed-layer chlorite/smectite, and minor talc. The results for samples from PCS Cory results are listed in Tables 7.2 and 7.3, and shown diagrammatically in Figures 7.1-7.3.

The results of the 23 samples analysed from Central Canada Potash (CCP) are listed in Table 7.4. Dolomite, quartz, chlorite, and illite, as identified from bulk-insoluble samples only (i.e. no HCl treatment or centrifuging), are present in all samples. Anhydrite is present in 19 of the samples. Although the CCP samples were analysed separately from the PCS Cory samples, the methods used were the same except that the <2 micron fraction was not analysed in the CCP samples. Identifying septechlorite and swelling chlorite was

impractical with bulk-insoluble samples; glycolated samples proved to be inconclusive.

Figures 3.2, 3.3, and 7.4 show typical X-ray spectra for the <2 micron fraction (clays) air dried, <2 micron fraction glycolated, and total insolubles, respectively. PCS Cory sample 40.7 was chosen because it has a high amount of anhydrite (Fig. 7.4). The difference between the glycolated and the air-dried samples (expansion of 14 Å peak to 16-17 Å) is typical of all the samples analysed, and is an indicator of the presence of swelling chlorite (Brown and Brindley, 1980). Both hematite and goethite are abundant, as indicated by the large peaks at 2.70 Å and 4.18 Å respectively, in sample CY 3.7 (Fig. 3.2).

Dolomite

Dolomite [$CaMg(CO_3)_2$] is probably the most abundant mineral in all the samples analysed. In the normal ore zone (PCS Cory), dolomite averages about 42% of the insolubles but in the anomalous ore zone it averages about 35% (Tables 7.2, 7.3). Where the amount of dolomite is very high (e.g. samples 16.21, 16.17, 36.9, and 40.6), there is <1% anhydrite. In both sections, anomalous and normal, there is slightly more dolomite (2-4%) in the insolubles of the clay seams than in the insolubles of the salts. The amounts

SALT DEPOSIT	INSOLUBLE MINERALS IN COMMON WITH THIS STUDY	MINERALS PRESENT BUT NOT FOUND IN THIS STUDY	REFERENCES
upper Prairie Evaporite Formation	dolomite, quartz, illite, chlorite, septechlorite, corrensite (swelling chlorite), hematite, goethite, anhydrite, spores and microfossils	smectite, mixed-layer chlorite/ smectite, vermiculite, minor sepiolite, gypsum, potassium feldspar, hydrocarbons	Droste (1963), Wardlaw (1968), McIntosh and Wardlaw (1968), Holter (1969), Mossman et al. (1982), Fuzesy, (1983) Nautiyal, (1975)
Permian Zechstein Formation (Europe)	minor dolomite, quartz, chlorite, muscovite (illite), amesite (septe-chlorite), corrensite (swelling chlorite), hematite, anhydrite	magnesite, talc, euhedral pyrite, potassium feldspar, organic material	Braitsch (1971)
Permian Salado Formation (New Mexico)	quartz, chlorite, amesite (septe-chlorite), muscovite (illite), corrensite (swelling chlorite), minor hematite and anhydrite	magnesite, minor talc, authigenic quartz, low-charge and high-charge corrensite	Jones (1972), Harville and Fritz (1986)
Permian San Andres Formation (north Texas)	dolomite, quartz, illite, chlorite, chlorite/swelling chlorite, 7Å serpentine-group mineral (septe-chlorite?), anhydrite	mixed-layer chlorite/smectite, chlorite/ vermiculite, saponite, mica, feldspar, opaque minerals	Hovorka (1987) Fisher (1988)
Upper Silurian Salina Group (north-east States and south Ontario)	dolomite, quartz, illite, chlorite, expanding chlorite (swelling chlorite) anhydrite	serpentine, talc, euhedral quartz and pyrite, potassium feldspar	Lounsbury (1963), Dellwig and Evans (1969), Bodine and Standaert (1977)

Table 7.1. Comparison of the insoluble minerals found in this study with those found in four major evaporite salt deposits.

Key to Tables 7.2 and 7.3, and Figures 7.1, 7.2, 7.3.

A, B, D, and G are potash rock types (Langford et al., 1987). Clay rock types, from Boys et al. (1986), are summarized: Gn. = greenish-grey, Bn. = brown, Mot. = mottled Gn. and Bn., M = massive insolubles, D = disseminated salts, S = obvious sylvite, "clay" means insolubles. The insoluble portion is % insols. Insols. = insolubles, m. = moderate, o = orange, g. = greyish, v. = very, l. = light, and pink. = pinkish. Compare Insols. colour to Hematite - goethite, and to Rock type. XRD minerals are in approximately decreasing abundance (from XRD analysis of total insolubles): D = dolomite, A = anhydrite, Q = quartz, I = illite, Ch = chlorites. % Dol & Anhyd. is the HCl-soluble portion of the insolubles. This is divided into % Dolom. and % Anhy. based on an estimate of % anhydrite using XRD on a spiked sample that was subsequently used as a standard for comparison with the remaining samples. Of the clay minerals, which are about 1/3 of the insolubles, illite, chlorite (includes swelling chlorite), and septechlorite make up about 99 per cent. Therefore the Il:Chl:SChl ratio closely represents the total percentage of the clay minerals.

Sample number	Seam number	Rock type	% Sylvite	% Insols.	Insols. colour	Hematite, goethite (h+>h>h-)	XRD minerals	% Dol & anhyd.	% Dolom.	% Anhy.	Il:Chl:SChl
16.21		D	62	6.5	m.o.pink	g-, h+	D,Q,(A)	51	50	1	40:32:28
16.17	415	Gn. M-S clay	22	26.6	g.o.pink	h-	D,Q	55	55	0	40:27:33
16.14	415	Gn. D(M) clay	5.9	14.2	pink.grey	nil	D,Q,A	46	41	5	40:31:29
16.11	415	Mot D(M)S clay	16	22.8	v.l.brown	h	Q,A,D	47	32	15	37:24:39
16.5	414	Mot. M(D) clay	1.9	36	v.l.brown	h-	D,A,Q	51	46	5	45:28:27
3.22	412	Bn. M clay	5.8	33	v.l.brown	h	D,Q	46	46	0	42:28:30
3.21		G	8.5	10.8	v.l.brown	h-	D,Q,A	47	40	7	34:23:43
3.17	411	Gn. D-S clay	55	15	pale red	h+	D-Q	39	39	0	49:31:20
3.16		D	21	5.9	pale red	g-, h+	D,Q,A	44	40	4	52:37:11
3.9		A	62	14.6	m.o.pink	g-, h	D,Q	42	42	0	53:32:15
3.7		A	78	3.3	m.o.pink	g+, h	D,Q	40	40	0	54:31:15
3.5		A (clay rich)	54	20.7	g.o.pink	g-, h	D,Q	41	41	0	48:39:13
3.2		A	62	5.6	m.o.pink	g+, h	D,Q	44	44	0	54:31:15
3.19		B	47	2.7	m.o.pink	g+, h	D,Q	42	42	0	51:28:21
36.9	Middle	Gn. D-S clay	9.8	21.8	g.o.pink	h-	D>Q	51	51	0	48:29:23
36.4	410 (top)	Gn. D clay	1.7	20.7	pink.grey	nil	D,A,Q	45	40	5	46:19:35
36.10	410	Mot. D clay	0.8	11.9	l.brown	h+	D,Q,A	45	39	6	55:30:15
Average above ore zone (n=5)			22	21				50	45	5	40:28:31
Standard deviation (n=5)			21	10				3	8	5	3:3:4
Average of ore zone(n=11)			37	14				44	42	1	40:30:22
Standard deviation (n=11)			26	9				3	3	2	6:5:10
Avg of ore zone clays (n=4)			10	23				45	44	1	46:27:27
StD of ore zone clays (n=4)			22	7				4	5	2	3:5:6
Avg of ore zone salts (n=7)			48	9				43	41	2	49:32:19
StD of ore zone salts (n=7)			23	6				2	1	3	7:5:10
Avg of clay seams		(n=9)	15	22				47	43	4	46:28:27
StD		(n=9)	17	8				4	7	5	5:4:6
Avg of salts		(n=8)	49	9				44	42	2	47:31:22
StD		(n=8)	22	6				3	3	2	7:5:11

Table 7.2. Analyses of samples from the reference section of the ore zone and above, a composite of sections 16, 3, and 36. Presented in stratigraphic order; samples 3.22 to 36.4 comprise the ore zone (Fig. 7.2). Refer to Key on p. 74.

Sample number	Seam number	Rock type	% Insols.	Insols. colour	Hematite, goethite (h+>h>h-)	XRD minerals	% Dol & anhyd.	% Dolom.	% Anhy.	Il:Chl:SChl
40.1	413	Mot. D clay	10.1	l. grey	nil	D,A,Q,Ch,I	46	38	8	54:21:25
40.4	412	Mot. M clay	43	l.brown	h+	D,A,Q,Ch,I	51	36	15	53:24:23
40.5		Hal. orange	4.9	v.l.brown	h	D,A,Q,Ch,I	42	32	10	54:27:19
40.6	411	Mot. M(D clay	53	v.l.brown	h-	D,Q,Ch,I	43	43	0	47:24:29
40.7		Hal. brown	7.2	v.l.brown	h	A,D,Q,I,Ch	57	37	20	50:23:27
40.10		Hal. orange	23.2	v.l.brown	nil	D,A,Q,Ch,I	44	29	15	63:27:10
40.12	Middle	Mot. M(D clay	19.5	v.l.brown	h	D,Q,A,I,Ch	42	37	5	48:23:29
40.13		Hal. brown	3.6	l.brown	h+	D,A,I,Q,Ch	47	32	15	56:25:19
40.16	410 (top)	Mot. D clay	8	v.l.brown	h	D,A,Q,I,Ch	38	32	6	56:23:21
Averages (Avg)		(n=9)	19				46	35	10	53:24:22
Standard deviation (StD)		(n=9)	17				5	4	6	5:2:6
Avg of clay seams		(n=5)	27				44	37	7	52:23:25
StD		(n=5)	18				4	4	5	3:1:3
Avg of salts		(n=4)	10				48	33	15	56:26:19
StD		(n=4)	8				6	3	4	5:2:6

Table 7.3. Analyses of samples from the salt anomaly section, #40. Hal. = halite. Rock types explained in text. Refer to Key on p. 74.

Central Canada Potash (CCP), clay seams, XRD results 04/88.

Sample #	Clay seam, CCP terminology	Clay rock type (Boys,1986)	Wt % insols	XRD minerals present	% Dolom.& anhyd.
	N41E7:				
1	13ft clay seam	Gn D(M)	9.5	D,Q,A,Ch,I	43
2	11ft above mining back	Mot D(M)	13.2	D,A,Q,Ch,I	45
3	7ft above mining back	Bn M(D)	41.7	D,Q,Ch,I	44
4	5ft above mining back	Mot M(D)	37.9	D,Q,Ch,I,A	44
5	4ft above mining back	Mot D	26.6	D,A,Q,Ch,I	48
6	No.1 clay seam	Gn D	15.6	D,A,Q,Ch,I	44
7	No.2 clay seam	Bn M	73.6	D,Q,Ch,I	42
8	No.3 clay seam	Gn DS	31.6	D,Q,A,I,Ch	47
9	No.4 clay seam	Gn M(D)S	40.2	A,D,Q,Ch,I	49
10	No.5 clay seam	Gn D	22.4	D,Q,I,Ch	43
	N6E13:				
11	No.4 clay seam	Gn M(D)S	27.9	D-A,Q,Ch,I	43
12	No.4 clay seam, duplicate	Gn M(D)	18.3	D,A,Q,I,Ch	41
13	No.5 clay seam	Gn D	21.3	D,Q,Ch,I,A	47
14	No.6 clay seam	Gn D(M)S	45.3	D,Q,I,Ch,A	40
15	No.6 clay seam, duplicate	Mot D(M)S (red&Gn)	39.8	D,Q,Ch,I,A	41
16	12ft below mining floor	Gn D(M)S	33.6	D>A,Q,I,Ch	44
17	12ft below mining floor, duplicate	Gn DS	11.6	D,A,Ch,I,Q	41
	Anomaly, W4N49:				
18	13ft clay seam	Mot M	60.3	D>Q,Ch,I,A	61
19	7ft above mining back	Bn M	58.4	Q,D,A,I,Ch	44
20	4ft above mining back	Bn M(D)	40.5	D,Q,Ch,I	46
21	No.1 clay seam	Bn M(D)	38.9	D,Q,A,Ch,I	44
22	No.2 clay seam	Mot D	14.6	A,D,Q,Ch,I	46
23	No.3 clay seam	Gn D(M)	16.1	D,A,Q,Ch,I	51
			Avg 32 StD 17		Avg 45 StD 4

Table 7.4. Analyses of insolubles from clay seams of the Central Canada Potash mine.

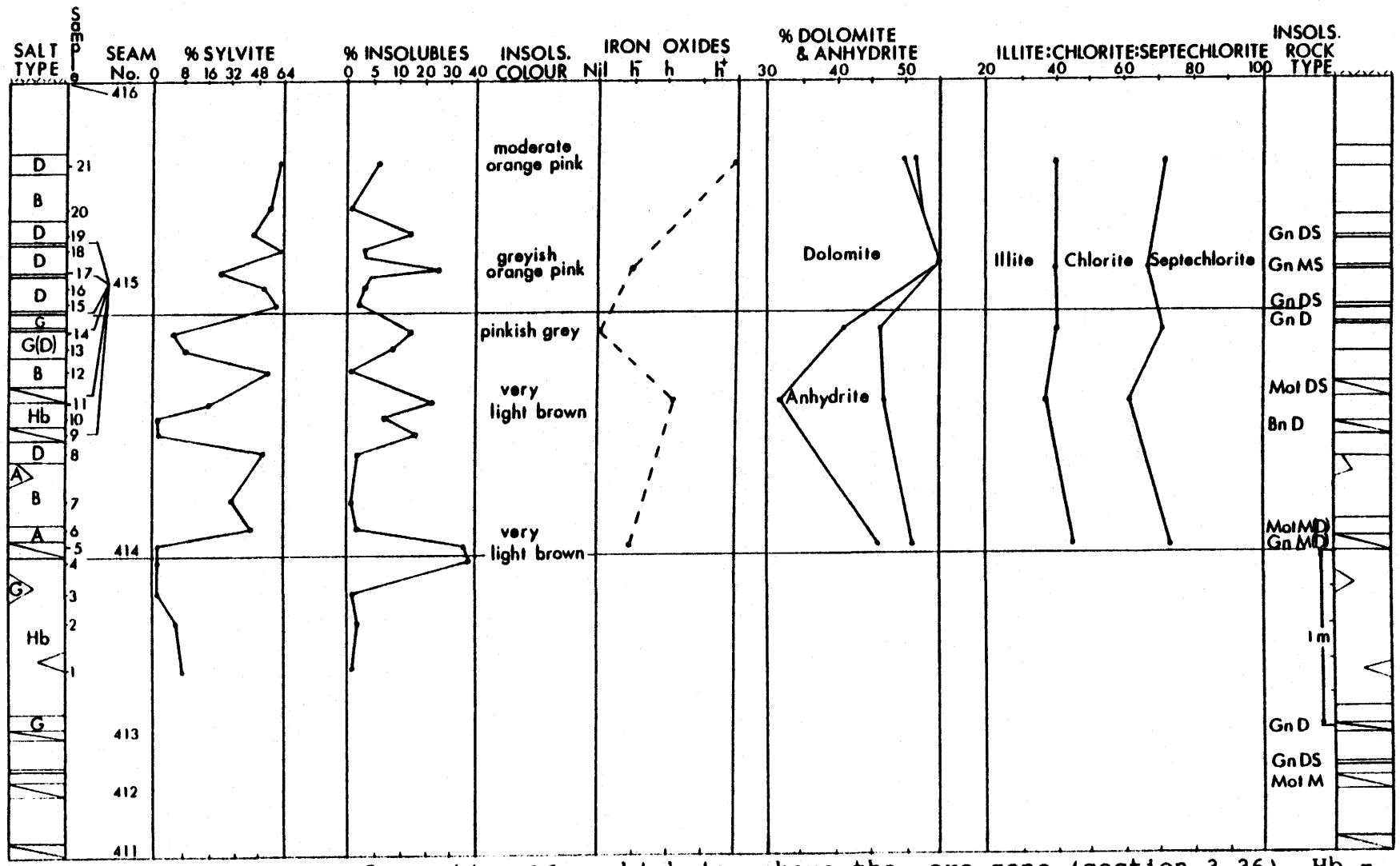

Fig. 7.1. Analyses of section 16, which is above the ore zone (section 3,36). Hb = brown halite. Refer to Key on p. 74.

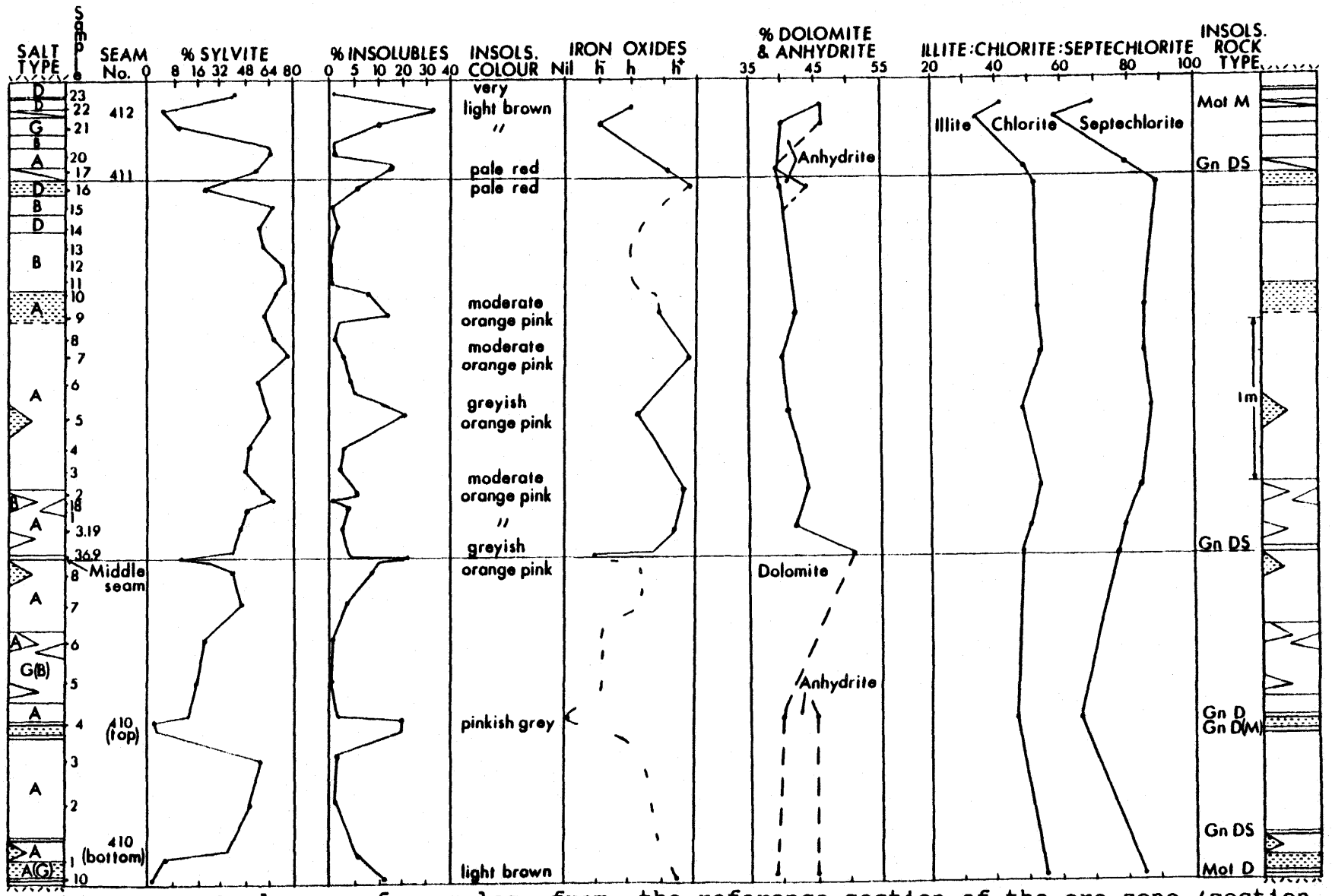

Fig. 7.2. Analyses of samples from the reference section of the ore zone (section 3,36). Refer to Key on p. 74.

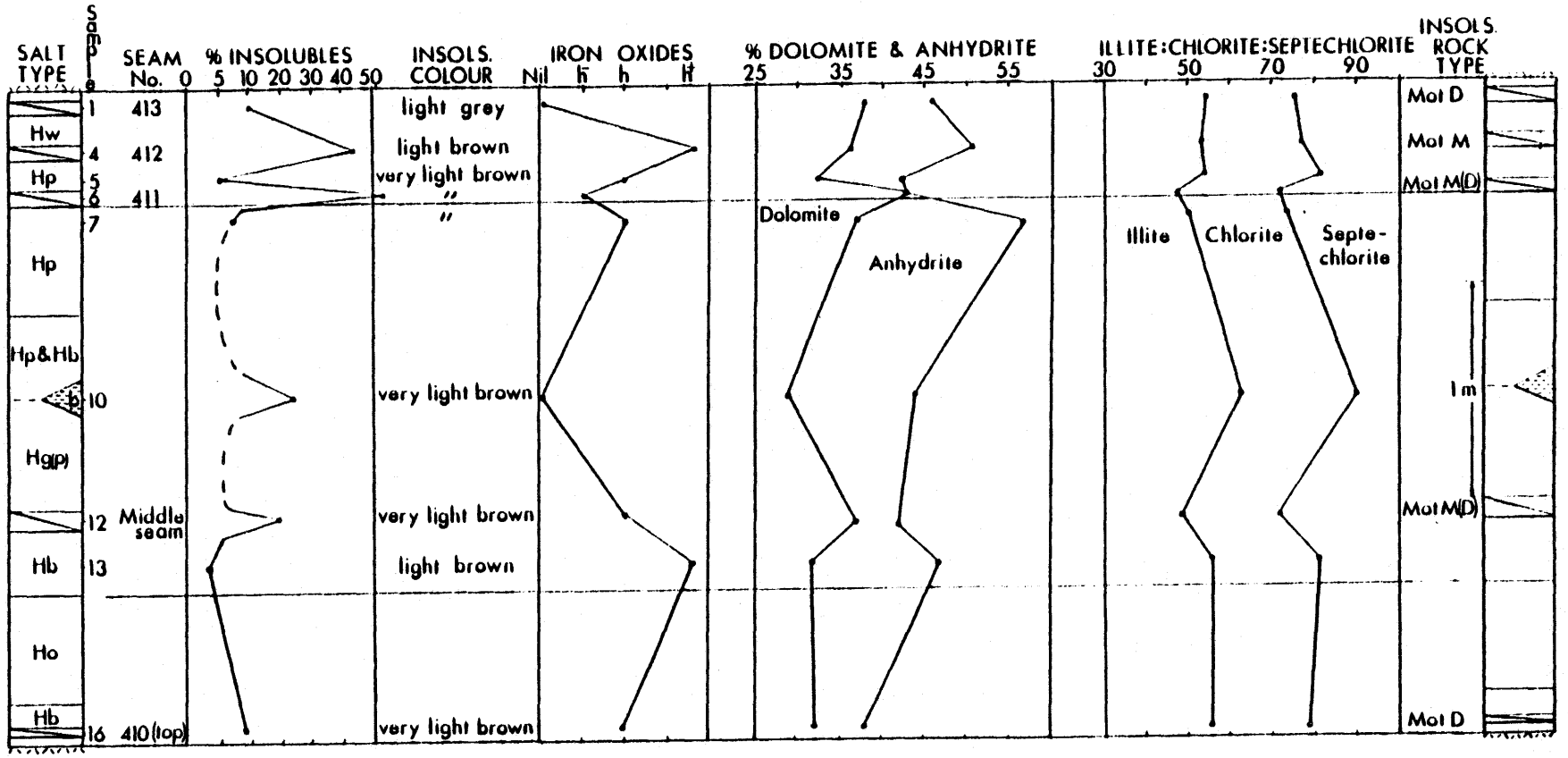

Fig. 7.3. Analyses of samples from section 40 of the salt anomaly. Salt types: H = halite, o = orange, g = grey, p = pink. Refer to Key on p. 74.

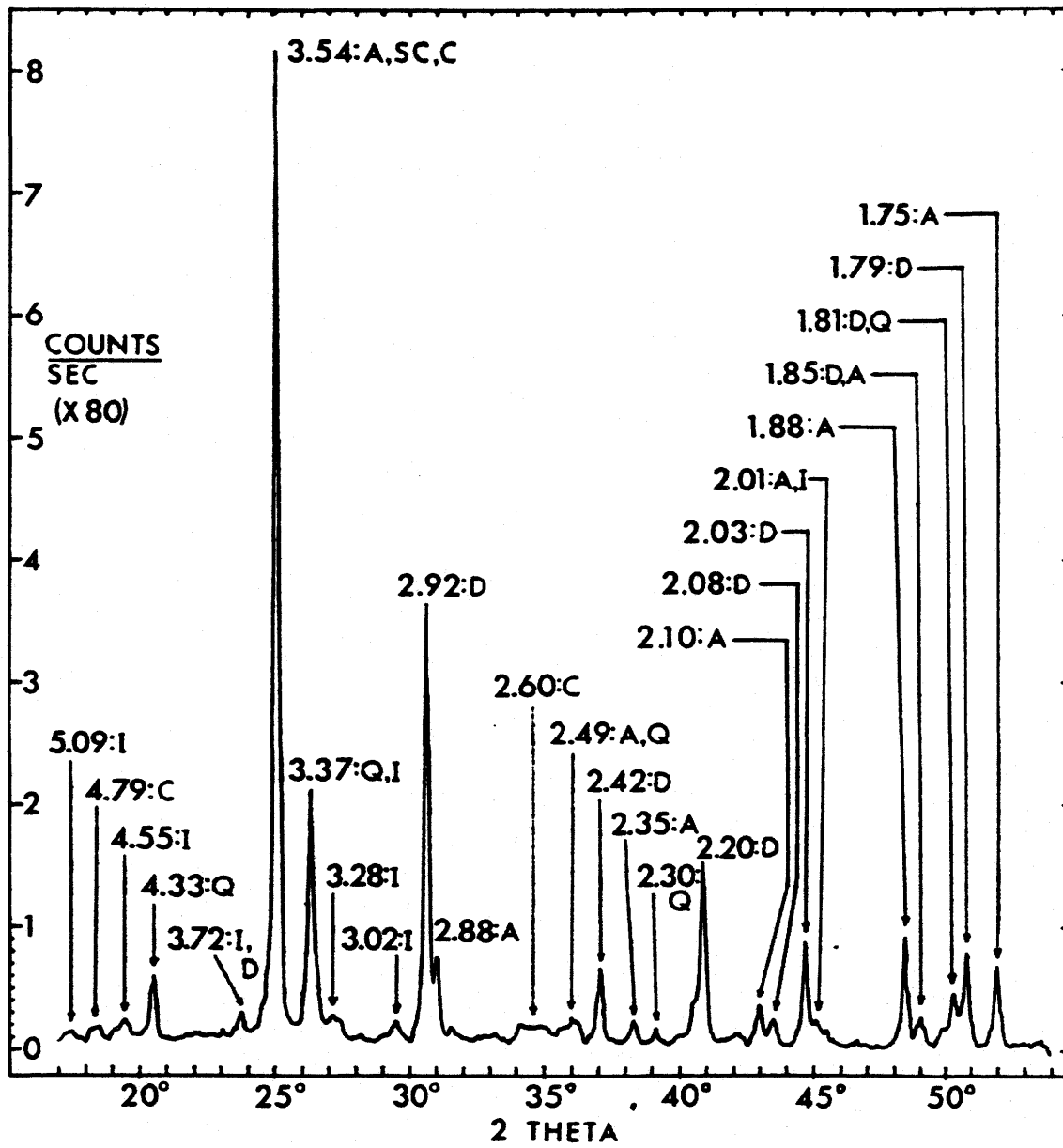

Fig. 7.4 X-ray diffractogram of sample 40.7: insolubles air dried. Scanned at 40kV, 80mA, and 4°/min. Minerals: A = anhydrite, C = chlorite, D = dolomite, I = illite, Q = quartz, and SC = septechlorite. D spacings in angstroms (Å).

of dolomite + anhydrite in the clay seams of the Central Canada Potash mine are similar to those in PCS Cory -about 45% of the total insolubles.

Clay minerals

Illite and chlorite were identified in all the bulk-insoluble samples from the clay seams of the Central Canada Potash mine. The <2 micron fraction was separated from the Cory samples to permit more detailed examination of the clay minerals. The clay minerals from PCS Cory, in approximate order of decreasing abundance, are: illite, chlorite, septechlorite, and mixed-layer swelling-chlorite/chlorite. Smectite and kaolinite were not apparent after 3 samples were boiled in HCl, nor after glycolation of samples. Not all samples were treated with hot HCl or other tests. Most of the percentages of difference are close to the margin of error, 10%, so qualitative differences are stressed.

Illite [$(K,H_3O)Al_2Si_3AlO_{10}(OH)$] is chemically similar to muscovite. Brindley (1981) points out that the term illite is used for all clay-grade micas. It forms as a weathering product of feldspars, by diagenetic alteration of other clay minerals, and as a product of hydrothermal alteration (Deer, Howie, and Zussman, 1966). The formation of illite is favoured by alkaline conditions and by high concentrations of aluminum and potassium. It has a 2:1 tetrahedra:octahedron ratio. The

diffraction pattern consists of a 10 Å basal spacing with an "associated integral series" (Mossman et al., 1982, p. 2129).

There tends to be a bit more illite in the ore zone than above it (Table 7.2). There is slightly less illite, and more septechlorite, in the halite layer about 80 cm above the 414 seam, and in the 412 seam than in the rest of normal section (Figs. 7.1, 7.2). The 411 and Middle clay seams in the anomaly have less illite and anhydrite, and more septechlorite, than in the rest of the anomaly. There is less illite in the clay minerals in the salts and insoluble seams of the ore, than in the clays in the salts and insoluble seams of the salt anomaly (Tables 7.2, 7.3). This may indicate that some diagenetic formation of illite took place. The potassium may have come from dissolved sylvite, the aluminum from the chlorites.

Chlorite [chlinochlore: $(Mg,Fe)_6(Si,Al)_4O_{10}(OH)_8$], including swelling chlorite, has a basal spacing of 14 Å with an associated integral series. Non-swelling chlorites have 2:1, tetrahedral:octahedral, layering while ideal corrensite, a type of swelling chlorite, has 1:1 layering (Hower, 1981). Considerable cation exchange occurs in the chlorites - especially magnesium for iron and aluminum (Deer, Howie, and Zussman, 1966). The chlorites of salt deposits tend to be very high in magnesium, indicating syndepositional formation in a

hypersaline brine (Braitsch, 1971, Bodine and Standaert, 1977, Harville and Fritz, 1986, Fisher, 1988).

In the normal section, chlorite and swelling-chlorite/chlorite, are about one third of the total clay minerals (Table 7.2). In the anomalous section they are a bit less than one third of the clay minerals (Table 7.3). Where the sylvinite is very rich in insolubles, chlorite is abundant (sample 3.5, Fig. 7.2). The amount of chlorite in the clays of the anomaly does not vary significantly. Where septechlorite is above average in the normal section (samples 16.11, 3.21, 36.4, Table 7.2), chlorite is below average. Three points of evidence suggest the chlorites are fairly magnesium-rich. The basal (001) spacing is fairly wide, at least 14.35 Å; the same peak survived (although diminished) in the 3 samples heated to 650°C, and it shows a high intensity with respect to the (002) 7 Å peak (Brown and Brindley, 1980). The 14 Å peak of magnesian chlorite disappears at 800°C, while that of iron-rich chlorite disappears at 600°C (Brown and Brindley, 1980). The 14 Å peak disappeared when the samples were heated to 725°C, which suggests that some iron is present (Brown and Brindley, 1980).

Septechlorites are a series of trioctahedral phases that "can occur as the low temperature polymorph of any composition which forms a chlorite" (Nelson and Roy, 1958,

p.721). Mineralogically and chemically, they are chlorites with a trioctahedral unit that repeats with a 7 Å periodicity along the c-axis (Nelson and Roy, 1958). They lack the 14 Å peak that characterizes normal chlorite. Although the term 'septechlorite' has been used by only a few authors (e.g. Nelson and Roy, 1954&1958; Deer, Howie, and Zussman, 1966; Velde et al., 1974; Mossman et al., 1982), natural 7 Å chlorites have been recognized by many others, including Brindley (1951), Hey (1954), Shirozu (1958a&b), Brown and Bailey (1962), Carroll (1970), Braitsch (1971), Velde (1973), Velde (1985), and Fisher (1988).

A double peak at 3.54 and 3.59 Å is the main criterion used to detect the presence of both chlorite (3.54 angstroms) and septechlorite (3.59 Å, Fig. 3.2). A slight shoulder on the 7 Å peak (Fig. 3.2) may also be present. However, Brown and Bailey (1962) found a fairly uncommon 14 Å chlorite, Ib polytype, that also had a peak at 3.59 Å.

On average, both for anomalous and normal sections, there is more septechlorite in the insolubles of the clay seams than in the insolubles of the salts (Tables 7.2, 7.3). The normal and anomalous ore zones have about equal amounts of septechlorite. Septechlorite is particularly abundant above the ore zone (Table 7.2). In the normal ore zone between the 411 and the Middle insoluble seams the amount of septechlorite

is below average and chlorite is above average. In the two samples that were heat-treated there was an initial slight decrease in the septechlorite 3.59 Å peak at 300°C. Further heating shows a relative strengthening of the septechlorite peak at 3.59 Å until 650°C where the only clay peaks remaining are those of illite and 14 Å chlorite. From the limited evidence obtained, septechlorite appears to be stable up to about 650°C while the basal 14 Å reflection of chlorite survives this heat.

Mixed-layer swelling-chlorite/chlorite is present, but not abundant, in all the Cory samples analysed. It has been included in the 'chlorite' portion of the illite:chlorite:septechlorite ratios. Swelling-chlorite/chlorite, or corrensite, is present in other salt deposits (Discussion, p. 129; Droste, 1963; Lounsbury, 1963; Braitsch, 1971; Harville and Fritz, 1986; Fisher, 1988).

Quartz

Quartz (SiO_2) is ubiquitous in the insolubles of both the salts and the clay seams. It can be detected prior to centrifuging of the sample by the presence of a large XRD peak at 3.34 Å (combined illite and quartz) and by a peak at 4.26 Å. Although little attempt was made to determine the relative amounts of quartz it probably occurs to the extent of several percent, i.e. 2-15% (Mossman et al., 1982). There seemed to be

an abundance of quartz from a massive seam (sample #19, 58% insolubles) at the Central Canada Potash mine.

Anhydrite

The amount of anhydrite ($CaSO_4$) ranges from 0 to about 20% of the insolubles. Where anhydrite is present, the amount of sylvite is usually <16% (Tables 7.2, 7.3). There is more anhydrite in the PCS Cory mine southwest leach-collapse anomaly (Fig. 7.3) than in the normal potash. The anhydrite content of the insolubles in the anomaly averages about 7% in the clay seams and 15% in the salts (Table 7.3). This is considerably higher than an average of 3% of the insolubles in the clay seams and salts of the normal ore zone (Table 7.2). The high standard deviations of the percentages of anhydrite indicate that it varies considerably from one sample to the next. Although the anomalies in both mines may be anhydrite-enriched, there is one sample in each that does not appear to have any anhydrite. The anhydrite enrichment in the anomaly seems to be at the expense of dolomite because the combined percentage of dolomite + anhydrite is similar to that of the normal ore zone. In the 412 seam of both potash mines there is abundant anhydrite in the salt-anomaly samples, but almost no anhydrite in the ore samples (Tables 7.2, 7.3). Euhedral bent laths of anhydrite, such as those found near a leach anomaly in PCS Cory mine (Plate 13a), suggested an eogenetic origin (post deposition but prior to significant burial) to Fuzesy

(1983). Clearly much of the anhydrite is authigenic and possibly, secondary.

Iron oxides

The iron oxides present in the Patience Lake Member, as determined by X-ray diffraction, are hematite (Fe_2O_3) and goethite [FeO(OH)]. Wardlaw (1968), McIntosh and Wardlaw (1968), and Fuzesy (1983) found goethite and hematite in the sylvinite, while Mossman et al. (1982) found hematite in the clay seams. Comparing the most intense X-ray diffraction peak heights for hematite (2.70 Å) and, when present, goethite (4.18 Å) between samples, permitted the determination of which sample had the higher amount of iron oxides. The distribution of the iron oxides is variable, unlike the distribution of dolomite, quartz, and clays.

Iron oxides are abundant in reddish and dark brown samples (Figs. 7.1-7.3). Most of these samples have abundant sylvite. Samples of D-type potash are also rich in iron oxides. Pale orange to orange B-type potash has less hematite and other insolubles than A-type potash. The insolubles in the sylvinite are almost always greenish-grey, which is thought to be due to the absence of hematite, and that any iron present is mostly ferrous or bound into chlorite (Fig. 7.2, compare samples 3.5 and 36.9 to 36.4). In other words, hematite, and

to a lesser degree goethite, are responsible for most red, orange, and brown colours in the evaporites.

The iron oxides take the form of tiny red platelets included in the margins of sylvite grains, and are presumed to be hematite (Plate 10b). Rarely, they form a primary inclusion pattern (Plate 11a). The marginal zones of carnallite ($KMgCl_3 \cdot 6H_2O$) and sylvite are commonly completely imbued with hematite (Wardlaw, 1968).

Goethite is especially common in the potash-rich salts of unit M3 in the ore zone (Table 7.2). It has not been found in the clay seams, nor in the PCS Cory leach-collapse anomaly - both of which may have considerable amounts of hematite. Most sylvite has hematite rather than goethite inclusions.

7.2 THE DISTRIBUTION OF INSOLUBLE MINERALS IN CLAY SEAMS

In general, there is little difference between the insoluble mineralogy of the clay seams and that of the insolubles in the salts. As previously mentioned, the brown and mottled clay seams have more hematite than green seams. As Mossman et al. (1982) found, the proportion of illite tends to be greater than that of either chlorite species. Illite is

more abundant in the anomaly than in the normal potash. In the PCS Cory salt anomaly, however, the salts have more anhydrite than the clay seams. The variability of clay ratios within a sample, and between sections for a given seam (Mossman et al., 1982), makes further comparisons inconclusive. No explanation exists for these small-scale heterogeneities, yet they probably reflect a combination of depositional and diagenetic conditions.

The upper two seams of the 415 seam that were analysed (Fig. 7.1) have similar illite:chlorite:septechlorite ratios. The third seam (sample 16.11) has somewhat less illite, chlorite, and dolomite, and relatively more septechlorite and anhydrite than the upper two. The anhydrite content is at a maximum in sample 16.11, which is just above 15 cm of halite.

The 5% anhydrite in the insolubles of samples from the 414 and 415 seams (#16.5 and #16.14), although not anomalously high, may be related by secondary redistribution, to the anhydrite-rich seam about 50 cm above (Fig. 7.1). As Mossman et al. (1982) found in the Cominco potash mine, illite forms a high proportion of the clay minerals (in this case, 45%) in the 414 seam when compared with the other samples above the ore zone (Table 7.2).

In PCS Cory, only the 413 seam from the salt anomaly was analysed. The insolubles contain about 38% dolomite, 8% anhydrite and virtually no iron oxides. The illite is fairly high (54% of the clays) compared to the other clay minerals (Table 7.3). The 413 seam in both sections in the CCP mine also have significant amounts of anhydrite (Table 7.4).

The insolubles of the 412 seam in PCS Cory contain no anhydrite in the normal section but 15 percent anhydrite in the anomalous section. The illite proportion of the clay minerals is also higher in the anomalous section (53 vs 42 for the normal section). A similar phenomenon is noticed in the 412 seam of the Central Canada Potash mine, with no anhydrite in the normal section, and abundant anhydrite in the anomaly.

The mineralogy of seam 411 is similar to that of the other clay seams in the normal ore zone (Table 7.2). The 411 seam in both sections lacks anhydrite (Tables 7.2, 7.3). The illite:chlorite:septechlorite ratios are 49:31:20 and 47:24:29 for the normal and anomalous samples respectively.

The Middle clay seam has a high amount of dolomite (51%) when compared with the other clay seams in the ore zone, otherwise its mineralogy is comparable. In the anomalous section the Middle seam has less dolomite (37%), more

anhydrite (5%), less chlorite, and more septechlorite than in the normal section.

An increase in anhydrite content of the insolubles in the 410 seams is matched by a decrease in the sylvite content of the accompanying salts (Table 7.2). The 410 (top) seam of the anomaly has a similar anhydrite content to its normal counterpart (Tables 7.2, 7.3). The bottom 410 seam in the normal section is fairly similar in the clay ratios to the 410 seam in the anomaly.

7.3 THE DISTRIBUTION OF INSOLUBLE MINERALS IN POTASH AND HALITE

Pale orange sylvinite, B- or G(B)-types, usually is poor in insolubles, and only one sample was analysed for its mineralogy. The other types of sylvinite average about 4% insolubles, most of which are greenish-grey. Brown insolubles are most common in halite, and in potash that lies close to brown or mottled clay seams. Insolubles in the salts of anomalies are commonly brown or greenish-grey and brown. Interstitial clots of insolubles in anomalous halite tend to be more common than in normal potash. Many collapse structures may be found with large irregular blebs, 1-4 m^2, of very insoluble-rich salt.

The insoluble mineralogy of eight PCS Cory sylvinite samples was analysed. Hematite was present in all eight, and goethite was present in all but the G-type sample between the 412 and 411 seams (Table 7.2). No goethite was found in the clay seams. On average, there is slightly less dolomite in the sylvinite samples (41%) than in clay seam samples (45%). The ratio of the clay minerals in the sylvinite is similar to that in the clay seams. The highest, and the only significant, anhydrite values are in the two samples closest to the 411 and 412 clay seams.

The insolubles of the anomalous halite samples (4) differ from the insolubles of the sylvinite samples in several respects. The most obvious difference is colour; the halite insolubles are all light or very light brown. The anhydrite content in the anomalous halite is more than in sylvinite, while dolomite is less than it is in sylvinite. The amount of anhydrite is very variable and there is no goethite in the halite samples of the anomaly. There is generally more illite, and less chlorite in the halite than in the sylvinite (Tables 7.2, 7.3).

PART 3. DISCUSSION

Chapter 8. THE ORIGIN OF THE INSOLUBLE MINERALS

8.1 INSOLUBLES IN OTHER EVAPORITE SALT DEPOSITS

All the insoluble minerals found in this study have been found in other evaporite salt sequences. It is pertinent to review the findings of previous authors in three major salt deposits: the Permian Zechstein of Europe, the Permian salts in south-western United States, and the Upper Silurian salts in the Salina Group of the eastern States and southern Ontario. These, and the insoluble minerals of the Prairie Evaporite Formation, are compared to the minerals of this study in a summary table (Table 7.1). Minerals not found in this study, but common elsewhere include: magnesite, euhedral quartz, feldspar, smectite or mixed-layer chlorite/smectite, and minor talc.

In the Permian Zechstein salts of Europe, magnesite was found to be the principal authigenic carbonate; dolomite is only minor and is ferroan (Braitsch, 1971). Anhydrite is also abundant. Quartz and muscovite (or illite) are most commonly of detrital origin. Other clay minerals in the salts include: clinochlore (chlorite), amesite (septechlorite), corrensite, and minor talc (Braitsch, 1971). Hematite,

believed to be the most important iron mineral in all salt deposits, is present as inclusions in sylvite and carnallite, and is thought to have recrystallized when sylvite formed from carnallite (Braitsch, 1971). In the potash salts the amount of iron is proportional to the amount of insolubles. Other, less common insolubles found in the Zechstein salts include: euhedral pyrite, potassium feldspar, and organic matter, including hydrocarbons and unspecified fossils (Braitsch, 1971).

In the Permian Salado Formation of New Mexico, magnesite is a common carbonate in the clay seams (Harville and Fritz, 1986). Quartz and the high magnesian clays, chlorite, amesite (septechlorite) and corrensite, are considered to be authigenic (Harville and Fritz, 1986). Relatively coarse muscovite and minor amounts of hematite, anhydrite, and talc were also found (Jones, 1972, Harville and Fritz, 1986). Harville and Fritz (1986) found that "high-charge" corrensite (interstratified chlorite/vermiculite) was more common with the bittern salts, such as sylvite and langbeinite, and that "low-charge" corrensite (interstratified chlorite/smectite) was more common in halite and anhydrite. They also suggest that thick clay seams represent major seawater influxes, disseminated insolubles resulted from undisturbed precipitation and deposition, and that clay

linings on sylvite resulted from solutions that dissolved pre-existing minerals.

The "mudstone" of the Permian San Andres Formation of northern Texas "is composed of silt-size quartz, feldspar, mica, opaque minerals, dolomite, and anhydrite" (Hovorka, 1987, p.1032). These are in a matrix of clay minerals which, in approximate decreasing abundance, are: illite, irregular interstratified chlorite/smectite, chlorite/vermiculite, chlorite/swelling chlorite, chlorite, saponite (a Mg-smectite), and a 7 angstrom serpentine-group mineral (Hovorka, 1987, Fisher, 1988). Fisher (1988) concluded that the Mg-enriched clays resulted from syndepostional alteration, and that the illites were slightly altered in a similar hypersaline environment. He found that the clays could be used to identify areas, such as solution-collapse breccias, where evaporites had formerly been present. Also, similar clay minerals in non-evaporitic strata, such as limestones or dolomites, could record the post-burial passage of hypersaline evaporite brines (Fisher, 1988).

Bodine and Standaert (1977) also suggested, with the aid of primary textures and bromine geochemistry, that the Mg-enriched chlorite in the Upper Silurian Salina Group formed in the marine environment, and that illite underwent some recrystallization in a hypersaline environment. Other fairly

minor minerals found include: euhedral quartz and pyrite, talc, potassium feldspar, and serpentine (Bodine and Standaert, 1977). Anhydrite and dolomite are the most common minerals in seams and "shale balls" (Dellwig and Evans, 1969, Bodine and Standaert, 1977). Lounsbury (1963) found that some of the chlorites showed a slight basal expansion. Fossil fragments, such as brachiopods, were found with the salts (Dellwig and Evans, 1969).

8.2 THE ORIGINS OF THE MINERALS FOUND IN THIS STUDY

The detrital minerals include quartz, dolomite, micas, some clays such as illite and chlorite, and organic material such as spores and fossil fragments. However, most of the illite and chlorite probably resulted from authigenic, pre- and post-burial, alteration of detrital micas and clays. Insolubles that probably formed authigenically in the hypersaline depositional environment include some chlorite, septechlorite, mixed-layer swelling-chlorite/chlorite, goethite, and possibly hematite. The hematite is authigenic (Sonnenfeld, 1984). Some anhydrite appears to be secondary, some syndepositional and possibly detrital.

As Mossman et al. (1982) suggested, the detritus was probably transported by winds and/or, more likely, by intermittent floods. As suggested by Harville and Fritz (1986)

for the Permian Salado Formation of New Mexico, thick clay seams, eg. # 412, 407, 406, and 401, probably represent major flooding events while disseminated insolubles represent a stronger eolian influence. Residual insolubles from dissolved salts probably contributed significantly to clay seams. Fine material transported in brines can spread for long horizontal distances before settling (Sonnenfeld and Hudec, 1985). Both marine and meteoric water were probably involved. Channel features up to tens of metres wide and 1-2 m deep and large spores indicate a meteoric water influence (Mossman et al., 1982).

Although Fuzesy (1983) suggested an early diagenetic origin for anhedral dolomite inclusions in potash, most is probably detrital, derived from adjacent areas of exposed carbonates (Wardlaw, 1968). To form dolomite in the middle of potash would require a considerable freshening of the brine, which would leave behind significant amounts of halite and anhydrite. Alternatively, there would have to be some mechanism for producing it under hypersaline conditions. Table 7.1 indicates that magnesite not dolomite, is the major carbonate in potash salts of the Zechstein and Salado Formations. Alternatively, to form dolomite rather than magnesite authigenically would require excess calcium, which Kendall (1989) suggests may have been available in large amounts from deeply circulating groundwater.

Detrital minerals, other than dolomite and fossil fragments, include illite or its mica precursors (Bodine and Standaert, 1977), chlorite, and quartz. Some illite may have formed diagenetically from chlorite and free K^+ in the leach-collapse salt anomaly. No terrestrial clays remain unaltered in hypersaline brines (Sonnenfeld, 1984), and magnesium enrichment, especially of chlorites, is diagnostic of marine brine alterations (Braitsch, 1971, Bodine and Standaert, 1977, Harville and Fritz, 1986, Fisher, 1988). It is likely that all clays formed, or were at least altered, authigenically.

The septechlorite and mixed-layer swelling-chlorite/chlorite are authigenic, and probably formed in the syndepositional hypersaline brine environment. Sedimentary chlorites found on ocean and estuary bottoms are the 7 Å type, whereas those in sedimentary rocks are mostly 14 Å (Velde, 1973). Septechlorite forms at, or near, the earth's surface, and may be the precursor to many Mg-chlorites (Brown and Bailey, 1962, Velde, 1973, 1985). It has never been found forming in recent sediments at depths greater than 80m (Velde, 1985). Berthierine, an iron-rich septechlorite, forms at or very near the sediment-seawater interface, while chamosite, also iron-rich, is thought to have a diagenetic origin (Velde, 1985). Although it can persist to high pressures and temperatures (2Kbars, near 500°C, Velde, 1985), it converts to normal (14 angstrom) chlorite at about 100°C (Velde, 1985),

which is the **maximum** crystallizing temperature determined from fluid-inclusions (average =55°C) in halite in the Patience Lake Member (Chipley and Kyser, 1989). Mossman et al. (1982) suggested an authigenic (syndepositional or diagenetic) origin for septechlorite, sepiolite, and vermiculite. The absence of otherwise ubiquitous septechlorite in a Second Red Beds sample supports this concept.

Minor amounts of swelling-chlorite/chlorite are present in every sample analysed. Mixed-layer clays are very common in hypersaline brines (Sonnenfeld, 1984), and poorly crystalline 14 angstrom phases retain small quantities of expandable phases at low temperatures (Velde, 1973), indicating a syndepositional origin for the swelling-chlorite/chlorite. Swelling chlorite, or corrensite, has been reported present in salts by several authors (Droste, 1963, Lounsbury, 1963, Braitsch, 1971, Harville and Fritz, 1986, Fisher, 1988). Although corrensite is a swelling chlorite, Harville and Fritz (1986) recognised two types: high-charge corrensite, a regular interstratified chlorite/vermiculite, and low-charge corrensite, a regular interstratified chlorite/smectite.

The types of clay found, can reflect the salinity of the environment in which they formed (Braitsch, 1971, Sonnenfeld, 1984, Harville and Fritz, 1986). Harville and

Fritz (1986) found high-charge corrensite (a type of swelling chlorite) to predominate in potash salts, low-charge corrensite in halite and anhydrite, and Braitsch (1971) found amesite, a high-Mg-Al septechlorite, to predominate in potash residues. Septechlorite in breccias or in rocks that have been exposed to fluids may be useful to indicate an origin in bittern brine fluids.

One effect of the anomaly-producing fluids was to increase the amount of anhydrite in the insolubles at the expense of dolomite. The occurrence of euhedral anhydrite indicates that it is authigenic. The increased anhydrite content in the insolubles of the PCS Cory leach-collapse anomaly indicates a post-burial (diagenetic) origin. The calcium required to form anhydrite may have come from the dolomite. The diagenetic fluids that were responsible for dissolving the potash probably contained the needed sulphate. Other anhydrite may have been mechanically deposited along with dolomite, and some may have formed syndepositionally, as is common in other salt deposits (Braitsch, 1971, Jones, 1972, Hovorka, 1987). Further research should determine whether or not the anhydrite content of insolubles in salts and the 412 clay seam close to an anomaly may be used to indicate anomalous ground.

Oriented goethite fibers in carnallite suggest that the two grew together in the primary environment (Wardlaw, 1968, McIntosh and Wardlaw, 1968). Goethite is the initial precipitate expected when the Eh and pH conditions leave the stability field of ferrous iron, and enter that of ferric iron (Turner, 1980). Goethite is then dehydrated to hematite if the redox potential (Eh) values are high enough to stabilize Fe_2O_3 (Sonnenfeld, 1984). Goethite recrystallizes into random hematite when carnallite is converted to sylvite (Wardlaw, 1968, Braitsch, 1971). Red sylvite is considered to be secondary after carnallite (Schwerdtner, 1964, Wardlaw and Schwerdtner, 1966, McIntosh and Wardlaw, 1968, Wardlaw, 1968, Fuzesy, 1983, Sonnenfeld, 1984). However, the presence of goethite in sylvite suggests that some primary red sylvite has been preserved. The rare primary inclusion pattern in sylvite crystals (Plate 11a) supports this possibility.

The low iron content of seawater (average 0.002 ppm, Drever, 1982, p.234) indicates that most of the iron would have had to come from continental weathering products (Braitsch, 1971). In fine-grained alluvium, most iron is transported as hydroxide grain coatings, and adsorbed on the surfaces and edges of clay minerals (Turner, 1980). Braitsch (1971) found that the iron content of Zechstein salts was directly related to the insoluble content. Likewise, the hematite and goethite content in sylvinite is greatest in

samples that have significant amounts (>2-3%) of insolubles. Therefore, it seems likely that the process of stripping the iron from the sediments, converting it to goethite, incorporating it as inclusions into carnallite, and recrystallizing it to hematite, was restricted to the immediate vicinity (within 10 cm) of the insolubles. The precipitation of iron as goethite or hematite probably occurred beneath the sediment surface, which is where most of the potash minerals seemed to have formed (p. 156), as it does in continental red beds (Turner, 1980). This would explain the low hematite content of B-type sylvinite that is low in insoluble content, and red hematite-rich "roots" extending down from sub-clay units (Plate 5).

Sonnenfeld (1984) states that primary halite is never red, but leaching of potash commonly produces secondary reddening (Plates 4a,b, 12). Where sylvite is absent and the hematite content is appreciable, as in salt anomaly section 40 (Fig. 7.4), it is possible that pre-existing sylvite, or carnallite, left behind its iron oxides when it was dissolved. In a similar manner, the presence of hematite in clay seams may indicate possible disconformities created by the dissolution of overlying potash-bearing beds. In other words, it could be residual. For example, the mottled disseminated clay seam at the base of the type section (sample 36.10) is low in sylvite and high in hematite, which would indicate this

as a disconformity over which potash was dissolved in a flooding event.

Chapter 9. GEOLOGICAL HISTORY

The geological history of the Prairie Evaporite Formation may be understood in terms of primary and secondary processes. These merge as the formation has been continually crystallized, dissolved, and recrystallized since the first salts precipitated in the Middle Devonian (Holter, 1969). Although this study was confined mostly to the Patience Lake Member at PCS Cory, the results add to the understanding of the processes acting in both the primary and secondary environments of the Prairie Evaporite Formation.

The Prairie Evaporite Formation is a "modified primary evaporite" because there are enough surviving primary features to indicate the nature of the depositional environment. In the lower Prairie Evaporite Formation, Wardlaw and Schwerdtner (1966) noted halite-anhydrite seasonal layers. Chevron textures are abundant in the halite (Wardlaw and Schwerdtner, 1966). Whether the brines were shallow or deep, eg. 180 m during deposition of the lower Prairie Evaporite Formation, as suggested by Wardlaw and Schwerdtner (1966), is poorly understood. Recent data indicate a shallow-brine origin (Utha-aroon, pers. comm., 1989), which is important when choosing a depositional model for the upper Prairie Evaporite Formation.

9.1 SYNDEPOSITIONAL HISTORY

Models of deposition

There are several depositional models that can explain the origin of large salt deposits. Briefly, these are: 1) continental playa, 2) supratidal salina, 3) supratidal sabkha, 4) barred basin, and 5) marine-marginal shelf (Hovorka, 1987). Early interpretations suggested that the Prairie Evaporite Formation originated in a deep-water basin barred from the open ocean by the Presqu'ile Formation carbonate reefs in the northeast (Fig. 1.1; Wardlaw and Schwerdtner, 1966; Holter, 1969). For the lower half of the Prairie Evaporite Formation this may have been the case, but the potash beds in the upper half were deposited in a shallow, areally extensive, salt pan (Wardlaw and Schwerdtner, 1966, Holter, 1969, Baar, 1974). The overwhelming evidence for this includes the following surficial features: washout channels, polygons, desiccation cracks, microkarst pits, and chevron halite textures. The marine-marginal shelf model of Hovorka (1987) can explain many of the depositional features of the upper Prairie Evaporite Formation. However, the "marginal shelf" of the Middle Devonian Elk Point Basin was probably more like a vast epeiric sea that stretched deep into the continent.

The main characteristics of the marine-marginal shelf model are that the depositional area is extensive, there are thick accumulations of evaporites, the facies are shallow-water to subaerial, the setting is a marine-marginal shelf, and that there is "good" exchange with marine environments (Hovorka, 1987). The potash beds of the Prairie Evaporite Formation are one of the most areally extensive in North America (Zharkov, 1984). The primary features described here and elsewhere (eg. Meijer Drees, 1986) attest to the shallow-water and periodically subaerial conditions.

There is biostratigraphic evidence (Braun, pers. comm., 1986) that the Presqu'ile barrier reefs correlate with the Dawson Bay Formation rather than with the Prairie Evaporite Formation. This suggests that there may **not** have been a well-defined barrier between open marine water and the Elk Point Basin as suggested by Holter (1969). The lack of a barrier reef argues in favour of the salts being deposited on a large, shallow-water shelf. As with most large evaporites, the thick salts would have accumulated not from the evaporation of one single large volume of seawater, but due to periodically supplied water that kept up with a continuously and steadily subsiding 'basin' (Fowler and Nisbet, 1984). There may have been a continuous influx of seawater induced by evaporation within the basin that was interrupted by episodic marine flooding events of greater magnitude.

Sources of solutes and insolubles

The contribution of meteoric waters during deposition is speculative. Even though a large portion of the Middle Devonian Elk Point Basin in the north, northeast and east may have been in contact with marine sources (Williams, 1984), it was essentially an epicontinental sea during deposition of the Prairie Evaporite Formation, and as such, probably received significant contributions of meteoric water runoff (Utha-aroon, pers. comm., 1989). Large terrestrial spores, and acritarchs and chitinozoans of marine origin, found in a clay seam from the ore zone, may indicate mixing of marine brines and fresh water (Cashman, pers. comm., 1988). Spores in marine sediments are chiefly water transported, rivers being a major source of input (Birks and Birks, 1980). Friedman (1980, p. 602) suggests "that the distinction between marine and non-marine evaporites is subjective and not really meaningful", and that the sites of evaporite formation probably swung between the extremes of brines and fresh-water runoff.

Unusual sources of water, whether in the primary or post-burial environments, are also indicated by a lack of sulphate and magnesium minerals in the Prairie Evaporite Formation, and by the simple mineralogy of the potash deposits: halite, sylvite, carnallite, minor polyhalite

[$K_2Ca_2Mg(SO_4)_4 \cdot 2H_2O$], and minor insolubles. This raises the question: why are the numerous sulphate and magnesium minerals, such as those found in the Permian Zechstein beds of Europe and the Permian deposits of New Mexico (Borchert and Muir, 1964), conspicuously missing?

Sulphate remained in marine brines after formation of the Muskeg anhydrites, and Kendall (1989) suggests that CaCl-bearing groundwaters from springs emerging from Winnipegosis Formation mounds undergoing dolomitisation were responsible for removing it as anhydrite. In order for this sulphate depletion to allow for later precipitation of K- and Mg-chlorides without Mg-sulphates, would require that groundwater-brine mixing continue after the carbonates were buried, or that the sulphate-depleted brines were stored in porosity (Kendall, 1989).

From oxygen and hydrogen stable isotope data, it appears that the primary fluid inclusions from chevron halite crystals of the Patience Lake Member potash contain a large component of formational waters (Chipley and Kyser, 1989). However, subtle changes in fluid chemistry without altering the chevron texture may have occurred after burial in a manner similar to that suggested by Walls et al. (1979) for radiaxial calcites. This implies that mixed marine, meteoric, and formational waters formed the upper Prairie Evaporite

Formation (Kendall, 1989). Surface runoff and groundwater from the Winnipegosis reefs have been cited as possible "freshwater" sources (Kendall, 1987).

There are several possible sources of the solutes, principally Na, K, Cl, and Mg, that formed all the salts of the Prairie Evaporite Formation (Fig. 9.1). Recycled solutes from dissolved strata were probably a major contributor. In this manner, all the potassium from the brines which formed the salt of the lower Prairie Evaporite Formation may have been concentrated in the brines of the upper Prairie Evaporite Formation. Sources of new solutes, in probable decreasing importance, were marine floods, meteoric floods, groundwater, and aerosols (wind and rain, Fig. 9.1).

The same sources of solutes, except perhaps groundwater, also provided insolubles (Fig. 9.1). Recycled insolubles from dissolved strata were likely to have been major contributors to clay seams. The sources of new solutes were also sources of new insolubles, probably in the following decreasing importance: marine and meteoric flooding, aerosols, and groundwater (Fig. 9.1). In the brines all the soluble minerals were formed, while only the insolubles septechlorite, goethite, hematite, and perhaps some of the anhydrite and dolomite were formed. Other insolubles, such as micas, illite, and chlorites, were significantly altered.

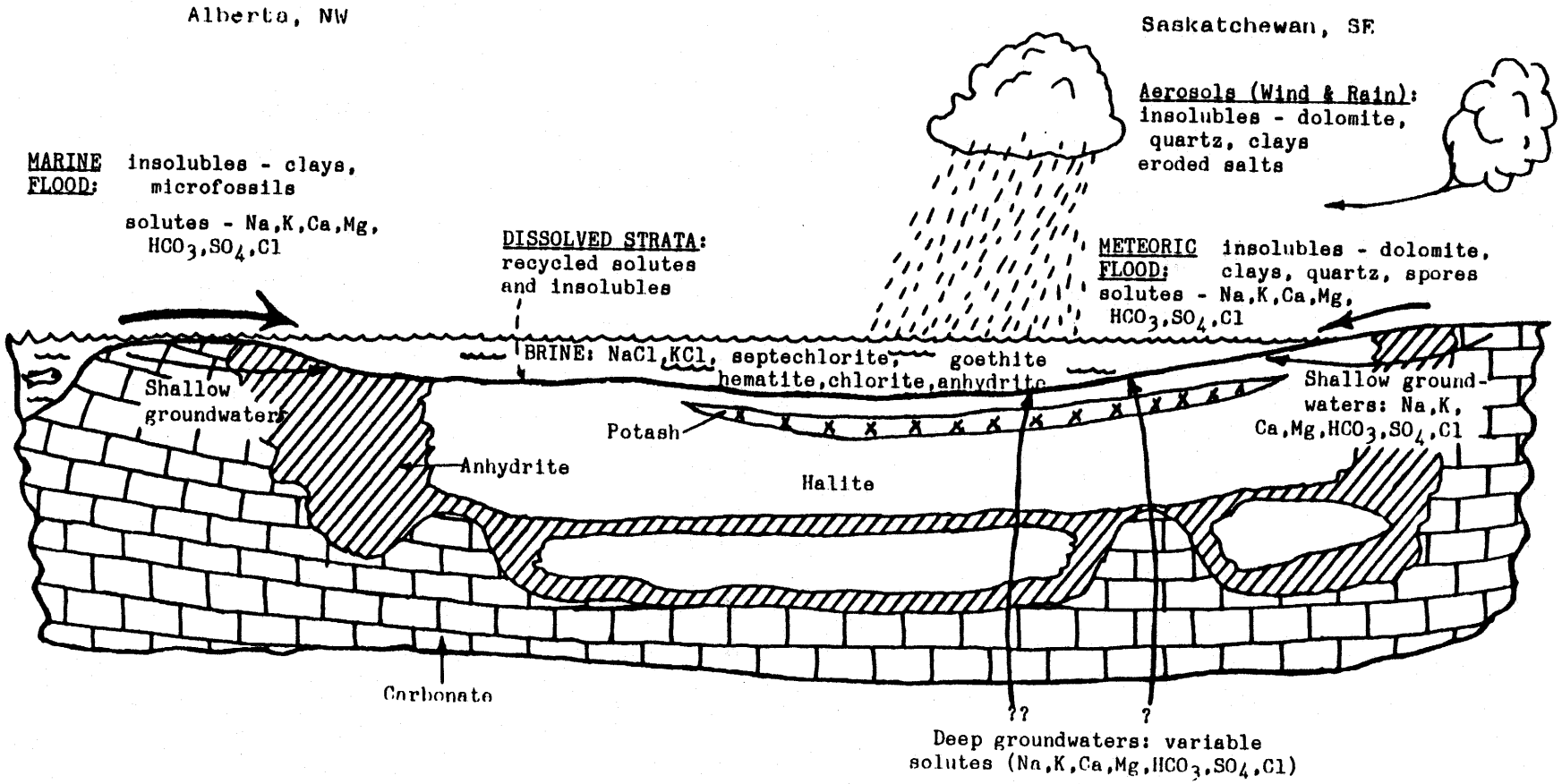

Fig. 9.1. Sources of solutes and insolubles during potash deposition of the Prairie Evaporite Formation. Authigenic minerals derived from the brine are also indicated. Brine depth is exaggerated.

Origins of the potash cycle

A close look at the potash cycle comprising unit M2 of the ore zone (Figs. 4.6-4.8 in pocket) shows that, although the salts have been recrystallized and hematite partly remobilized, the distribution of insolubles probably reflects primary processes. Even where secondary leaching has removed sylvite, the insolubles, other than some hematite, have not been significantly remobilized (Fig. 5.2). The disseminated insolubles in potash were likely transported by wind (Mossman et al., 1982, Harville and Fritz, 1986). It is expected that flood-transported insolubles would leave a more laterally-continuous record, and that some signs of brine freshening may remain.

Commonly, the disseminated insolubles increase upward in amount below a clay seam and there are some disseminated insolubles just above the clay seam, but in the potash near the middle of the cycle there are negligible amounts of insolubles. Two idealised models are proposed, both of which involve wind transport, to explain the distribution of the disseminated insolubles in the potash cycle. A combination of both models is probably a better explanation than either one by itself.

The first model assumes more-or-less constant wind velocity, although this is not likely to have occurred, and varies the location of the source area of the insolubles as the brines dry up. While a clay seam is being deposited after a flood, chevron halite may be forming (Plate 10c). Those insolubles that are late to settle are disseminated in the salts immediately overlying the clay seam (Fig. 9.2A, graph). At this time the brine is relatively deep and has a large surface area so that much of the wind-borne insolubles, derived by deflation from the subaerial basin margins, may have dropped out before reaching the centre of the basin (Fig. 9.2A). If these conditions continue for some time, salts low in insolubles may form, which eventually become B-type potash in the middle of the cycle. With continued evaporative drawdown the brine level drops to expose peripheral saline mudflats, whose salts and insolubles can then be deflated and transported toward the centre of the basin (Fig. 9.2B). The lower that the brine level drops, the greater the surface area exposed to deflation. Thus wind-deposited insolubles may increase toward the basin centre because the source area is closer. The effect is to develop an upward increasing amount of insolubles in a potash cycle prior to desiccation (Fig. 9.2C). On a larger scale, the increasing amount of insolubles in succesively higher potash members of the Prairie Evaporite Formation (Holter, 1969), may indicate that the entire basin was becoming increasingly desiccated.

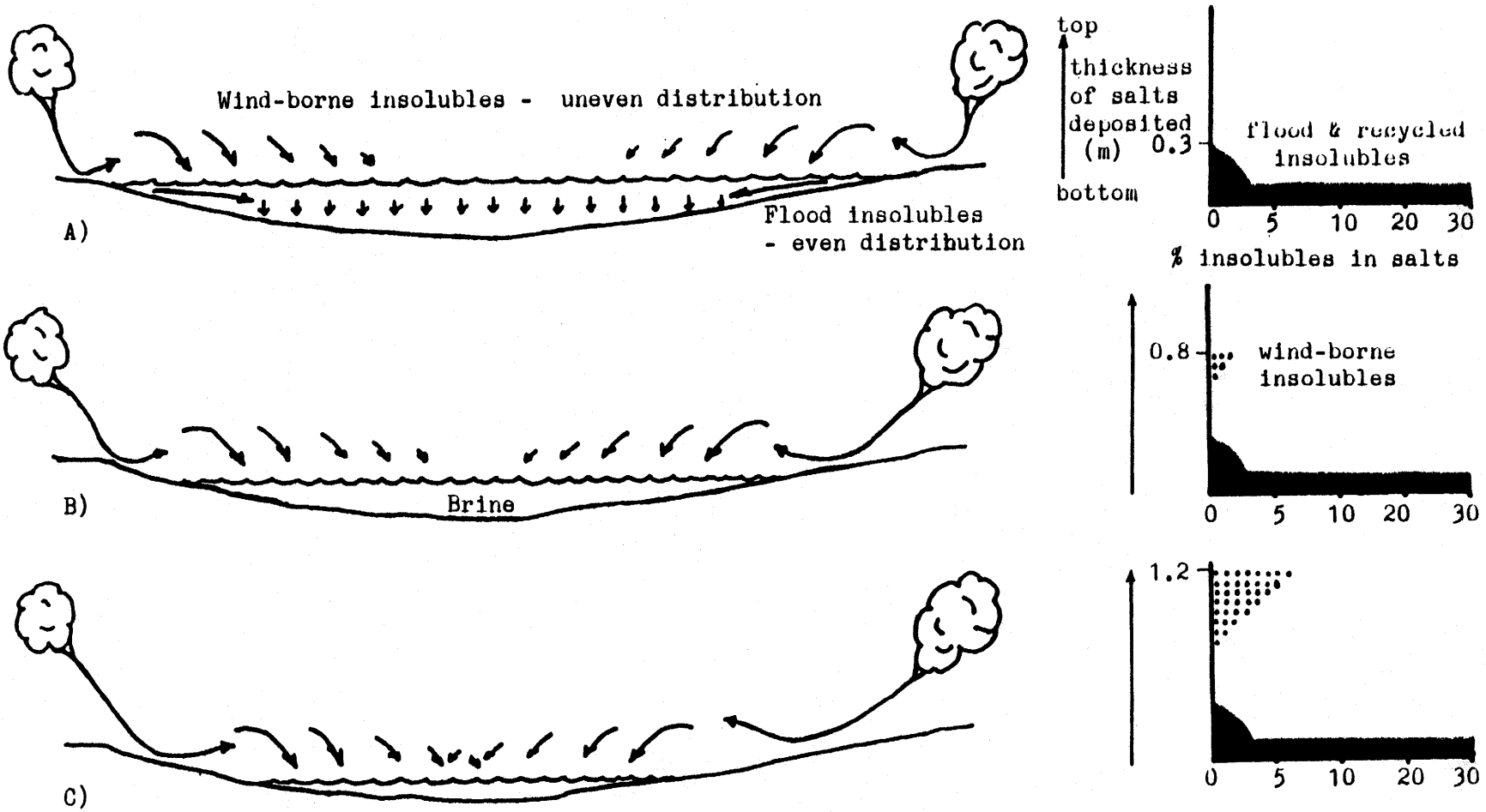

Fig. 9.2. Schematic diagram of the variable-source, constant-wind-power model to explain the distribution of insolubles in the potash cycle. The amount of wind-borne insolubles in the middle of the basin (see graphs), increases as the source gets closer due to evaporation of the brine. No preferential wind direction is implied.

The alternative model assumes a more-or-less constant source of insolubles from the subaerial basin margins, but varies the power of the wind. The amount of disseminated insolubles in the potash cycle reflects the strength and influence of winds across the vast brine and salt flats. Preceeding each flood, marked by the clay seams, wind velocity may increase, reaching a maximum prior to flooding. Strong winds may even contribute to flooding by pushing marine waves toward the ephemeral salt basin. As wind velocity increases, so does evaporation and salinity. More insolubles are then deposited, and more carnallite (or sylvite) may crystallize, incorporating iron oxides from the insolubles. In the middle of the potash cycle, winds may decrease during salt formation, and slightly less sylvite (e.g. pale G-type in unit M2, Fig. 4.7) in some potash cycles may represent lower salinity due to decreased evaporation - a result of decreased humidity difference between the brine and the still air above. After the flood, residual wind-borne insolubles would be disseminated in the salts above the clay seam.

Unit M1, at the base of the ore zone, may represent an incomplete potash cycle in which an overabundance of insolubles prevented insoluble-poor B-type potash from forming a coherent bed in the middle, as it does in normal potash cycles. There are two main conditions that could have prevented the top of unit M3 from forming into a clay seam: an

insufficient supply of insolubles, and/or fast salt growth. A secondary redistribution of insolubles is possible, although not likely because, even in salt anomalies where significant dissolution and recrystallization occurs, the insolubles are not transported very far. If the top of unit M3 had been a clay seam, then it, and units M4 and M5 would form a potash cycle. The rest of unit M3 may also represent one or two incomplete potash cycles.

The fact that hematite-poor B-type potash does not occur where there are significant amounts of insolubles suggests that the iron oxides were derived from the local insoluble material. The process of stripping the iron from the sediments, converting it to goethite, incorporating it as inclusions into carnallite, and recrystallizing it to hematite, was restricted to the immediate vicinity (within 10 cm) of the insolubles. The originally pale orange to white potash in the middle of the potash cycle would have represented the most quiet period of deposition when iron-giving sediments, primarily clays, were unavailable, or the chemical conditions, principally pH and Eh, were outside of the stability field of ferric iron. It is not understood how greenish-grey insolubles and organic material, which seem to indicate reducing conditions (Hovorka, 1987), can coexist with hematite-imbued sylvite. In fact, the greenish-grey insolubles are most common in red sylvinite.

Effects of flooding

The continuity of bedding indicates that depositional conditions were very similar over a wide area (Holter, 1969). The clay seams probably represent detritus which resulted from marine, and possibly meteoric, flooding events (Lowenstein and Hardie, 1985, Harville and Fritz, 1986, Hovorka, 1987). The onset of potash deposition was preceeded by significant flooding as seen in several thick clay seams (# 401/402, 407, 414, Fig. 4.1). The thick seams may represent more than one flooding event, the net result of which was to build up the concentrations of insolubles and potassium.

According to the rock record, potash overlying halite or potash, flooding does not necessarily result in significant brine freshening. Possible explanations for this include: 1) a shallow stratified brine from which the surficial fresh waters were evaporated, or 2) diagenetic interstitial brines reacted with the minerals to form potash, or both 1) and 2). Diagenetic alteration of halite is most intense within the first few metres of burial and is essentially complete within 45 m (Casas and Lowenstein, 1989). However, as discussed later (p. 166), leaching at depth continues today.

After flooding, the expected sequence of precipitates would start to form in brines of lower, or perhaps equal, salinity to those which were dissolved. This would vary according to the difference in salinities between the floodwaters and the material they come in contact with. Gradual increases in salinity could be expected after floods of low salinity (Fig. 9.3b,c). This would take the form of halite overlain by low-grade sylvinite, which is overlain by A- or B-type sylvinite (eg. from seam 408 up to seam 410, Fig. 4.1), or where patchy, G-type potash grades up into A-type (potash cycles 2, 3, and 6, Figs. 4.1, 4.5). Where the clay seams are overlain by high-grade potash, the brines that resulted from the flooding event(s) were initially of high salinity, or interstitial brines caused recrystallization (Fig. 9.3d,e).

Halite that horizontally overlies sylvinite, without significant intervening insolubles, probably reflects brine freshening. A gradual decrease in salinity is suggested by the gradational contact between sylvinite of the Allan Marker Bed and overlying halite (Fig. 4.1). In contrast, an abrupt contact between sylvinite and overlying halite indicates a more rapid brine freshening (20 cm below seam 408, Fig. 4.1). It seems unlikely that these are secondary contacts because the overlying halite is colour-banded. The brine freshenings were likely caused by floods that did not dissolve salts with

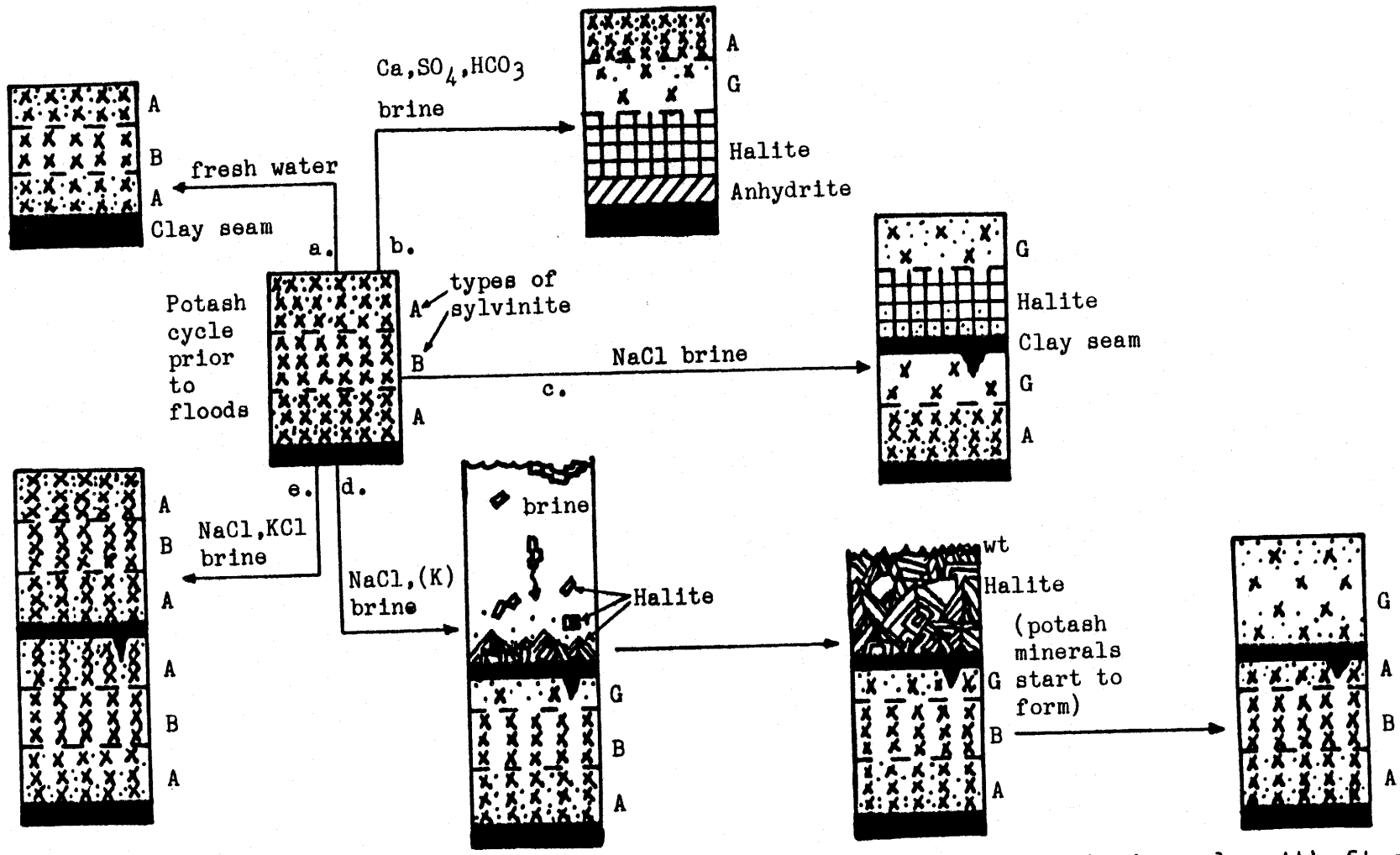

Fig. 9.3 Conceptual model to show the results of flooding a potash cycle with five waters of different compositions. Route d. includes two intermediate steps. Flooding with fresh water (a.) dissolves potash cycle, which eventually returns to potash if in a closed system. Flood of NaCl brine (c.) does not dissolve entire potash cycle; partial dissolution of B-type potash leaves G-type. Interstitial refluxing brines of decreasing salinity would be needed to change b.-d. to e. See text for further details.

significant amounts of insolubles because there are negligible insolubles at the contacts.

Floodwaters probably acquired significant solutes prior to reaching the areas of potash deposition. Once NaCl-saturation was reached, only sylvite would be dissolved, leaving a selectively leached unit of salt. Some potash minerals would survive if either the settling insolubles protected them from the brines or the brines reached KCl-saturation (Fig. 9.3c-e). Interstitial carnallite formation could replace that which had been previously dissolved as long as there was access to interstitial MgCl-KCl-brines. Once MgCl-KCl-saturation was reached, carnallite would form in the brine pond but, more commonly, within a halite mush. In that way, beds which normally would have recorded a freshening event, would show potash after interstitial carnallite precipitation. According to McIntosh and Wardlaw (1968) carnallite was the main primary potash mineral to precipitate and it was quickly converted to sylvite.

Interstitial formation of potash minerals

The halite films between sylvite crystals (Plates 1a, 10a,b, 11c,d) are ambiguous in origin, but seem to indicate that the sylvite or its precursor, carnallite, grew interstitially in a halite "mush". These halite films may be

primary. The thin halite films between sylvite crystals could have formed in two ways - either the sylvite (or carnallite) grew in a matrix of halite as a pore-filling cement, or NaCl-saturated fluid moved through and between sylvite crystals, dissolving the sylvite as it moved prior to crystallizing. The former mechanism seems the most likely. Diagenetic alteration of halite is most intense within the first few metres of burial and is essentially complete within 45 m (Casas and Lowenstein, 1989). Dissolved sylvite leaves behind hematite within halite (Plate 4a,b,), but very little halite has hematite inclusions. Besides, it would be hard to imagine an NaCl-saturated fluid moving through more soluble material, such as sylvite or carnallite, without quickly becoming KCl-saturated.

Vertically elongated carnallite in halite of the Esterhazy Member suggests that the carnallite precipitated interstitially (Utha-aroon, pers. comm. 1988). Other petrographic evidence, such as sylvite cross-cutting primary fluid inclusions in halite (Plate 11c), suggests that sylvite is younger than halite. From petrographic evidence McIntosh and Wardlaw (1968) also concluded that sylvite and carnallite are younger than the halite in ore beds. Nevertheless, some halite would probably still be forming at the same time as the carnallite. Wardlaw (1968) suggests that carnallite and goethite grew together. Although an indirect analogy due to

differences in oxidation states, Turner (1980) indicates that the goethite or hematite of continental red beds probably formed beneath the sediment surface. Therefore, the potash minerals probably formed beneath the sediment surface. With the support of early analogues, such as those on early diagenesis of halite (Casas and Lowenstein, 1989), the speculation that the timing of these events would have been fairly early, ie. penecontemporaneous, is made in the face of abundant evidence for secondary formation of sylvite (eg. Baadsgaard, 1987).

There are three main ways in which salts associated with clay seams may form. Chevron halite crystals with only minor insoluble inclusions, which are common in clay seams (Plate 10c), could have grown in a shallow brine and settled into the insolubles. Alternatively, they could have grown as displacive salts in existing clay that was not buried too deeply to inhibit the different rates of crystallization manifested in the patterns of fluid inclusions (Roedder, 1984, see discussion on chevron halite below). Salts also grew in the pore spaces after the insolubles were mostly deposited, forming various textures depending on the rates of crystallization, and deposition (Plate 4c). Many of these salts incorporated insolubles as they grew. Salts, commonly sylvite, in desiccation cracks are commonly elongated perpendicular to the crack walls. This suggests a rapid,

competitive growth of crystals. Many salts may have been selectively dissolved and recrystallized by post-burial fluids.

Very fine, straight bedding in halite (colour-banded halite) indicates the absence of secondary disruption or deformation, but does not preclude non-destructive recrystallization (Dellwig, 1972, Hardie et al., 1983, Hovorka, 1987). Colour-banded halite is caused by the alternation of halite with thin bands or laminae of insolubles, such as anhydrite, dolomite, clays or combinations thereof (Hovorka, 1987). These less soluble minerals may be due to periodic influxes of fresher waters, some eolian sedimentation, or both (Mossman et al., 1982, Harville and Fritz, 1986, Hovorka, 1987). It is uncertain whether or not these influxes were due to seasonal fluctuations. Dellwig (1972) attributed the alternation of cloudy halite layers with clear halite layers to seasonal fluctuations in conditions such as temperature and rate of precipitation. Annual cycles in water level and the salinity of saline playas are common in the modern environment (Last, 1989).

Shallow-brine and desiccation features

The following features in the Patience Lake Member indicate deposition in a shallow brine, salt-pan environment

(Fig. 6.1): desiccation polygons, desiccation cracks, microkarst pits, and chevron halite crystals. Wave or current action in shallow water is indicated by what appear to be catenary ripple marks in anhydrite interbeds above the White Bear Member of the Prairie Evaporite Formation at the Cominco potash mine (Meijer Drees, 1986). The Prairie Evaporite Formation is a "modified primary evaporite" because the many primary features which have survived extensive secondary processes indicate the original environment of deposition.

Desiccation polygons are evidence of subaerial exposure. In the desiccation stage of a salt pan, the continued growth of halite cement just beneath the dry surface causes lateral expansive growth of the surface crust which leads to disruption of the crust into metre-scale polygons (Lowenstein and Hardie, 1985). This process is similar to that which forms tepee structures on the edges of mega-polygons in carbonate crusts (Kendall and Warren, 1987). Subsequent flooding can cause pools of brine to form in the polygons that, upon preservation, form lenticular bodies of halite or sylvinite. The cracks may become enlarged by dissolution and filled with mud and, eventually, more salt. The old polygonal cracks may determine the position of subsequent cracks resulting in stacked polygons, which seems to have been the case in polygons observed in the PCS Cory large leach anomaly.

The cracks in the clay seam shown in Plates 8b and 9c were more likely formed subaerially (desiccation cracks) than under water (syneresis cracks, Mossman et al., 1982). Syneresis cracks tend to be shorter, more curved, and less interconnected. However, Dellwig (1972) considered similar cracks to have formed under water. Many crack networks in the clay seams of the potash mines have polygonal shapes characteristic of desiccation (Dellwig, 1972, Mossman et al., 1982).

Microkarst pits and washout channels indicate dissolution at, or near, the paleosurface because there is no disruption of overlying beds. Disturbed beds up to 50 cm above the washout channel in PCS Cory indicate that the channel formed under, but close to, the paleosurface. Baar (1974) observed similar washout features in the Esterhazy Member and attributed them to rainwater channels leading to a central sink area. Microkarst pits "formed in the unsaturated zone above the brine-water table by processes physically similar to the formation of vadose karst pits in limestone" (Hovorka, 1987, p1036), and were then filled in by insolubles and halite. Modern salt karsts (eg. <7X2 m) have been filled within a matter of a few years (Last, 1989).

Chevron textured halite is caused by the entrapment of thousands of fluid inclusions along growth zones of the

halite crystal (Roedder, 1984, Lowenstein and Hardie, 1985). Rapid growth is marked by the inclusion-rich zones, slower growth by the clearer bands. This may have occurred during diurnal temperature fluctuations, which are possible only in shallow brines (Roedder, 1984). Diurnal fluctuations in modern saline playas are known to affect the formation of different salts (Last, 1989). Chevron crystals are commonly vertically-oriented, vertically-elongated, and formed during competitive upward crystal growth into a free-standing, saturated brine.

Somewhat perplexing are the depleted stable isotope values, similar to those of Saskatchewan basinal brines, of the fluids in chevron halites (Chipley, pers. comm., 1988). Were the original brines depleted, do chevron textures form in a burial environment, or were the fluids in the inclusions replaced without destroying the structure? Until a mechanism for changing the rate of crystal growth to produce vertically-oriented, upright-pointing chevrons in the post-burial environment is found, then it is safe to assume that the chevrons are primary. Hence, their depleted stable isotopes are most likely the result of very subtle, molecule-by-molecule neomorphic processes that replaced the fluids without altering the texture (see Walls et al., 1979). That chevron crystals are uncommon in the Patience Lake Member indicates a possibility of extensive recrystallization, or only minor chevron formation in the first instance. Chevron halite tends

to be most common in clay seams; it is likely that either the insolubles protected the crystals from dissolution, or the insolubles and the chevron halite formed in a similar environment that was different from that of the rest of the sylvinite.

Potash rock types

The four sylvinite rock-types recognized in this study combine the ore-grade aspect of Klingspor's (1966) classification, and some of the colour and composition categories of McIntosh and Wardlaw (1968). The rock-types are not only useful in describing and mapping the potash, but are also genetically significant. Using them to describe lithology in the Patience Lake Member has led to recognition of a potash cycle. The rock-types and potash cycle have been identified in other potash mines in the Patience Lake Member in the Saskatoon region, but it is not yet known whether they will be applicable elsewhere. Perhaps three shortcomings of the rock-type classification are that it does not include carnallite, neither does it account for crystal size, nor for subtle changes in ore grade.

Iron oxide inclusions are concentrated in thin outer zones of sylvite crystals in D-type potash as opposed to thick zones in A-type. This may be due to one of two processes. The

most probable is that A-type sylvinite represents fast growth of sylvite (or its precursor carnallite) with the result of including a lot of hematite (or its precursor goethite) in thick zones. The sylvite of D-type potash would have grown more slowly, displacing the hematite until just at the end of crystal growth when large amounts of hematite were rapidly included. D-type sylvinite is most common within the 30 cm directly beneath insoluble seams, which suggests that the insolubles may have acted as insulation while the salts grew slowly. However, goethite and hematite also precipitate in the same brine environment (Sonnenfeld, 1984). Therefore, in the case of D-type potash, the iron oxides may not have formed until the very end of carnallite formation, or much of the carnallite may have grown before the arrival of iron-bearing sediments.

Where G-type sylvinite, which has less sylvite than other types of sylvinite, is laterally continuous in the regular bedded sequence (e.g. in unit M2, Fig. 4.7), it may be a result of lower salinity during primary deposition. Where it is associated with anomalies, such as near a salt anomaly contact (centre of Fig. 5.4), it is more obviously due to secondary redistribution of KCl.

9.2 POST-BURIAL HISTORY

From previous work there are abundant evidence and descriptions of the secondary or post-burial history of the Prairie Evaporite Formation. These include Cretaceous radiometric age dates (Baadsgaard, 1987); high fluid inclusion temperatures and depleted stable isotope values of halite (Chipley and Kyser, 1989), unusual bromine and rubidium values for halite and sylvite (Wardlaw, 1968), secondary distribution of carnallite (Holter, 1969), halite and sylvite crystals preferentially aligned with regional structures (Clark, 1964), petrographic relationships (Schwerdtner, 1964; Wardlaw and Schwerdtner, 1966; McIntosh and Wardlaw, 1968; Wardlaw, 1968; Holter, 1969; Fuzesy, 1983), some salt anomalies, and most collapse structures (eg. McIntosh and Wardlaw, 1968; Mackintosh and McVittie, 1983).

According to McIntosh and Wardlaw (1968) the three major geological events to form the potash deposits were: 1) deposition of halite and carnallite, 2) brines transformed carnallite to sylvite possibly leaving some carnallite and recrystallizing some halite, and 3) leaching of residual carnallite from the ore beds while localized, more intense leaching removed sylvite leaving salt anomalies. Both of Holter's (1969) hypotheses for the genesis of the potash beds involve post-burial replacement of carnallite by sylvite due

to $MgCl_2$ being leached by downward percolating halite-saturated brines. The $MgCl_2$ brines later precipitated carnallite in areas that commonly cross-cut bedding. His mechanism for salt dissolution involves basement faulting that stimulated the release of water from the permeable beds and mounds of the Winnipegosis Formation.

Wardlaw (1968) suggests that the carnallite-sylvite transition occurred soon after deposition. Surface leaching of carnallite to form sylvite, is the best explanation for Quaternary potash in Ethiopia (Holwerda and Hutchinson, 1968). However, both Holter (1969) and Baadsgaard (1987) suggest that the Cretaceous was a time of major dissolution and subsequent recrystallization in the Prairie Evaporite potash. Using Rb-Sr and K-Ca systematics, Baadsgaard (1987) concluded that "the formation of sylvite from primary carnallite likely took place near the end of the Devonian, and extensive <u>in-situ</u> recrystallization of the salts occurred during a period of salt removal in the Cretaceous. Since the Upper Cretaceous, sylvite has been locally converted to carnallite by the sporadic action of Mg-rich brines." The role and timing of the effects of secondary fluids on the Prairie Evaporite Formation are clearly very complex.

Formation waters within the Saskatchewan Sub-basin are thought to be recharged from the central Montana uplift

(Wittrup, 1987), which resulted from Cretaceous mountain building. Large volumes of salt have been dissolved in southeast Saskatchewan. Numerous collapse features, and leach-collapse anomalies indicate that the dissolution of salt has been going on for some time. Leaching of the salts continues today as seen in salt springs and seepages on the edge of the sedimentary basin (Fuzesy, 1982), and in our own accelerated solution mining and accidental floods. Unusually depleted values of deuterium and ^{18}O of fluids from ore-zone halite suggest that the salts may have formed from basinal fluids derived from meteoric waters (Chipley and Kyser, 1989).

Origins of the salt anomalies

Many features associated with collapse anomalies are obviously secondary. These include: elongated salt beds, folds in the salt strata, collapse features, split clay seams with injected salt, and coarse recrystallized halite, all of which indicate post-burial salt movement. Recent (10-20 years) movement that formed mylonites and filled old mine openings, shows how quickly the salt can move.

The leach-collapse anomaly in the southwest of PCS Cory overlies the flank of a Winnipegosis mound, which probably provided an aquifer and structural irregularities to cause the anomaly in a manner similar to that suggested by

Gendzwill (1978) and Wilson (1985). The leach anomaly in the north of PCS Cory (Fig. 5.5) seems to be secondary, in that red and orange halite derive their colour from hematite leached from sylvite (see p. 138). However, because bedding is preserved, it remains speculative as to whether this occurred in the post-burial environment. The large leach anomaly in the vicinity of the #2 shaft, PCS Cory (Figs. 2.1, 4.3), preserves bedding, has very little orange halite, includes preserved polygons, and therefore seems to be syndepositional. However, a small but deep collapse feature within it, indicates a post-burial component to its origin. Perhaps an original, fracture-induced depression in the primary environment developed a secondary fracture system. In Quaternary potash deposits of Ethiopia, Holwerda and Hutchinson (1968) found barren halite bodies lying along fracture zones.

Whether dissolution occurred on the salt-flat surface or subsurface can only be determined if the top of the anomaly may be seen, as in washout channels, or if blocks of overlying sediments (eg. Dawson Bay breccia) are found in collapse anomalies. Surface depressions can arise in several ways, including wind-erosion, surface dissolution due to channels leading into topographic lows (Baar, 1974), or spring discharges (Renaut, pers. comm., 1988). Subsurface salt dissolution can occur in many modern playas, and may cause subsidence and surface depressions in which funnel-shaped

collapse structures can develop (Renaut, pers. comm., 1988). Similar dissolution can also occur in the post-burial environment, resulting in the collapse of significant overlying strata (Gorrell and Alderman, 1968). Leach anomalies, which do not destroy clay seams, tend to be funnel- or saucer-shaped (Fig. 5.1c). In the sedimentary environment they could form if water undersaturated with respect to sylvite, but saturated with respect to halite, were to percolate down through the potash during evaporitic drawdown (Holwerda and Hutchinson, 1968). In the post-burial environment, if the water were to rise up a zone of permeability it could spread laterally into a saucer shape where it encounters a compacted, impermeable clay seam, such as the Second Red Beds (Renaut, pers. comm., 1989).

Colour changes in insoluble seams from 5 to 150 metres from an anomaly, are a long-known geologic indicator of some anomalies (Danyluk, pers. comm., 1987). A less obvious indicator is an unusual distribution of low-grade (G-type) potash beneath the 411 seam, such as large blebs (eg. >200 cm^2) of G-type potash cross-cutting units M4 and M5 about 5 m from the large leach anomaly, and a very thin sub-clay unit beneath the 411 seam, the lower contact of which is very irregular and gradational into G-type potash. This probably results from partial dissolution of sylvite at the extreme end of the leaching front. In some locations, the 412 seam is

underlain by 1-5 cm of brown halite, but this does not seem to indicate the proximity of an anomaly. Although they have similarities, all anomalies are different. Common indicators may exist equally for two very different types of anomalies. The leaching front may extend beyond the ore-anomaly contact, especially as seen along clay seams and, where it reaches KCl saturation, recrystallized sylvite may be expected.

Linn and Adams (1966) noticed that pods and lenses of langbeinite, leonite, kainite, recrystallized halite, and recrystallized sylvite occur in ore near the salt anomalies in potash deposits of Carlsbad, New Mexico. The coarsely crystalline halite and sylvite were localized along clay seams and at the contacts between halite marker beds and ore members (Linn and Adams, 1966). Other than the G-type potash, no recrystallized salt, unusual minerals, or significant changes in crystal size were noticed in the ore beds close to any of the PCS Cory anomalies; however, detailed petrographic studies were not carried out.

Within the potash cycle, the sporadic distribution of lenses and blebs of one potash rock type in another is postulated to be the result of post-burial recrystallization. The unusual wispy distribution of hematite in B-type potash and the lack of other insolubles suggests that the minor amounts of hematite were derived from fluid transport and

secondary recrystallization. The finely layered sylvinite, such as in unit M2 of sections 100 (Fig. 4.6 in pocket) and 44 (Fig. 5.2 in pocket), is of ambiguous origin.

The timing of halite overgrowths and euhedral anhydrite laths is unknown although, most likely, secondary. Secondary halite overgrowths may be found around chevron and hopper fluid inclusion textures (Plate 11b). They are especially common within, and near, salt anomalies. Authigenic anhydrite laths adjacent to sylvite (Plate 13a) are a contradiction to the evaporite phase rule. The evaporite phase rule of Borchert (1972) states that only adjacent members of the evaporite series can precipitate together simultaneously. Secondary anhydrite found in the halite of a secondary leach-collapse salt anomaly (see p. 122), would be in harmony with the evaporite phase rule. This would indicate that the anhydrite laths in Plate 13a formed at the same time as the leach salt anomaly, which was only 1m away. However the timing of the leach anomaly is ambiguous.

In the leached portions of anomalies #1 and #2, stratigraphically lower units show a higher degree of replacement of sylvite by halite than do overlying units. There are two basic mechanisms to explain this. Whatever the source of leaching fluids, whether from above, below, or the sides, they exited downward. The salinity either increased as

the fluids reached lower levels, thereby precipitating more halite in lower units, or fluids of more-or-less constant salinity resided longer in lower than in higher units. If the salinity increased downward, then at even lower levels recrystallized sylvite may be expected. Compacted clay seams, such as those closely spaced at the top of the ore zone, acted as permeability barriers that served to retain fluids while salts formed. Another mechanism to explain the different volume reductions in different units, would require that the higher units had greater contact with aquifers (Reeves, pers. comm., 1989). In anomaly #3 the banded halite between seams 413 and 414 remained essentially undisturbed, while under- and overlying units showed significant losses of volume. This suggests that a chemical gradient provided a significant drive to move the fluids; as sylvite was dissolved by NaCl-saturated fluid, the permeability was increased in these strata allowing for further brine migration.

Different strengths of leaching result in secondary facies

The effects of leaching decrease from the interior of the anomalies toward their edges. They range from weak to strong, from selectively preserving delicate laminae and chevron textures near the edges of anomalies to deforming and destroying salt beds near the centres. The red halite found only in anomalies represents a late or weak stage in the

leaching process in which sylvite has been dissolved and potassium has been removed without unduly disturbing the hematite. The hematite may have restricted the subsequent growth of halite because it is only found in small, anhedral halite crystals. Orange and pink halite result from advanced recrystallization after fluids have had enough time, and/or chemical conditions were appropriate (i.e. reducing), to remove much of the hematite. Brown halite derives its colour from the insolubles that were likely enriched by hematite. An abrupt contact between red and grey halite (section 112, Fig. 5.5 in pocket) may represent a chemical front within the leaching fluids.

The dissolution process has varied in scale. The largest and most completely dissolved areas are the no-salt area south of Saskatoon and the eroded northeast edge of the Prairie Evaporite Formation (Fig. 1.1). Based on the anomalies studied and the observations of Holter (1969), four secondary facies (Fig. 9.4) showing decreasing effects away from the centre of leaching, can be recognized. In the "centres" of these areas (the most extremely leached) there are collapse breccias of mud and limestone where salts and anhydrite of the Prairie Evaporite Formation have been completely dissolved (Holter, 1969). Farther from the centre, the next secondary facies to be encountered would be collapse breccias of mud, limestone, and anhydrite; recrystallized halite would also be

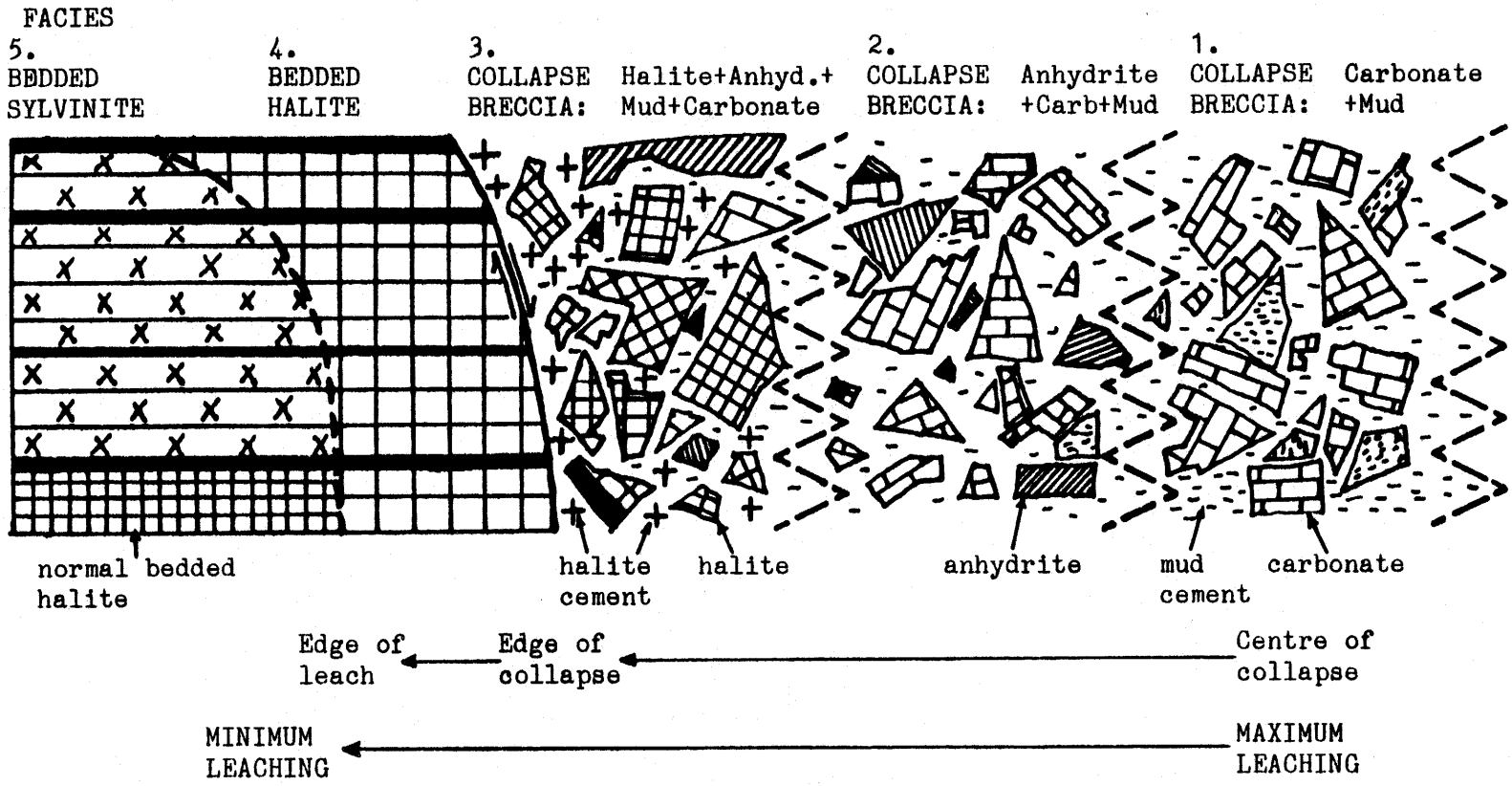

Fig.94.Cross-section of one half of an idealized solution-collapse structure showing relationships between secondary facies. Scale varies, e.g. from edge of leach to centre of collapse may be 100 to 500 or more metres.

found in the breccias. Leach salt anomalies, which preserve bedding, would be still farther from the source of leaching fluids. Finally, subtle disturbances in the potash beds, such as changes in clay seam colour, would mark the extreme limit of the leaching front.

The secondary facies are similar to primary facies because both follow the evaporite phase rule of Borchert (1972). However, the two processes are opposite in nature and direction because, while one forms the chemical sediments in the depositional environment, the other destroys them in the post-burial environment.

Several factors determine the extent to which the deposits may be dissolved. These include: time, and the salinity, amount and gradient of the leaching fluid. The location of the leach centre is probably determined by structural irregularities, such as basement faults (Smith and Pullen, 1967), the central Montana uplift, or underlying fractured Winnipegosis mounds (Gendzwill, 1978, Wilson, 1985), and by the availability of an aquifer. Most salt anomalies encountered in the potash mines, many being partially exposed, seem to be the less intense end of the spectrum of secondary facies.

In some areas, one facies may be negligible, as in the case where bedded sylvinite contacts halite breccia (Fig. 5.4), but it is highly unlikely that several facies would be missing as suggested in some of Holter's (1969) structural cross-sections. In the cross-sections that correlate into the no-salt area of southwest Saskatchewan (Holter, 1969, Figs. 33, 36, 37), it is misleading to see potash members abutting the no-salt depressions. The change is most likely more gradational than the cross-sections indicate, and, if even for a short distance, potash has probably been leached farther from the edge of the no-salt area. There is a limit to what well data can indicate. Nevertheless, on the northeastern edge of, and within the Prairie Evaporite Formation, Holter (1969) was able to identify gradual thinning and impoverishment of salts as leached centres were approached. He suggested that "greater" leaching, such as in the southwest no-salt area, led to more abrupt thinning of beds. Fresh headwaters from the Cretaceous Montana Uplift were probably the chief factors that led to "greater" (ie. faster) leaching.

There are other variations or problems associated with identifying secondary facies that result from the dissolution of evaporites. Depositional and dissolution thinning of the Prairie Evaporite Formation may be differentiated by the presence of collapse breccias that involve significantly thick portions of overlying rocks

(Oglesby, 1987). Also, depositional thinning by onlap is characterized by bottom to top thinning of the Prairie Evaporite Formation (Oglesby, 1987). Different leaching events can lead to confusing relationships between the secondary facies. The timing of leaching events may be determined by knowing the last units to have collapsed in the overlying rock record (Smith and Pullen, 1967, Gorrell and Alderman, 1968). Within the Patience Lake Member potash mines, unless the breccias include fragments of at least the Second Red Beds or Dawson Bay Formation, the collapse breccias are not necessarily diagnostic of secondary leaching. Minor leaching of potash in the post-burial environment can lead to leach anomalies that are indistinguishable from those that may have formed in the depositional environment.

Chapter 10. CONCLUSIONS AND RECOMMENDATIONS

The main success in this study lies in developing and applying a simple, yet effective, classification of potash rock types. As a result, the stratigraphic norm has been set for the Patience Lake Member, especially for the ore zone. The implications for interpreting the geological history of potash are significant. It has also been demonstrated that this can have repercussions on the ability to locate salt anomalies.

10.1 GEOLOGICAL HISTORY

The potash deposits of the Middle Devonian Prairie Evaporite Formation were most likely formed in a vast, continental, epeiric sea. The shallow brines were commonly evaporated to the point of desiccation, exposing huge salt flats. Although the ocean was a prime source of solutes and insolubles, the contribution of meteoric waters was probably significant. Highly saline floods and refluxing interstitial brines probably resulted in potash formation above clay seams. Other floods and interstitial brines were less saline, and resulted in facies changes.

The potash cycle is a result of the cyclic deposition of the insolubles. As the disseminated insolubles were most likely wind transported (Harville and Fritz, 1986),

their amount may be directly related to the proximity of their source and the wind velocities. High amounts of disseminated insolubles and abundant iron oxide inclusions in sylvite are found in A-, D- or G-type potash. It seems likely that the process of stripping the iron from continental weathering products, converting it to goethite, incorporating it as inclusions into carnallite, and recrystallizing it to hematite, was restricted to the immediate vicinity (within 10 cm) of the insolubles. The minor iron oxides in insoluble-poor B-type potash probably came from secondary redistribution processes. The differences in the potash rock-types reflect genetic differences, such as salinity, rate of crystallization, and influence of insolubles. Except where there was collapse of strata, the post-burial redistribution of insolubles, other than iron oxides, was insignificant. In the primary environment, possible disconformities created by the dissolution of overlying potash-bearing beds may be indicated by an abundance of residual hematite in clay seams.

Dolomite, which was mostly deposited by wind and flood, is the most abundant insoluble mineral. Other detrital minerals include quartz, micas, clays, perhaps some anhydrite, and organic remains, such as spores and microfossils. Septechlorite, mixed-layer swelling-chlorite/chlorite, and some chlorite probably formed in the syndepositional environment. Magnesium enrichment, especially of chlorites, is

diagnostic of marine brine alterations. In the syndepositional environment, goethite was formed as inclusions in carnallite beneath the sediment surface. When carnallite was altered to sylvite, the goethite probably recrystallized to hematite (Wardlaw, 1968). Some post-burial anhydrite formed in the salt anomalies.

Thin halite rims between sylvite crystals indicate that the sylvite or its likely precursor, carnallite, grew in a crystalline halite "mush". Nucleation and interstitial growth of potash salts beneath the salt surface is not surprising because, as Braitsch (1971) and others (eg. Borchert, 1972) point out, very little water is left by the time potash salts precipitate from a marine source. Halite would continue to crystallize at the same time.

The effects of leaching vary in scale from megascopic to microscopic - from collapse structures to preserved chevron halites in sylvinite and leach anomalies. At the large scale, there may be up to five secondary facies, ranging from collapse breccias of carbonates and mud to bedded sylvinite. The leaching was progressively weaker from the centre of anomalies to their edges. The degree to which hematite inclusions are retained in halite after sylvite is dissolved is a possible indicator of the relative strength of leaching. Where bedding is preserved, it is likely that the

mechanism of dissolution and recrystallization was slow and sub-microscopic, with fluids travelling along grain boundaries - similar to the molecule-by-molecule neomorphic replacement that has preserved fossils.

In leach anomalies that preserve bedding, lower beds having a better replacement of sylvite by halite than higher beds, suggests that the salinities of the fluids may have increased vertically downward, or that leaching fluids exited downward. The sylvinite beds provided a chemical gradient for the movement of NaCl-saturated fluids.

10.2 INDICATORS OF ANOMALOUS GROUND

Perhaps the most successful methods of predicting anomalies have been carried out by Mackintosh and McVittie (1983). Seismic surveys and ore bed contouring indicate broad, relatively flat areas that generally produce good mining conditions. Closed lows and sharply changing elevations suggest the probability and direction of problem areas. Seismic methods can be used to identify Winnipegosis mounds and major solution collapse features, but are less effective in identifying salt anomalies. The location and delineation of the mounds and local collapse structures by seismic surveys are extremely helpful in the potash mining industry. Drilling shallow holes in the roof of mine entries can identify the top

of a saucer-shaped leach anomaly while an increase in the KCl of the ore beds provides an additional warning of a leached zone (Mackintosh and McVittie, 1983). Radar and sonar methods have had limited use in the detection of collapse features (Mackintosh and McVittie, 1983).

Geologic indicators close to an anomaly include: colour changes in insoluble seams from 5 to 150 metres from an anomaly, and in the case of PCS Cory, at least, unusual amounts of G-type potash within 2 m beneath the 411 clay seam. Once the normal variation of potash in the Patience Lake Member was established, especially in the ore zone, peculiarities were able to be recognized. The low-grade (G-type) potash was found either as large blebs (eg. >200 cm^2) cross-cutting units M4 and M5 (just below seam 411) about 5 m from an anomaly, or as a layer with an irregular, gradational upper contact. These are probably the effects of partial leaching of sylvite. The Winnipegosis mound beneath the leach-collapse anomaly identified by seismic methods was another helpful indicator. Common indicators may exist equally for two very different types of anomalies.

Within an anomaly, indicators of a major collapse feature may include: stretched clay seams, folded beds, small collapse features (1-20 m), split clay seams with injected salt, and unusual (eg.>10 m) drops in elevation.

Unfortunately, any number, or none, of these indicators may be found in the vicinity of a major collapse feature.

10.3 CONCLUDING COMMENTS

The variability of anomalies makes it very hard to predict whether or not it would be economical to mine a passageway through, around, or back off from, an anomaly that has been encountered. It is primarily for this reason, and the present lack of data on salt anomalies, that further research is recommended. Nevertheless, the results of this study indicate that if there are indicators of a major collapse to an anomaly, it would be unwise to try and mine a passageway through the structure. Rather the miner should be made to back off from, or go around the anomaly. Although in plan view anomalies are of irregular and lobate shapes, the general outline tends to be circular. Presently, there are insufficient data on attempts to circumnavigate an anomaly.

The first research proposal is that a compendium be made on all the salt anomalies in Saskatchewan. This would help the mine geologist to understand what the possible variations of an anomaly may be.

More specifically, research is recommended into the distribution of anhydrite in both salts and clay seams from

normal potash right into the interior of an anomaly. This is based on the finding of this project that anhydrite amounts were significantly higher in a vertical suite of samples from a leach-collapse anomaly than from samples in ore. The results of such a project would test the hypothesis that anhydrite amounts may increase close to an anomaly.

Further petrographic research may reveal new or recrystallized minerals in the proximity of some anomalies, as found by Linn and Adams (1966) in the Carlsbad salts of New Mexico. The leaching front may extend beyond the ore-anomaly contact, especially along clay seams, and where it reached KCl saturation, recrystallized sylvite may be expected. Some specific targets to aim for include: unusual distributions of sylvite-poor G-type potash blebs cross-cutting ore-zone units in the close vicinity of an anomaly, ore-grade and crystal-size analyses as an anomaly is approached, and checking for corroded chevrons and other overprints on primary halite as an anomaly is approached.

A close look at the salts and brines of the tailings piles of the potash mines may reveal hitherto unknown aspects of potash deposition. A better, more accurate model of the small-scale processes and features involved in potash deposition would be a helpful comparison-tool for finding indicators of the proximity of salt anomalies.

A palynological study of the clay seams of the potash mines and of the Prairie Evaporite Formation would be beneficial. Biostratigraphic correlations could be made that are not only useful to determine relative ages, but may correlate ("fingerprint") between clay seams or sets of clay seams. This could give indications of the stratigraphic origin of insolubles in salt anomalies. Also, the extent of a meteoric water influence could be determined by studying the distribution of large spores.

There are two important advantages to continuing research into the geology and geochemistry of the Prairie Evaporite and associated formations. First, an increased understanding of the primary and secondary environments of formation can lead to improving strategies for ore grade control. For example, a primary shallow-water-subarial environment of potash deposition implies that some anomalies have resulted from surface runoff leading into sinkholes. With this knowledge, predicting the locations of these anomalies may be made easier. And secondly, a geologic solution to the problems of ore grade control is inexpensive compared to other methods.

REFERENCES

Anderson, S.B. and Swinehart, R.P., 1979. Potash salts in the Williston Basin, U.S.A. Econ. Geol., **74**: 358-376.

Baadsgaard, H., 1987. Rb-Sr and K-Ca isotope systematics in minerals from potassium horizons in the Prairie Evaporite Formation, Saskatchewan, Canada. Chem. Geol., **66**: 1-15.

Baar, C.A., 1974. Geological problems in Saskatchewan potash mining due to peculiar conditions during deposition of potash beds. In: Coogan, A.H. (Editor), 4th Symposium on Salt, N. Ohio Geol. Soc., Cleveland, **1**: 101-118.

Baillie, A.D., 1953. Devonian system of the Williston Basin area. Manitoba Mines Branch, Publ. 52-5.

Birks, H.J.B. and Birks, H.H., 1980. Quaternary palaeoecology. Edward Arnold, London, 289 pp.

Bishop, R.A., 1954. Saskatchewan exploratory progress and problems. In: Clark, L.M. (Editor) Western Canada Sedimentary Basin, Am. Assoc. Petrol. Geol., Tulsa, pp. 474-485.

Bodine, M.W.Jr. and Standaert, R.R., 1977. Chlorite and illite compositions from Upper Silurian rock salts, Retsof, New York. Clays Clay Mineral., **25**: 57-71.

Borchert, H. and Muir, R. O., 1964. Salt deposits: The origin, metamorphism and deformation of evaporites. Van Nostrand, Princeton, 300 pp.

Borchert, H., 1972. Secondary replacement processes in salt and potash deposits of oceanic origin. Geology of saline deposits, Proc. Hanover Symp., 1968, pp . 61-68.

Boys, C., Langford, F.F., Renaut, R.W., & Danyluck, T., 1986. The clay rocks in the PCS Mining Limited, Cory Division Potash Mine, Saskatchewan. In: Summary of Investigations 1986, Sask. Geol. Surv., Misc. Report 86-4, pp. 179-182.

Braitsch, O., 1971. Salt deposits: Their origin and composition. Springer, New York, 275 pp.

Brindley, G.W., 1951. X-ray identification and structure of clay minerals. Mineralogical Society, London, 345 pp.

Brindley, G.W., 1981. X-ray identification (with ancillary techniques) of clay minerals. In: F.J. Longstaffe (Editor), Short Course in Clays and the Resource Geologist. Mineral. Assoc. Canada, Edmonton. 199 pp.

Brodylo, L.A. and Spencer, R.J., 1987. Depositional environment of the Middle Devonian Telegraph salts, Alberta, Canada., Bull. Can. Petrol. Geol., **35**: 186-196.

Brown, B.E. and Bailey, S.W., 1962. Chlorite polytypism: I. regular and semi-random one-layer strucures. Am. Mineral. **47**: 819-850.

Brown, G. and Brindley, G.W., 1980. X-ray diffraction procedures for clay mineral identification. In: Brindley, G.W. and Brown, G. (Editors), Crystal structures of clay minerals and their X-ray identification. Mineralogical Society Monograph No. 5, 1980, London, 495 pp.

Carroll, D., 1970. Clay minerals: a guide to their identification. Geol. Soc. Am., Spec. Pap. 126, 80 pp.

Chipley, D.B.L., 1987. Potassium ion selective electrode analysis of potash samples. Unpublished report, PCS Mining Ltd.

Chipley, D.B.L and Kyser. T.K., 1989. Fluid inclusion evidence for the deposition and diagenesis of the Patience Lake Member of the Devonian Prairie Evaporite Formation, Saskatchewan, Canada. Sed. Geol., **64**: 287-295.

Clark, A.R., 1964. Petrofabric analysis of potash ore beds, Esterhazy, Saskatchewan., Unpublished M.Sc. thesis, Univ. Sask., Saskatoon, Saskatchewan.

Danyluck, T., 1981. Geology of the decline to the bottom of no.1 shaft, part A, potash section. Unpublished report, PCS Mining Ltd., Cory Division.

Deer, W.A., Howie, R.A. and Zussman, J., 1966. An introduction to the rock forming minerals. Longman, London, 528 pp.

Dellwig, L.F. and Evans, R., 1969. Depositional processes in Salina salt of Michigan, Ohio, and New York. Am. Assoc. Petrol. Geol. Bull., **53**: 949-956.

Dellwig, L.F., 1972. Primary sedimentary structures of evaporites. Geology of saline deposits, Proc. Hanover Symp., 1968, pp. 53-60.

Drever, J.I., 1982. The Geochemistry of natural waters. Prentice-Hall, New Jersey, 388 pp.

Droste, J., 1963. Clay mineral composition of evaporite sequence. In: Bersticker, A.C., Hoekstra, K.E., and Hall, J.F. (Editors), 1st Symposium on Salt, N. Ohio Geol. Soc., Cleveland, pp. 47-54.

Ellwood, R., Wong, M., Armstrong, K. and Mular, A.L., 1983. Assay of potash ore with ion electrodes. IN: McKercher, R.M. (Editor) Potash technology, Pergamon, Oxford, pp. 533-539.

Eugster, H.P., 1984. Geochemistry and sedimentology of marine and nonmarine evaporites. Eclog. Geol. Helv., **77**: 237-248.

Fisher, R.S., 1988. Clay minerals in evaporite host rocks, Palo Duro Basin, Texas Panhandle. J. Sed. Petrol., **58**: 836-844.

Fisher, R.S. and Hovorka, S.D., 1987. Relations between bromide content and depositional processes in bedded halte, Permian San Andres Formation, Palo Duro Basin, Texas. Carb. Evap., **2**: 67-82.

Fowler, C.M.R. and Nisbet, E.G., 1985. The subsidence of the Williston Basin. Can. J. Earth Sci., **22**: 408-415.

Friedman, G.M., 1980. Review of depositional environments in evaporite deposits and the role of evaporites in hydrocarbon accumulation. IN: Les evaporites: Mecanismes, diagenese, et applications., Bull. Cent. Rech. Explor.-Prod., pp. 589-608.

Fuzesy, A., 1982. Potash in Saskatchewan. Rep. Sask. Geol. Surv., **181**: 44 pp.

Fuzesy, L.M., 1983. Petrology of potash ore in the Middle Devonian Prairie Evaporite, Saskatchewan. IN: McKercher, R.M. (Editors) Potash technology, Pergamon, Oxford, pp. 47-57.

Garrels, R.M., 1960. Mineral equilibria at low temperature and pressure. Harper, New York, 254 pp.

Gendzwill, D.J., 1978. Winnipegosis mounds and Prairie Evaporite Formation of Saskatchewan - Seismic study. Am. Assoc. Petrol. Geol. Bull., **62**: 73-86.

Gornitz, V.M. and Schreiber, B.C., 1981. Displacive halite hoppers from the Dead Sea; some implications for ancient evaporite deposits. J. Sed. Petrol., **51**: 789-794.

Gorrell, H.A. and Alderman, G.R., 1968. Elk Point Group saline basins of Alberta, Saskatchewan, and Manitoba, Canada. IN: International conference on saline deposits, 1962, Geol. Soc. Am., Spec. Pap. **88**, pp. 291-317.

Goudie, M.A., 1957. Middle Devonian potash beds of Central Saskatchewan. Unpublished report, Sask. Dept. Min. Resources.

Grayston, L.D., Sherwin, D.F., and Allen, J.F., 1964. Middle and Upper Devonian. IN: Geological history of western Canada, Alta. Soc. Petrol. Geol., pp. 49-85.

Hardie, L.A., 1984. Evaporites: marine or non-marine? Am. J. Sci., **284**: 193-240.

Hardie, L. A., Lowenstein, T. K. and Spencer, R. J., 1985. The problem of distinguishing between primary and secondary features in evaporites. Sixth Symposium on Salt, 1983, N. Ohio Geol. Soc., Cleveland, Ohio, **1**: 11-39.

Harding, S.R.L. and Gorrell, H.A., 1967. Distribution of the Saskatchewan beds. Can. Min. Metall. Bull., **60**: 682-687.

Harville, D.G. and Fritz, S.J., 1986. Modes of diagenesis reponsible for observed succession of potash evaporites in the Salado Formation, Deleware Basin, New Mexico. J. Sed. Petrol., **56**: 648-656.

Hey, M.H., 1954. A new review of the chlorites. Mineral. Mag., **30**: 277-292.

Hite 1983. The sulphate problem in marine evaporites. IN: Coogan, A.H. (Editor) 6th Symposium on Salt, N. Ohio Geol. Soc., Cleveland, **1**: 217-230.

Holter, M.E., 1969. The Middle Devonian Prairie Evaporite of Saskatchewan. Rep. Sask. Dept. Min. Resour., **123**: 1-134.

Holwerda, J. G. and Hutchinson, R. W., 1968. Potash-bearing evaporites in the Danakil area, Ethiopia. Econ. Geol., **63**: 124-150.

Hovorka, S.D., 1987. Depositional environments of marine-dominated bedded halite, Permian San Andres Formation, Texas. Sedimentology, **34**: 1029-1054.

Hower, J., 1981. X-ray diffraction identification of mixed-layer clay minerals. In: F.J. Longstaffe (Editor), Short course in clays and the resource geologist. Mineralogical Assoc. Canada, Edmonton. 199 pp.

JCPDS, 1983. Powder diffraction file: Alphabetical index, inorganic phases. JCPDS Int. Centre for Diffraction Data, Swarthmore, Penn., 1023 pp.

Jordan, S.P., 1967. Sask. reef trend looks big. Oilweek, pp. 10-12.

Jones, C.L., 1972. Permian basin potash deposits, south-western United States. Geology of saline deposits, Proc. Hanover Symp., 1968, pp. 191-201.

Kendall. A.C., 1989. Brine mixing in the Middle Devonian of western Canada and its possible significance to regional dolomitization. Sed. Petrol., **64**: 271-285.

Kendall, C.G.St.C. and Warren, J., 1987. A review of the origin and setting of tepees and their associated fabrics. Sedimentology, **34**: 1007-1027.

Keyes, D.A., 1966. Geology of the IMC potash deposit Esterhazy, Saskatchewan. Second Symposium on Salt, N. Ohio Geol. Soc., Cleveland, Ohio, **1**: 95-101.

Kinghorn, R.R.F., 1983. An introduction to the physics and chemistry of petroleum. Wiley, Toronto, 420 pp.

Klaus, W., 1966. Utilization of spores in evaporite studies. Third Symposium on Salt, N. Ohio Geol. Soc., Cleveland, Ohio, **1**: 30-33.

Klingspor, A. M., 1966. Cyclic deposits of potash in Saskatchewan. Bull. Can. Petrol. Geol., **14**: 193-207.

Knauth, L.P. and Beeunas, M.A., 1986. Isotope geochemistry of fluid inclusions in Permian halite with implications for the isotopic history of ocean water and the origin of saline formation waters. Geochim. Cosmochim Acta, **50**: 419-433.

Langford, F.F. and Boys, C., 1987. Microstratigraphy of the potash mining zone west of Saskatoon, Saskatchewan. Progr. Abstr. Joint Annu. Meet. Geol. Assoc. Can., Miner. Assoc. Can., **12**: 65 pp.

Langford, F.F., Renaut, R.W., Boys, C., & Danyluck, T., 1987. A type stratigraphic section of the ore zone of a potash mine near Saskatoon, Saskatchewan. IN: Gilboy, C.K. and Visgrass, L.W. (Editors) Economic minerals of Saskatchewan, Sask. Geol. Soc. Spec. Publ., **8**, pp. 153-158.

Last, W.M., 1989. Sedimentology of a saline playa in the northern Great Plains, Canada. Sedimentology, **36**: 109-123.

Linn, K.O. and Adams, S.S., 1966. Barren halite zones in potash deposits Carlsbad, New Mexico. Second Symposium on Salt, N. Ohio Geol. Soc., Cleveland, Ohio, **1**: 59-69.

Lounsbury, R.W., 1963. Clay mineralogy of the Salina Formation, Detroit, Michigan. In: Bersticker, A.C., Hoekstra, K.E., and Hall, J.F. (Editors), 1st Symposium on Salt, N. Ohio Geol. Soc., Cleveland, pp. 56-63.

Lowenstein, T. K., 1982. Primary features in a potash evaporite deposit, the Permian Salado Formation of West Texas and New Mexico. In: Handford, C.R., Loucks, R.G., and Davies, G.R. (Editors) Depositional and diagenetic spectra of evaporites - A core workshop, Soc. Econ. Paleontol. Mineral. Core Workshop, **3**, Calgary, Canada, pp. 276-304.

Lowenstein, T. K. and Hardie, L. A., 1985. Criteria for the recognition of salt-pan evaporites. Sedimentology, **32**: 627-644.

Mackintosh, A.D. & McVittie, G.A., 1987. Detailed stratigraphy in the Cominco potash mine. Progr. Abstr. Joint Annu. Meet. Geol. Assoc. Can., Mineral. Assoc. Can., **12**: 1-69.

Mackintosh, A.D. & McVittie, G.A., 1983. Geological anomalies observed at the Cominco Ltd. Saskatchewan potash mine. IN: McKercher, R.M. (Editor) Potash technology, Pergamon, Oxford, pp. 59-64.

Meijer Drees, N.C., 1986. Evaporitic deposits of Western Canada. Geol. Surv. Can. Pap., pp. 85-20.

McGehee, J.R., 1949. Pre-Waterways Paleozoic stratigraphy of Alberta Plains. Bull. Am. Assoc. Petrol. Geol., **33**: 603-613.

McIntosh, R. A. and Wardlaw, N. C., 1968. Barren halite bodies in the sylvinite mining zone at Esterhazy, Saskatchewan. Can. J. Earth Sci., **5**: 1221-1238.

Milner, R.L., 1957. Effects of salt solution Saskatchewan. (Abstr.) In: First Int. Williston Basin Symposium, Conrad, Bismarck, N.D., 111 pp.

Mossman, D.J., Delabio, R.N. & Mackintosh, A.D., 1982. Mineralogy of clay marker seams in some Saskatchewan potash mines. Can. J. Earth Sci., **19**: 2126-2140.

Nautiyal, A.C., 1975. Occurrence of microplanktons in the Middle Devonian rocks of Saskatchewan and Alberta, Canada. Curr. Sci., **44**: 851-853.

Nelson, B.W. and Roy, R., 1954. New data on the composition and identification of chlorites. Proc. 2nd. Nat. Conf. Clays Clay Minerals., Nat. Res. Council, Washington D.C., **327**: 335-348.

Nelson, B.W. and Roy, R., 1958. Synthesis of the chlorites and their structural and chemical constitution. Am. Mineral., **43**: 707-725.

Oglesby, C.A., 1987. Distinguishing between depositional and dissolution thinning: Devonian Prairie Formation, Williston Basin, North America. IN: Carlson, C.G. and Christopher, J.E. (Editors) Fifth International Williston Basin Symposium, Sask. Geol. Soc. Spec. Publ. **9**, pp. 47-52.

Phillips, G.D., 1982. Nomenclature for use in Saskatchewan potash. Unpublished report of the seventh annual Canadian Institute of Mining and Metallurgy, district four meeting, Saskatoon, Saskatchewan, 18 pp.

Roedder, E., 1984. The fluids in salt. Am. Mineral., **69**: 413-439.

Schoen, R., 1962. Semi-quantitative analysis of chlorites by X-ray diffraction. Am. Mineral., **47**: 1384-1392.

Schreiber, B.C. (Editor), 1988. Evaporites and hydrocarbons. Columbia University, New York, 475 pp.

Schwerdtner, W.M., 1964. Genesis of the potash rocks in the Middle Devonian Prairie Evaporite Formation of

Saskatchewan. Bull. Am. Assoc. Petrol. Geol., **48**: 1108-1115.

Shearman, D.J. and Fuller, J.G., 1969. Anhydrite diagenesis, calcitisation, and organic laminites, Winnipegosis Formation, Middle Devonian, Saskatchewan. Bull. Can. Petrol. Geol., **17**: 182-193.

Shirozu, H., 1958a. X-ray powder patterns and cell dimensions of some chlorites in Japan, with a note on their interference colors. Mineral. J. Japan, **2**: 209-223.

Shirozu, H., 1958b. Aluminian serpentine and associated chlorite from Usagiyama, Fukuoka Prefecture, Japan. Mineral. Jour. Japan, **2**: 298-310.

Smith, D.G. and Pullen, J.R., 1967. Hummingbird structure of southeast Saskatchewan. Bull. Can. Petrol. Geol., **15**: 468-482.

Sonnenfeld, P., 1984. Brines and evaporites. Academic Press, Toronto, 600 pp.

Sonnenfeld, P. and Hudec, P.P., 1985. Clay laminations in halite: their cause and effect. Sixth Symposium on Salt, 1983, N. Ohio Geol. Soc., Cleveland, Ohio, **1**: 51-56.

Stewart, F. H., 1963. Marine evaporites. U.S. Geol. Surv. Prof. Paper 440-Y, 53 pp.

Turner, P., 1980. Continental red beds. (Developments in Sedimentology, 29), Elsevier, Amsterdam, 562 pp.

Velde, B,. 1973. Phase equilibria in the system $MgO-Al_2O_3-SiO_2-H_2O$: chlorites and associated minerals. Mineral. Mag. **39**: 297-312.

Velde, B., 1985. Clay minerals: A physico-chemical explanation of their occurence. (Developments in Sedimentology, 40), Elsevier, Amsterdam. 427 pp.

Velde, B., Raoult, J.-F. and Leikine, M., 1974. Metamorphosed berthierine pellets in Mid-Cretaceous rocks from north-eastern Algeria. J. Sed. Petrol., **44**: 1275-1280.

Walker, C.T., 1957. Correlations of Middle Devonian rocks in Western Saskatchewan. Sask. Dept. Min. Resources, Rep. **25**: 59 pp.

Walls, R.A., Mountjoy, E.W., and Fritz, P., 1979. Isotopic composition and diagenetic history of carbonate

cements in Devonian Golden Spike reef, Alberta, Canada. Bull. Geol. Soc. Am., **90**: 963-982.

Wardlaw, N.C., 1968. Carnallite-sylvite relationships in the Middle Devonian Prairie Evaporite Formation, Saskatchewan. Bull. Geol. Soc. Am., **79**: 1273-1294.

Wardlaw, N. C. and Hartzell, W., 1963. Geothermometry of halite from the Prairie Evaporite Formation. (Abstr.) Can. Mineral. Metall. Bull., **56**: 155.

Wardlaw, N.C. and Reinson, G.E., 1971. Carbonate and evaporite deposition and diagenesis, Middle Devonian Winnipegosis and Prairie Evaporite Formations of south-central Saskatchewan. Am. Assoc. Petrol. Geol., **55**: 1759-1786.

Wardlaw, N. C. and Schwerdtner, W. M., 1966. Halite-anhydrite seasonal layers in the Middle Devonian Prairie Evaporite Formation, Saskatchewan, Canada. Geol. Soc. Am. Bull., **77**: 331-342.

Warren, J.K., 1989. Evaporite sedimentology: importance in hydrocarbon accumulation. Prentice Hall, New Jersey, 285 pp.

Williams, G.K., 1984. Some musings on the Devonian Elk Point Basin, Western Canada. Can. Bull. Petrol. Geol., **32**: 216-232.

Wilson, N.L., 1985. A study of the Upper Winnipegosis mounds in south-central Saskatchewan. M.Sc. thesis, Univ. of Saskatchewan, Saskatoon, Sask., 104 pp.

Wittrup, M.B., Kyser, T.K., and Danyluk, T., 1987. The use of stable isotopes to determine the source of brines in Saskatchewan potash mines. IN: Gilboy, C.K. and Visgrass, L.W. (Editors) Economic minerals of Saskatchewan. Sask. Geol. Soc. Spec. Publ. **8**: 216 pp.

Worsley, N. & Fuzesy, A., 1979. The potash-bearing members of the Devonian Prairie Evaporite of southeastern Saskatchewan, south of the mining area. Econ. Geol., **74**: 377-388.

Yuan, J., Chengyu, H. and Keqin, C., 1985. Characteristics of salt deposits in the dry salt lake and the formation of potash beds. (Abstr.) Sixth Symposium on Salt, 1983, N. Ohio Geol. Soc., Cleveland, Ohio, **1**: 193-195.

Zharkov, M.A., 1984. Paleozoic salt bearing formations of the world. Springer, New York, 427 pp.

PLATE 1: A-TYPE SYLVINITE

a. The type sample of A-type sylvinite. Sylvite is red, and large crystals have dark or cloudy centres. Halite is clear or dark. Insolubles are pale grey. Very close observation at top centre will reveal thin "films" of halite between many sylvite crystals.

b. Smooth and rough cut A-type sylvinite. All are bulk type samples except the broken core which is sample 8.8.

c. Variations of A-type sylvinite. Large sample at left is 103.6, A(G)-type, and the small arrow indicates tops. Sample numbers (rock types as indicated) are: left to right, top row 16.8, 10.22, 15.7, 36.2; bottom row, 8.3, 36.3, 8.8 (first number of sample number indicates section - see Fig. 2.1).


A
a


A
Type A
A type
A
b

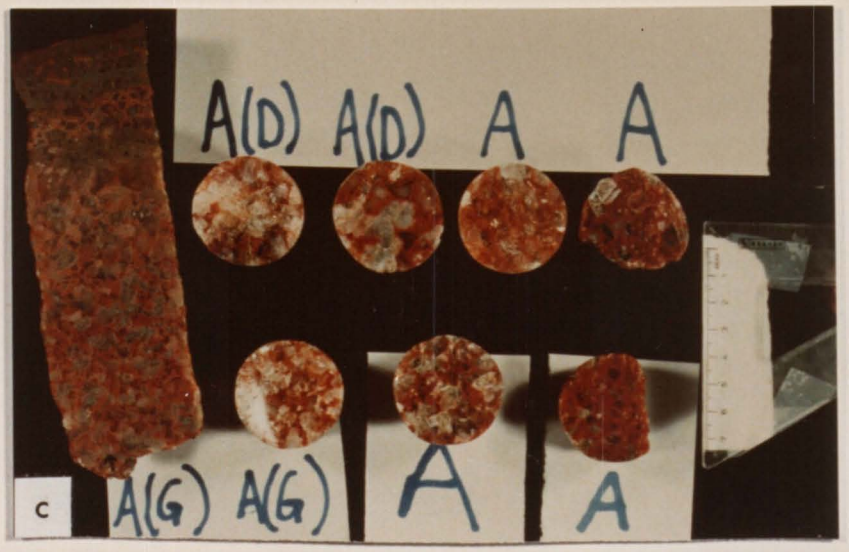
A(D) A(D) A A
A(G) A(G) A A
c

PLATE 2: B-TYPE AND D-TYPE SYLVINITE

a. Type sample of B-type sylvinite. In this view it is very hard to discern sylvite from halite; most milky white crystals are sylvite. Note the very small amount of greenish-grey insolubles in the centre.

b. Variations of B-type sylvinite. Sample numbers are, left to right: top row, 8.8, 11.12, 15.4, 4.4, 8.7, 8.6; second row (all B-types), 15.17, 15.14, 16.17, 14.18, 8A.16, 15.6; third row, 14.19, 8A.17, 29.5, 11.1, 11.2, 16.1.

c. Type sample of D-type sylvinite. Milky white and dark crystals with thin dark red rims are sylvite, halite is clear or with greeenish-grey insoluble inclusions. Insolubles are pale greenish-grey. Black lines are ink.


B
a

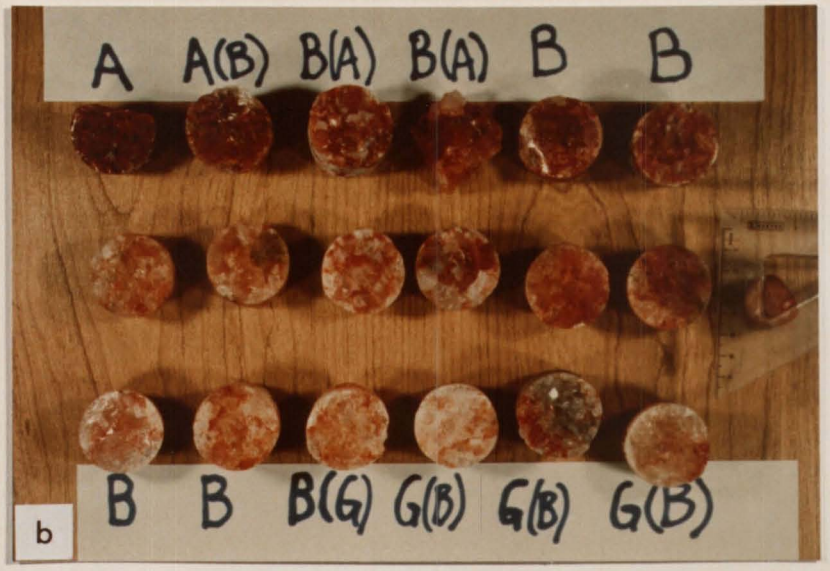
A A(B) B(A) B(A) B B
B B B(G) G(B) G(B) G(B)
b


c

PLATE 3: D-, G-, AND MIXED SYLVINITE TYPES

a. Variations of D-type sylvinte. Rock types not indicated are D-type. Sample numbers, clockwise from lower left, are: 8.8, 15.2, 14.9, 8A.15, 14.13, 15.1, 14.15, 14.20.

b. Type sample and variations of G-type sylvinite. Type sample is at far right. Rock types as indicated. Sample numbers are, left to right: top row, 8.8, 27.3, 15.16, 29.6, 8.5; bottom row, 25.1, 30.5, 28.4, 26.3, 22.8. See also variations of other rock types.

c. Lens of B-type in A-, to A(D)-type sylvinite. This sample has characteristics of all four main potash rock types. From left to right is pale A-type, then 2-3cm thick lens of B-type, then A-type, then large-grained D-type, which has thin red rims on sylvite crystals that have a somewhat patchy appearance (G-type).

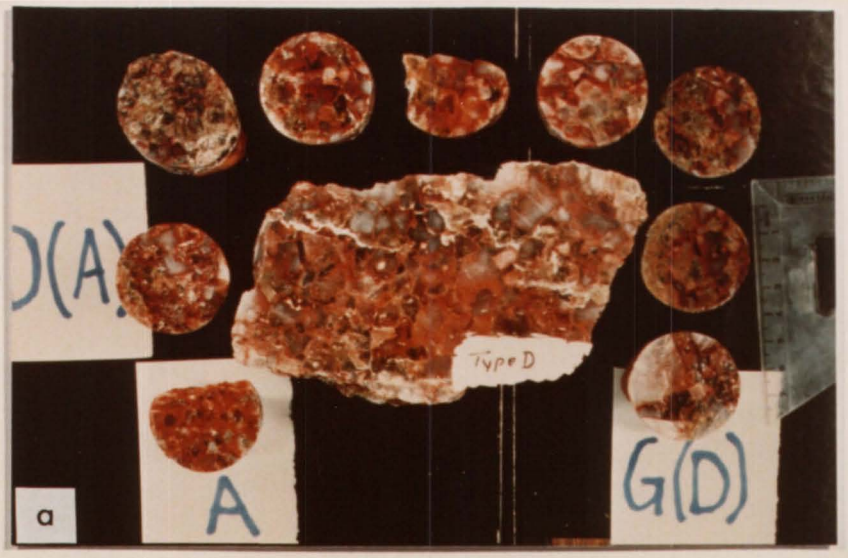
D(A)
Type D
A
G(D)
a

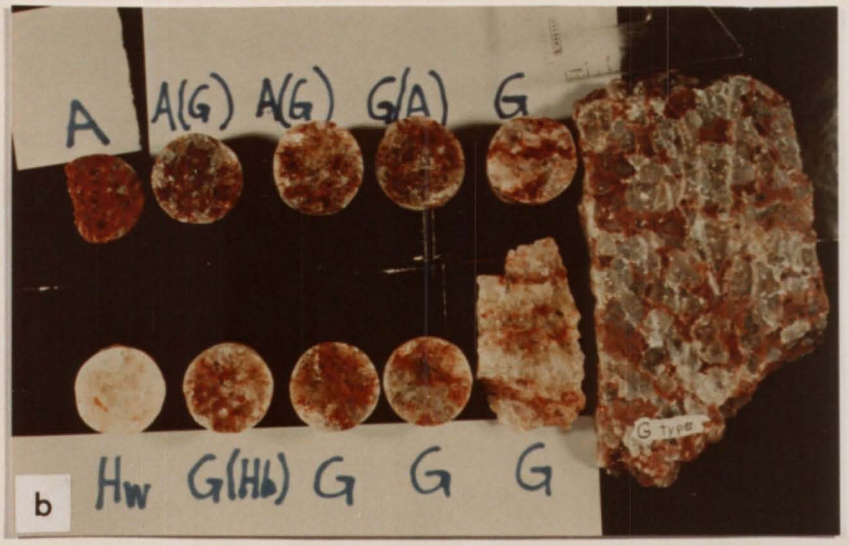
A
A(G) A(G) G(A) G
G Type
Hw G(Hb) G G G
b


A B A
c

PLATE 4: HALITE AND CLAY ROCK TYPES

a. Examples of all the main halite rock types. Rock types and sample numbers are, left to right: top row, type sample of orange halite from an anomaly, 37.2; red halite from Lanigan leach-collapse anomaly; A-type sylvinite, 8.8; bottom row, type sample of orange halite from bedded halite, 25.9; brown halite, 24.2; white halite, 25.1; grey halite, 24.4. Sylvite is red and present in samples 8.8, 25.1, and 25.9.

b. Close-up of red halite from Lanigan leach-collapse anomaly. The red insolubles are distributed mostly along boundaries of small halite crystals that act as a "matrix" to large halite crystals. Scale in mm.

c. Core samples of clay seams. Clockwise from centre left: mixed massive seam with disseminated salts and insolubles below and above, seam of disseminated salts and visible sylvite especially below insolubles, seam with disseminted salts, massive seam, mixed massive and disseminated seam.


a
0
10
20
30
40
50
60
70
80
90
100

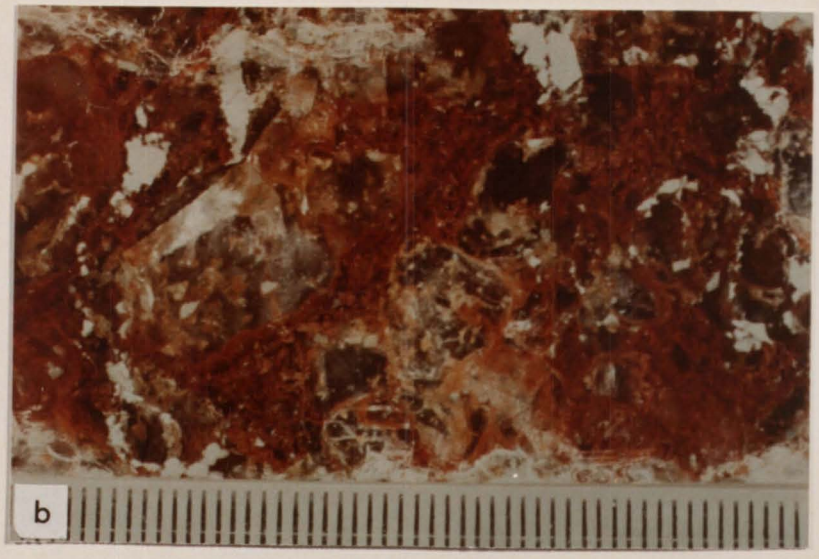
b

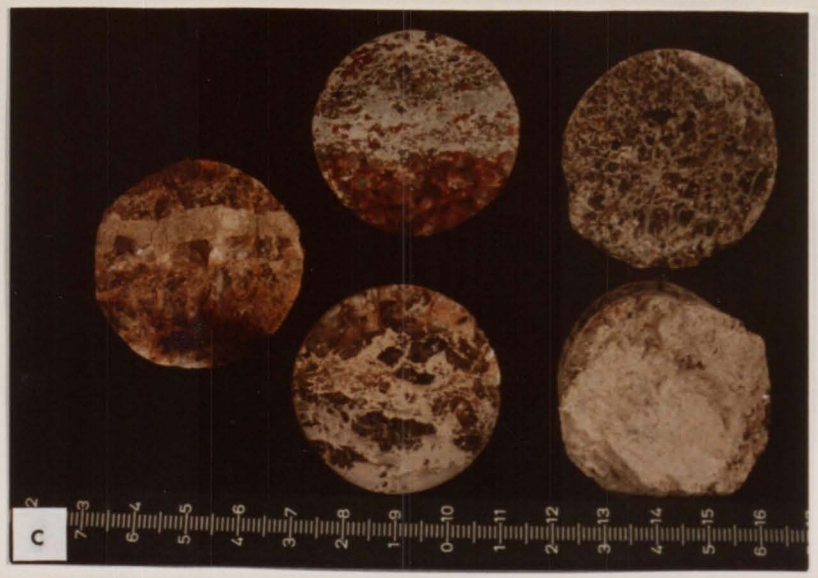
c

PLATE 5: THE TOP OF THE LOWER PATIENCE LAKE MEMBER

Banded halite, which indicates a flooding or brine freshening event, sits disconformably on clay seam #406 (seam numbers after Phillips, 1982). This marks the top of the lower Patience Lake Member (Figs. 1.3, 4.1). Potash cycles three and four (Figs. 4.1, 4.3) are shown: clay seam #404 overlain by red A-type syvinite then orange B-type followed by more red A-type, and seam #405 which completes one cycle. The next potash cycle, #4, clay seam-red-orange-red-clay seam, ends with seam #406. Note the bleb of red A-type extending down into B-type potash in the lower cycle. Taken from sections 26 and 27, PCS Cory potash mine (Fig. 2.1). Vertical curved marks are scars from the mining machine.

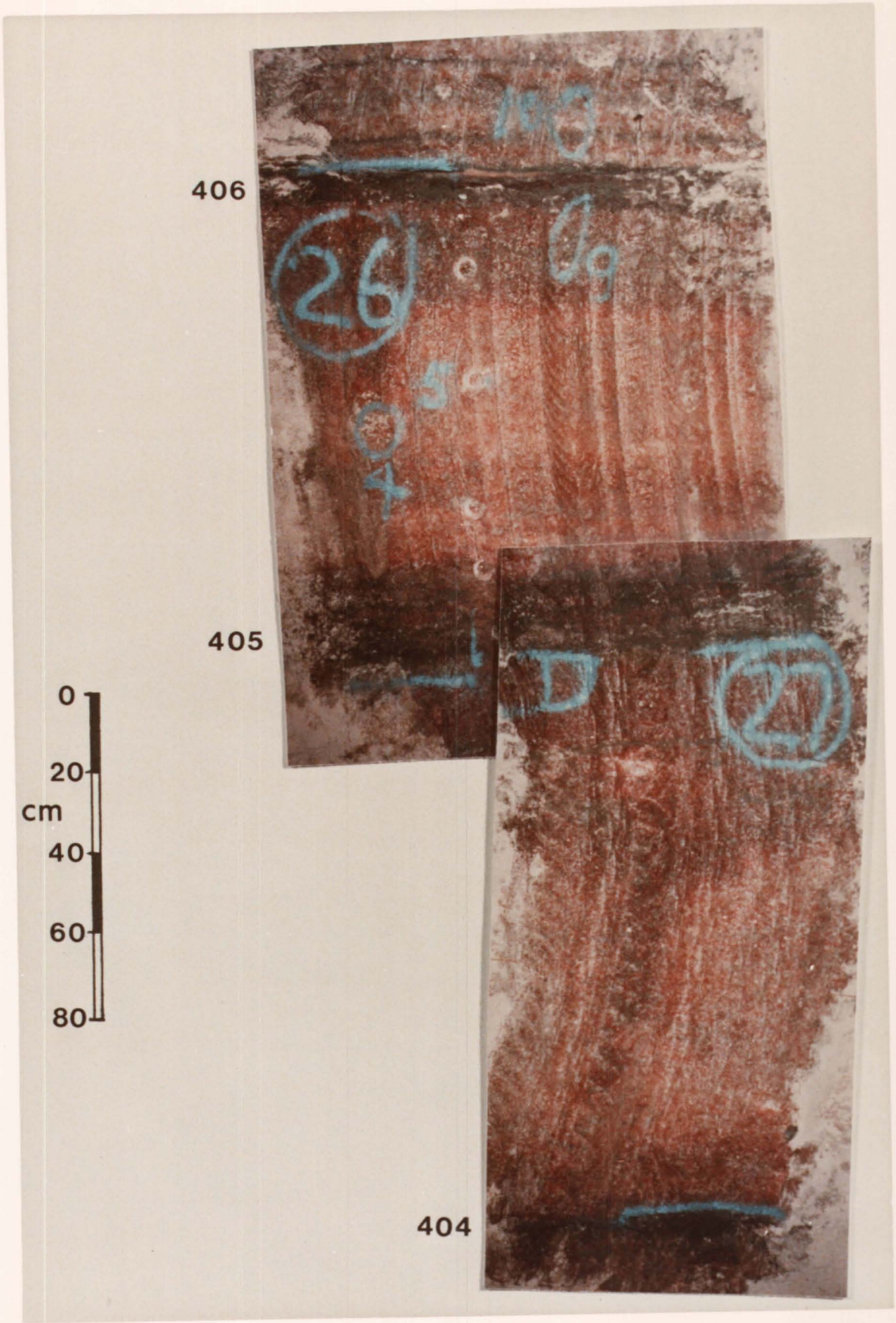
406
405
404
0
20
cm
40
60
80

PLATE 6: THE REFERENCE STRATIGRAPHIC SECTION, PCS CORY POTASH MINE.

The reference stratigraphic section is a combination of sections 3 and 36 (Fig. 2.1). The rock types are graphically represented in Fig. 4.5. Unit M1 at the base of the ore zone comprises the seams of #410 clay seam. Unit M2 includes a complete potash cycle. Unit M3 provides the bulk of high grade sylvinite. It is fairly insoluble-rich at the top (greenish-grey spots above the broom-head), and had it formed a clay seam then from it up to the top of unit M5, would be a potash cycle. Therefore the same interval is referred to as a discontinuous potash cycle. Unit M4 consists of pale orange B-type sylvinite. Unit M6 includes the #411, 412, and 413 clay seams; only the first two are shown here. Subtle colour-change layering may be seen above the 412 seam. Curved marks are scars from the mining machine. Horizontal black line in unit M3 and blue marks are paint.

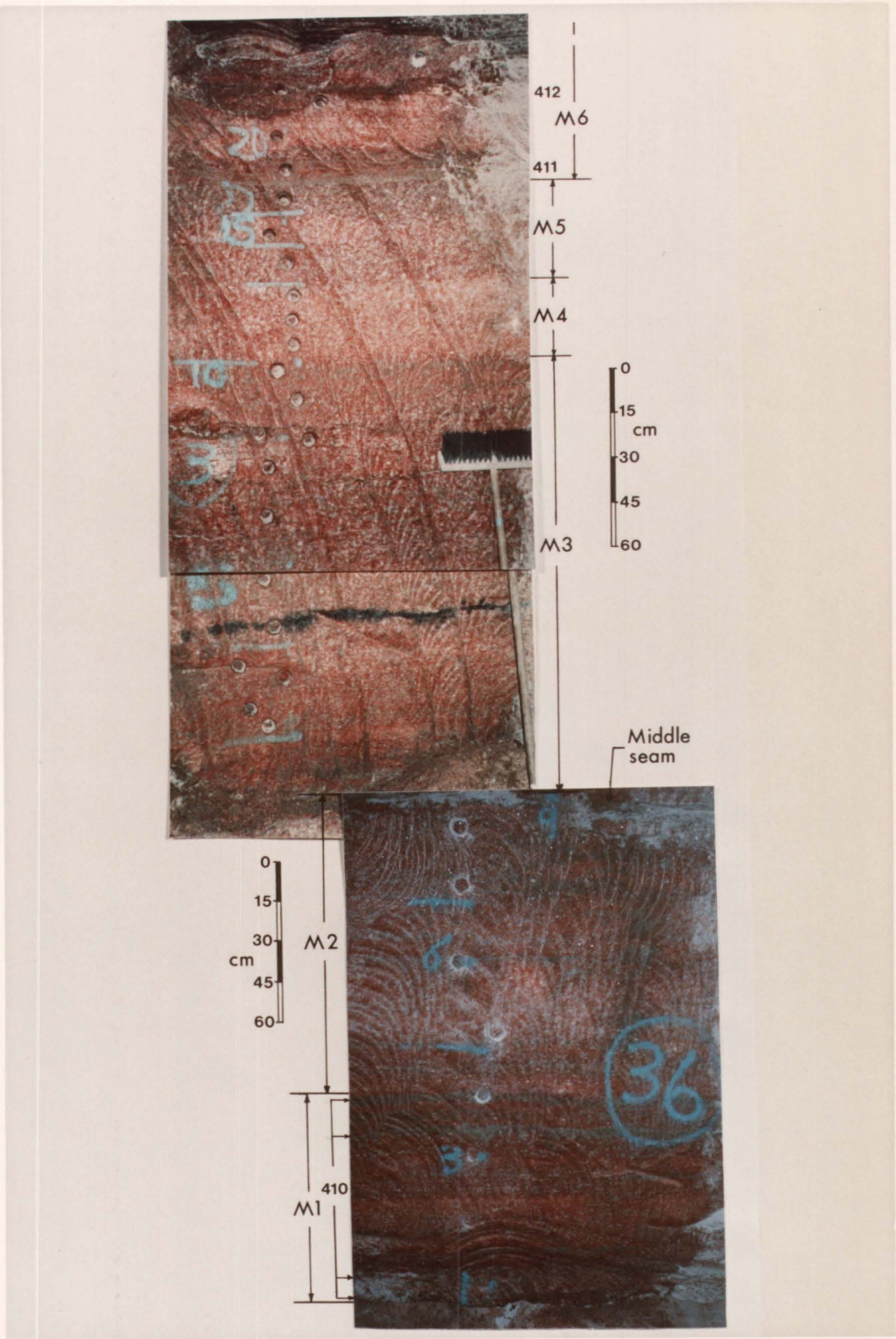
412
M6
411
M5
M4
0
15
cm
30
45
60
M3
Middle
seam
0
15
30
cm
45
60
M2
410
M1
36

PLATE 7: STRATIGRAPHIC SECTION #103 OF THE ORE ZONE.

Essentially the same stratigraphic level as that of the reference section (previous Plate), this shows the variability of rock types in the mine zone units, and a complete section of seam #410, unit M1. Section 103 is in the south of PCS Cory (Fig. 2.1), and is graphically represented in Fig. 4.8. Unit M2 represents a complete potash cycle. Note the enrichment of insolubles (greenish-grey spots) which marks the top of unit M3. Unit M6 is lacking the 413 seam in this view. Subtle colour-change layering may be seen above the Middle seam. Vertical marks are scars from the mining machine.

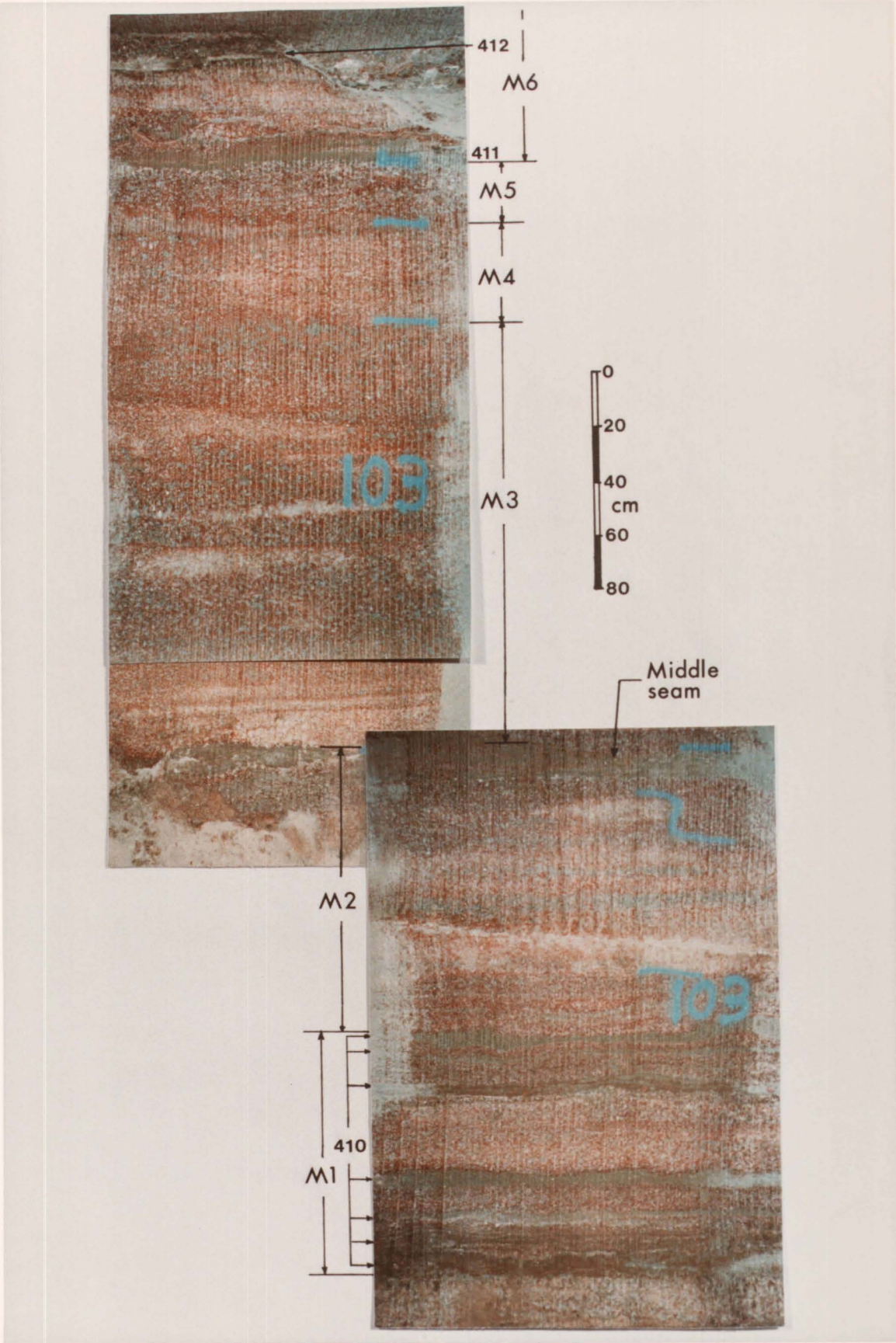
412
M6
411
M5
M4
M3
0
20
40
cm
60
80
Middle
seam
M2
410
M1
103
103

PLATE 8: UNIT M6 AND ABOVE THE ORE ZONE

a. Section 16 above the reference section of the ore zone (Fig. 4.4). From seam 413 to seam 414 is banded halite (sylvite <5%). Seam 415 includes all the clay seams from the blue number 10 to just below the 20. The bottom of 416 seam is at the top of the photograph. The curved marks are scars from the mining machine.

b. Unit M6 comprises the 413, 412, and 411 clay seams at the top of the ore zone. From section 114, which is graphically represented in Fig. 4.6. Seam 413 is used to guide the top of the mining machine. Seam 411, the bottom of which forms the datum for the ore zone cross-sections, is greener than seam 413. Close observation reveals a slight collapse and unusual desiccation cracks in the bottom right of seam 411. Note how the sylvinite contacting the seam is red. Seam 412 is massive and has desiccation cracks indicating subaerial exposure. The colour of the 412 seam changes abruptly, just below the vertical black paint mark, from brown on the left to greenish-grey on the right. Black and blue are paint.

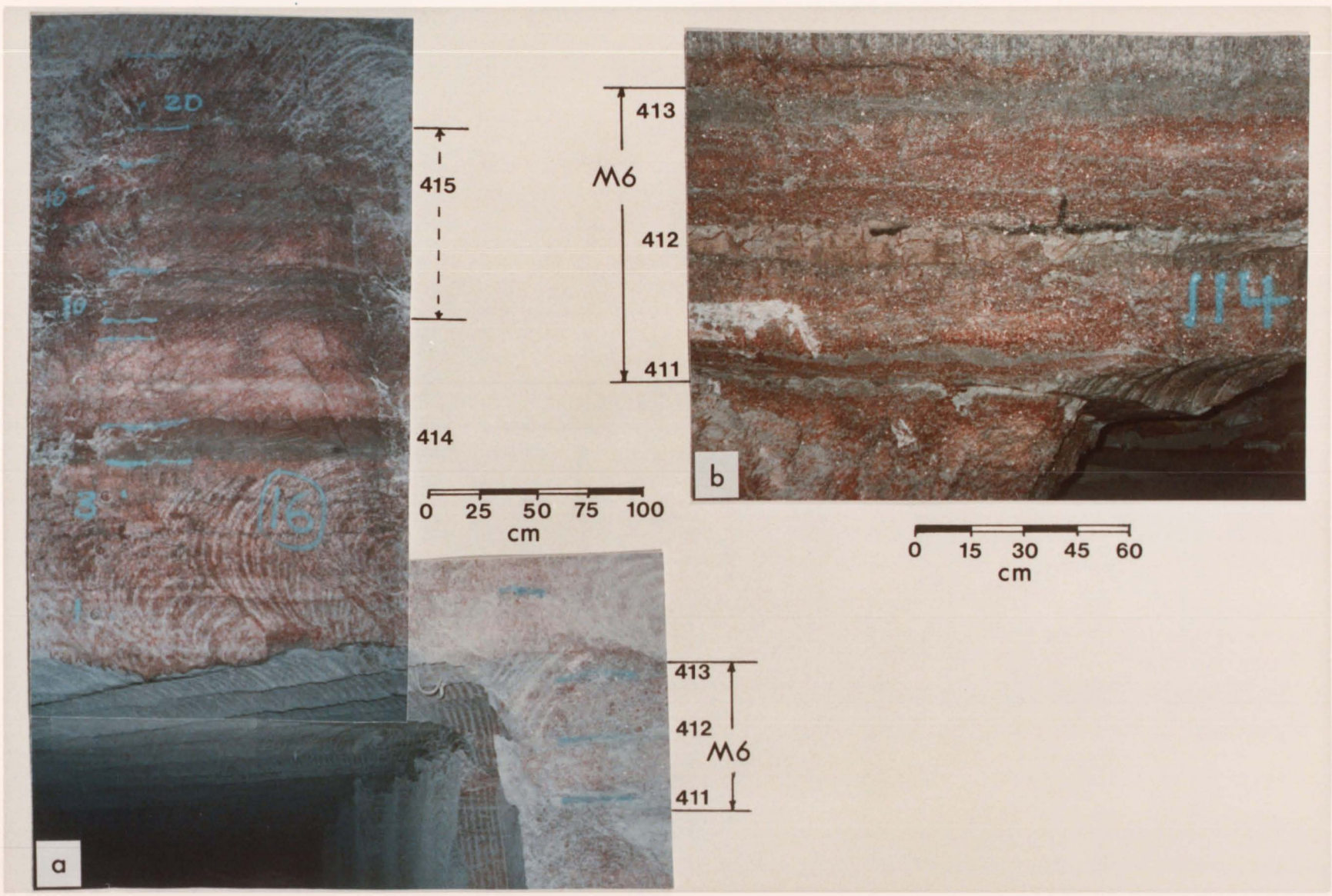
415
414
0 25 50 75 100
cm
413
M6
412
411
b
0 15 30 45 60
cm
413
412
M6
411
a

PLATE 9: SYNDEPOSITIONAL FEATURES IN THE PATIENCE LAKE MEMBER

a. "Colour-banded" halite, section 25 PCS Cory potash mine (Fig. 2.1). This unit divides the lower and upper Patience Lake Members, with seam 407 at the top.

b. Sample from the "colour-banded" halite (previous photo), showing small red sylvite crystals ("s"), and chevron halite ("c"). Alternating bands of mostly clear halite and mostly cloudy halite were thought to be caused by changing rates of precipitation due to seasonal fluctuations (Dellwig, 1972). The dark colour bands, dark grey cutting through the s, are mostly anhydrite and dolomite (Dellwig and Evans, 1969).

c. Desiccation polygons in halite of Cominco potash mine. These are in the upper Patience Lake Member. The dark red contacts between polygons contain sylvite. Polygons form under subaerial conditions (Lowenstein and Hardie, 1985). Some curved scars from the mining machine may also be seen.

d. Desiccation cracks in clay seam in the back (roof) of Central Canada Potash mine. These also indicate subaerial exposure. Steel plate is about 15cm along one side.

e. Microkarst pit filled with insoluble-rich halite. This is a dissolution feature and undisturbed overlying beds indicate dissolution at the paleosurface (see also Hovorka, 1987). From

banded halite between Patience Lake Member and Allan Marker Bed (Fig. 4.1) exposed in the decline to the base of the #2 shaft (Fig. 2.1).

f. Cross-section view of washout channels 2 m north of section 12 (Fig. 4.7). The white pods are underlain by insoluble-rich sylvinite that appear to form the channel bottoms. Very large sylvite crystals just to the mid-right of the left ladder indicate slow recrystallization. The extent of disturbance of overlying beds indicate these channel features formed very close to the surface (eg. 1-3m deep).

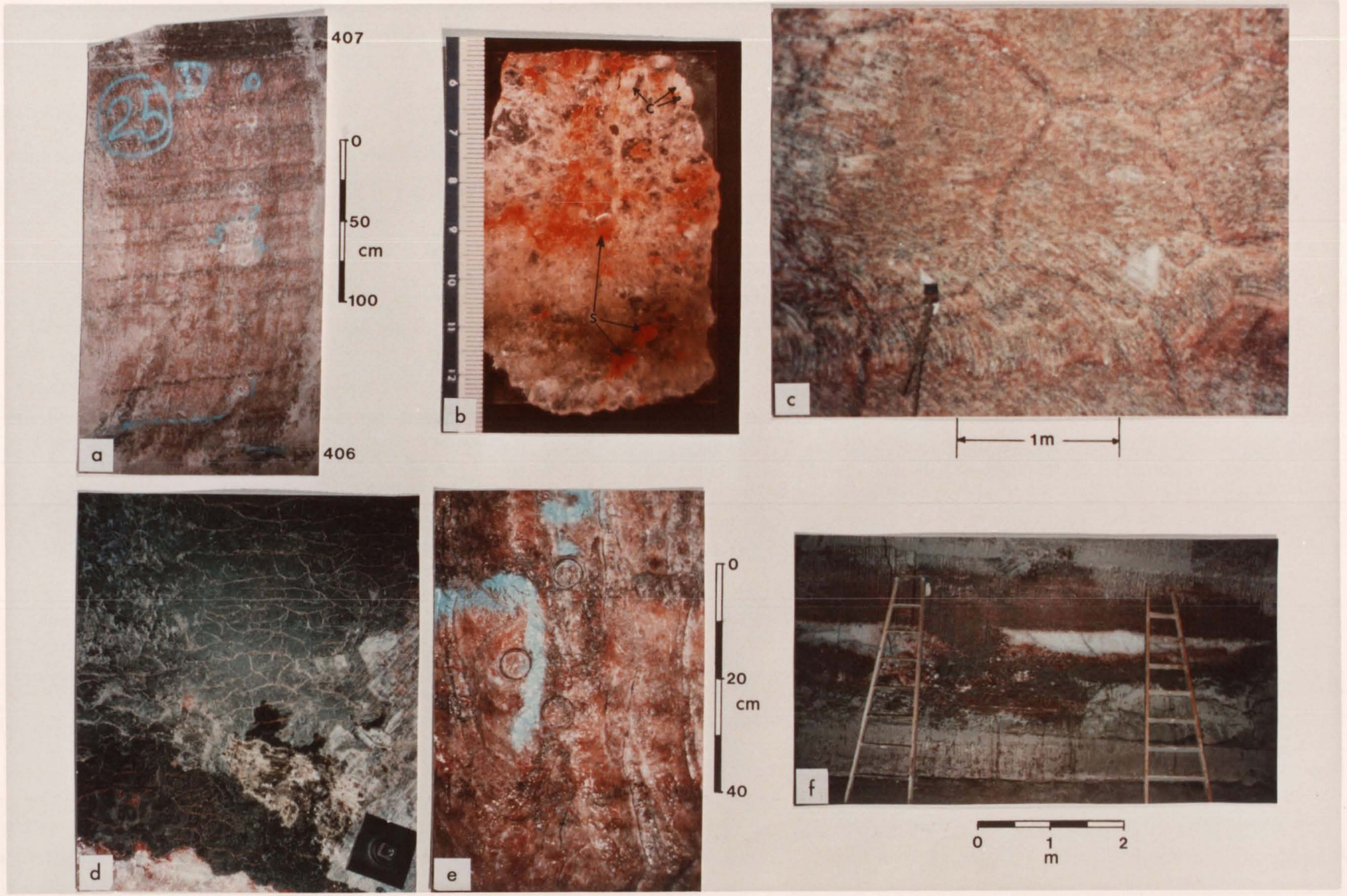
407
406
0
50
cm
100
a
b
C
S
c
1m
d
e
0
20
cm
40
f
0
1
2
m

PLATE 10: CHEVRON HALITE AND HEMATITE INCLUSIONS

a. Two halite crystals show chevron texture in A-type sylvinite; this is due to fluid inclusions trapped along growth margins of the halite crystal as it grows vertically upward in a shallow brine (Lowenstein and Hardie, 1985). The cloudy, inclusion-rich bands probably formed relatively quickly during periods of intense evaporation, while the clear bands formed during slower evaporation (Lowenstein and Hardie, 1985). This sample is from unit M1 of section 8 (Fig. 4.7). Small h indicates halite, s indicates sylvite. Small interstitial films of insolubles are present in halite, and between halite and sylvite. A thin halite film similar to that one indicated by the arrow, is shown in the next photograph. They form an interconnection between apparently separate halite crystals.

b. Photomicrograph of halite film between sylvite crystals. Small red platelets are believed to be hematite, and the rods are hematite or goethite. Small s indicates sylvite, h indicates halite. All photomicrographs are of samples from a section 1 m from a PCS Cory leach salt anomaly.

c. Chevron textured (cloudy) halite crystals (c) disseminated throughout insolubles. Some sylvite is present (s). Arrow indicates top, which is the direction the chevrons point in.


s
h
s
s h
h
M\M
a

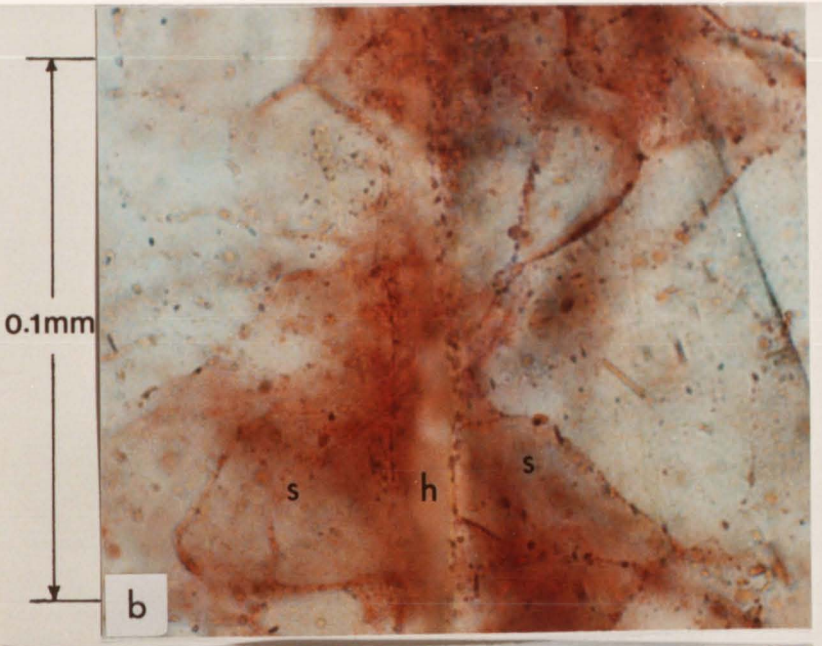
0.1mm
s
h
s
b


s
c
c
M/M
c

PLATE 11: BLACK-AND-WHITE PHOTOMICROGRAPHS OF SYLVINITE

a. Zoning of hematite inclusions (i) in sylvite crystal (s). Small h indicates halite, some of which cross-cuts the sylvite, indicating the halite is younger. Black material is insolubles. In all these photographs sylvite appears darker and of higher relief than halite. Hematite inclusions enhance this effect. Plane polarized light. All photomicrographs are of samples from a section 1 m from a PCS Cory leach salt anomaly.

b. Primary fluid inclusion pattern (f) in the centre of a halite crystal (h). The outer portions of the crystal are most likely recrystallized. "i" indicates insolubles. Plane polarized light.

c. Photomicrograph of "grow-together" (or "pull-apart"?) texture between sylvite crystals (s). The strands connecting sylvites in the middle are hematite. Halite (h) forms crystals as well as films between sylvite crystals. The impression is one of sylvite crystals growing together in a halite matrix mush. Hematite-rich contacts mark where sylvite crystals have grown together. In the upper left corner, the otherwise continuous fluid inclusion pattern (f) in the halite crystal

has been broken by sylvite. The timing of crystallization is rather ambiguous. Plane polarized light.

d. Another view of halite films (h, arrow) between sylvite crystals (s). It appears as if insoluble inclusions (i) are being transported into centre-right halite crystal. This is likely due to a squeezing-out effect produced by sylvite crystals growing in a halite mush. However, rounded edges of both sylvites and halites render the relative timing of crystallization ambiguous. Plane polarized light.

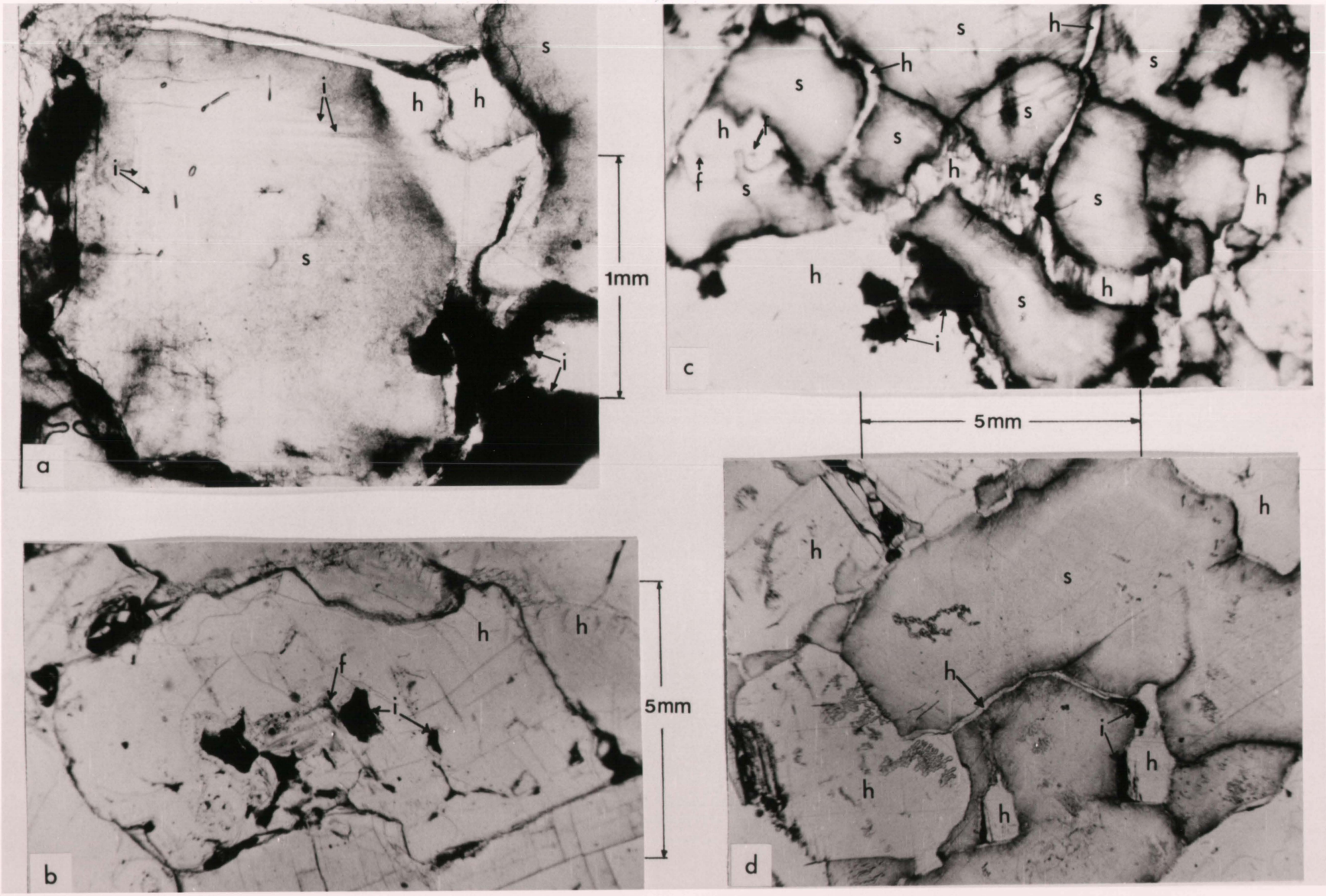
a
s
i
h
h
i
s
1mm
i
b
h
h
f
i
5mm
c
s
h
h
s
s
h
i
f
s
s
h
s
h
h
s
h
i
5mm
d
h
h
s
h
i
h
h
h

PLATE 12: THE EDGE OF LEACH-COLLAPSE SALT ANOMALY

a. Section 83 (Figs. 5.2, 5.3). The potash-salt anomaly contact is just starting to encroach on the ore zone from above; the 412 clay seam and above have had the sylvite removed. The 411 seam appears to be quite normal because the brown discolouration does not show very well. The 412 and 413 seams are unusually thin, and there is a slight collapse in the upper right of the 413 seam. A few small red remnant sylvite crystals may still be seen in the salt. Vertical marks are scars from the mining machine.

b. Section 47 (Figs. 5.2, 5.3). The contact between salt (orange and grey) and potash (red) is lower as the centre of the anomaly is approached. The contact is fairly insoluble-rich (grey). The orange in the halite is due to small amounts of hematite retained after dissolution of the sylvite. The 412 and 411 clay seams are noticeably changed in colour to mottled greenish-grey-and-brown. The Middle seam retains its greenish-grey colour since it has not been subjected to the anomaly-producing fluids.

c. Part of a small collapse feature (Fig. 5.4, between sections 42 and 44 in Figs. 5.2, 5.3). The last bit of sylvite may be seen in the bottom left corner as the contact dips below the floor. It is low-grade G-type sylvinite. A bleb of

sylvinite that survived dissolution may be seen to the upper-left of the "45". The grey is insoluble-rich halite; the white is recrystallized halite. The insoluble-rich halite beds dip down to the right in the centre-right of the photograph, due to collapse. Only the top of the 410 clay seam is recognizable. Vertical marks are scars from the mining machine.

d. Section 34B (Figs. 5.2, 5.3). Closest to the centre of the salt anomaly, this section shows a decrease in the thickness of the ore zone due to the sylvite that was removed and not replaced by halite. The thickness between the 411 and Middle clay seams is ordinarily about 2 m. Orange halite is a reminder of the sylvite that was present. Bedding is still fairly well preserved. The Middle clay seam has changed colour to mottled greenish-grey-and-brown. The 410 clay seam, normally not all visible so close to the 411 seam, is indicated in the lower left. Vertical marks are scars from the mining machine.

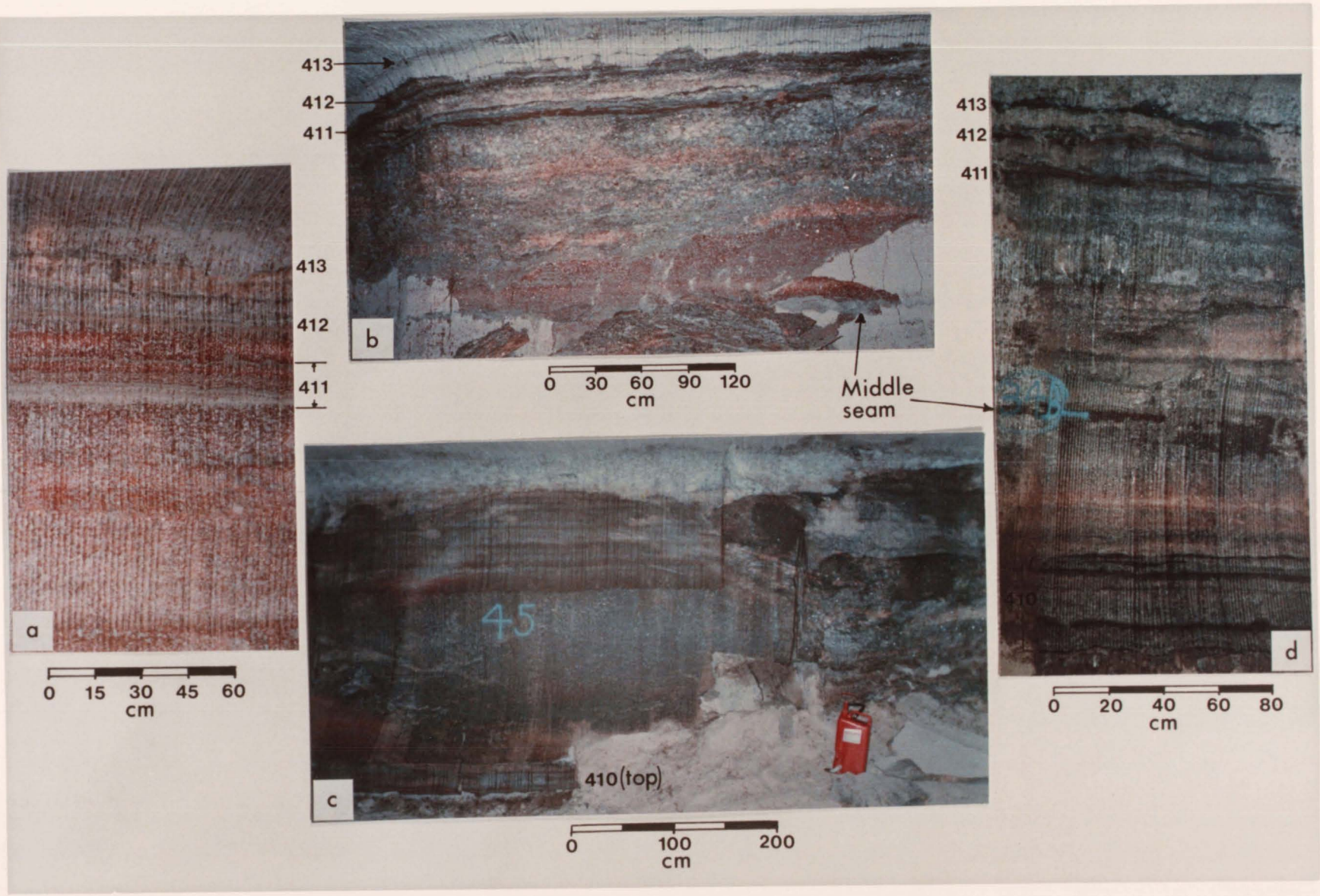
413
412
411
b
0 30 60 90 120
cm
Middle seam
413
412
411
a
0 15 30 45 60
cm
45
410(top)
c
0 100 200
cm
410
d
0 20 40 60 80
cm

PLATE 13: AUTHIGENIC ANHYDRITE AND STRUCTURALLY DEFORMED BEDS OF A COLLAPSE ANOMALY.

a. Bent euhedral anhydrite laths (a, arrow), similar to those found by Fuzesy (1983), indicate authigenic (syndepositional or diagenetic) origin. Sylvite indicated by "s"; "h" indicates halite. All photomicrographs are of samples from a section 1 m from a PCS Cory leach salt anomaly.

b. Elongation of salt beds is manifested in this stretched clay seam on the edge of a PCS Lanigan leach-collapse salt anomaly. Cracks are infilled with white halite. There is a component of rotation equivalent to that of a dextral simple shear regime. Whether the elongation and rotation occurred at the same time or not is unclear. The horizontal elongation on the outer parts of the anomaly are due to vertical downward movement in the centre collapse portion. Vertical marks are scars from the mining machine.

c. Close to the centre of a PCS Lanigan leach-collapse anomaly. This and the previous photograph are from the same salt anomaly. High-angle dipping salt beds are clearly noticed by the triangle formed by two clay seams. Notice the infilled polygon cracks (microkarsts) on the bottom of the lower clay seam. Folded beds increase in amplitude toward the centre of the collapse (Mackintosh, pers. comm., 1987). Round scars show the pattern dug by the mining machine.

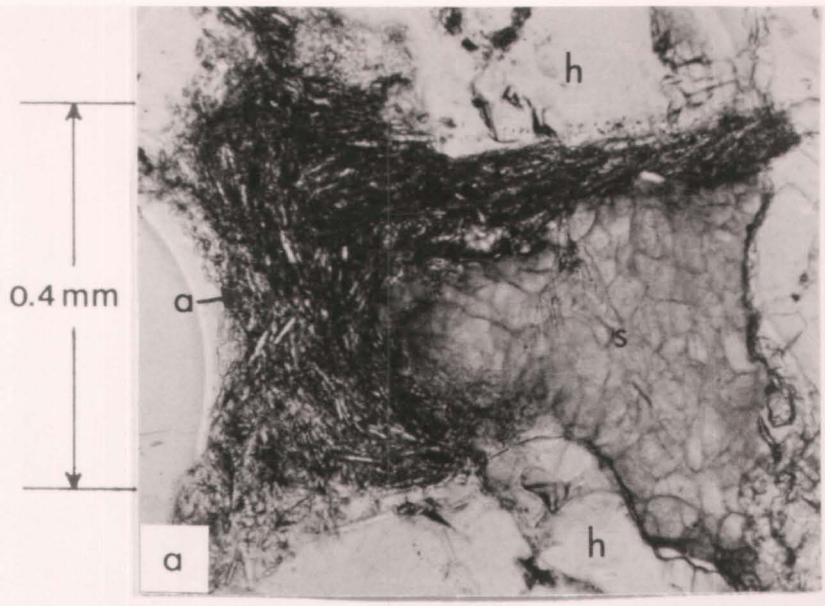
0.4 mm
h
a
s
h
a

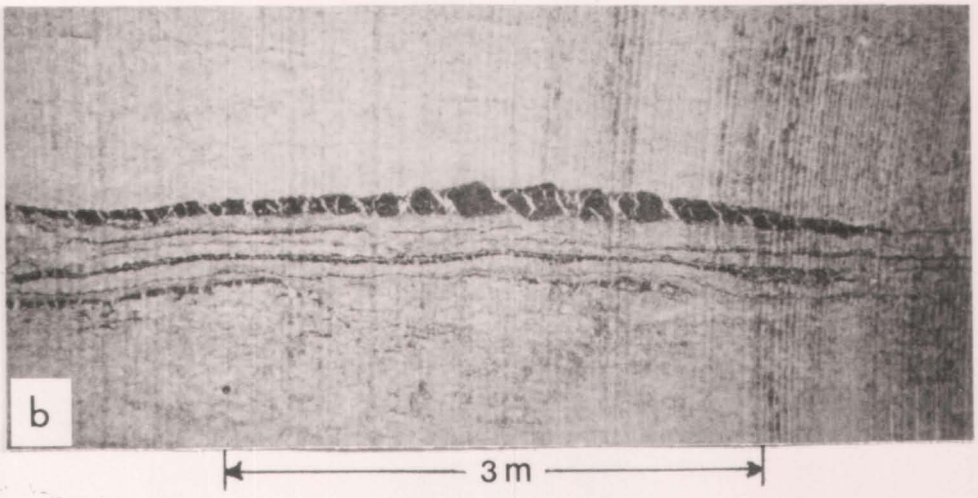
b
3 m

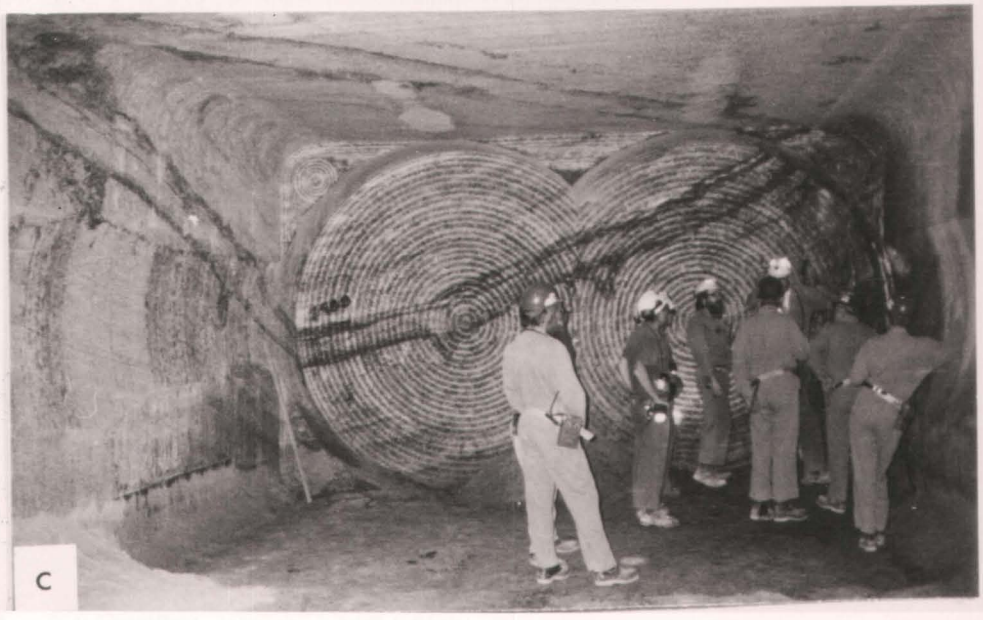
c

APPENDIX 1

Table A1. The data gathered on all the stratigraphic sections in PCS Cory mine. Des - descriptions, Ins - insoluble amount measured, Pho - photographs, OZ - ore zone, A - anomaly, a - above, b - below, Decl - decline, sw - southwest (Fig. 2.1).

Sect#	Sampl	Des	Ins	ISE K2O	Other analys	Pho	Strat. position	Break-through	Entry
1						y	OZ	#2 shaft	
1A	25	y	25		XRD.K	y	OZ	#2 shaft	
1B	10	y	10		XRD.K	y	bOZ	#2 shaft	
2	0	y				2	OZA	1W	
3	23	y	23	23	Clays,Mg,AA.K	y	OZ	516	5300
					XRD.K				
4	9	y	9	9		4	OZA	522	5300
4A-G	0	y				8	OZA	522	5300
5	24	y	24	24	XRD.K	y	OZA	520	5300
6	20	y	20	20	XRD.K	7	OZ	518	5300
7	14	y			XRD.K	11	OZ	512	5300
8,8A	22	y	19	19	XRD.K	y	OZ	321	3300
9	15	y	15		XRD.K	9	OZ	325	3300
10	25	y	25	25	XRD.K	y	OZ	330	3300
11,11A	17	y	17	17		14	OZ	334	3300
12	9	y				5	OZ	339	3300
13	22	y				9	OZ	341	3300
14	20	y	20	20		y	aOZ	326	3300
15,15A	22	y	22	22	AA.K	y	OZ	603	6300
16	22	y	22	22	Clays,AA.K.Na	y	aOZ	516	5300
17	12	y	12	12		3	aOZA	520	5300
18	0					8	aOZA	2W	
19	19	y				y	aOZA	2W	P.lot
19A		y				y	aOZA	2W	P.lot
20	6	y	6	6		6	OZA	531	
21	12	y	12	12		4	Decl		
22	17	y	17	17		4	Decl		
23	17	y	18	18		4	Decl		
24		y				6	aOZA	531	5300
25,25A	10	y	10	10		8	Decl		
26	10	y	8	8		4	Decl		
27	4	y	4	4		4	Decl		
28	8	y	8	8		5	Decl		
29	6	y	6	6		5	Decl		
30	8	y	8	8		5	Decl		
31	6	y	7			4	Decl		
32	8	y				6	Decl		
33	6	y				5	Decl		
34	6	y	6	6		2	OZswA	611.1	6200
34B	6	y	6	6		7	OZswA	611.1	6200
35	6	y	6	6		7	OZswA	608.1	6200
36	10	y	10	10		y	bOZ	516	5200
37	10	y				2	OZswA	611.1	6200
38						2	OZswA	611.1	6200
39						3	OZswA	610.1	6200
40	16	y	9		Clays	1	OZswA	610.1	6200
41						2	OZswA	609.1	6200
42		y				1	OZswA	609.1	6200
43						2	OZswA	609.1	6200
44		y				1	OZswA	609.1	6200
45	37					22	OZswA	609.1	6200

Sect#	Sampl	Des	Ins	ISE K2O	Other analys	Pho	Strat. position	Break-through	Entry
46									
47		y				1	OZswA	609.1	6200
48						1	OZswA	608.1	6200
49							OZswA		
50							OZswA		
51							OZswA		
52							OZswA		
53							OZswA		
54							OZswA		
55							OZswA		
56							OZswA		
57							OZswA		
58							OZswA		
59							OZswA		
60		y					OZswA	607.1	6200
61		y				2	OZswA	607.1	6200
62							OZswA		
63							OZswA		
64							OZswA		
65							OZswA		
66							OZswA		
67							OZswA		
68							OZswA		
69							OZswA		
70							OZswA		
71							OZswA		
72							OZswA		
73							OZswA		
74							OZswA		
75							OZswA		
76							OZswA		
77						1	OZswA	608.1	
78							OZswA		
79							OZswA		
80							OZswA		
81							OZswA		
82		y				1	OZswA		
83		y				3	OZswA	606.1	
84						2	OZswA		
85							OZswA		
86							OZswA		
87							OZswA		
88							OZswA		
89							OZswA		
90							OZswA		
91							OZswA		
92							sw		
93							sw		
94,94A		y					sw		
95	13	y				4	swOZ	604.1	6200
96						3	swOZ	605.1	6200
97							sw		
98							sw		
							sw		

Sect#	Sampl	Des	Ins	ISE K2O	Other analys	Pho	Strat. position	Break-through	Entry
100		y				1	OZ	Fuel dump	
101	14	y	14	14			OZ	653	6200
101A		y				1	bOZ	653	6200
102		y				2	OZ	610	6200
102A		y					OZ	610	6200
103	27	y	15	15		6	OZ	683	6200
103B		y					bOZ	683	6200
104	1	y							
105	9	y				2	OZ	204.1	2200
106	17	y				3	OZA	203.1	2200
107		y				2	OZA	203.1	2200
108	18	y				3	OZA	202.1	2200
109	10	y				2	OZA	201.1	2200
110		y				2	OZA	200.1	2200
111		y				3	OZA	299	2200
112	8	y				2	OZA	299	2200
113	12	y				2	OZ		36,C55
114	14	y				3	OZ	272	2300
115	25	y				3	OZ	295	2200
Tot.	707+	78	433	367		>257			

Des - descriptions , Ins - insolubles meaured, Pho - photographs
OZ - ore zone, A - anomaly, a - above, b -below, Decl - decline ,

APPENDIX 2

Table A2. Ionic Specific Electrode (I.S.E.) vs X-ray Diffraction (XRD) vs Atomic Absorption (AA) results of potassium analyses, and all the XRD results on K_2O. Insols - insolubles, first % Diff. (% difference) = $(\%K_2O_{ISE}-\%K_2O_{XRD})/\%K_2O_{XRD}X100$, second % Diff. = $(\%K_2O_{ISE}-\%K_2O_{AA})/\%K_2O_{AA}X100$.

SAMPLE NUMBER	% INSOLS	INSOLS. COLOUR	ROCK TYPE	I.S.E. % KCl	I.S.E. % K2O	XRD %K2O	% DIFF.	AA %K2O	% DIFF.
3.1	3.70	RD	A	51.64	32.62	31	5.23	34.46	-5.33
3.2	5.58	RD,GRY	A	61.57	38.90	39	-.27	41.76	-6.86
3.3	2.22	RD,GRY	A	59.48	37.58	37	1.56	40.21	-6.55
3.4	2.97	RDBRN	A	65.51	41.38	41	.94	44.51	-7.02
3.5	20.73	BRN,GRY	A	53.65	33.89	36	-5.85	34.69	-2.30
3.6	4.42	RDBRN	A	58.83	37.17	38	-2.19	39.71	-6.40
3.7	3.26	RDBRN	A	78.02	49.28	47	4.86	49.85	-1.13
3.8	1.23	RD	A	68.61	43.34	42	3.20	44.19	-1.91
3.9	14.61	RD	A	61.99	39.16	39	.41	43.33	-9.63
3.10	4.30	RD	A	69.73	44.05	44	.12	45.99	-4.21
3.11	.30	RD	B	77.11	48.71	45	8.25	49.25	-1.09
3.12	.52	RD	B	75.45	47.66	45	5.92	47.48	.39
3.13	.64	RD	B	60.93	38.49	34	13.21	41.99	-8.33
3.14	2.08	RDBRN	A(D)	59.07	37.31	37	.85	39.01	-4.35
3.15	.59	RDBRN	B(D)	66.66	42.11	41	2.72	42.8	-1.60
3.16	5.89	PRPL	A(D)	21.46	13.56	15	-9.61	13.85	-2.11
3.17	14.97	PRPL		55.93	35.33	35	.96	33.81	4.51
3.18	.85	RDBRN	B	68.44	43.24	41	5.46	43.73	-1.13
3.19	2.70	RDBRN	B	46.88	29.62	30	-1.27	30.56	-3.08
3.20	.46	RDBRN	B	48.97	30.94	29	6.68	31.04	-.34
3.21	10.84	BRN		8.49	5.36	7	-23.41	6.17	-13.11
3.22	32.97	BRN		5.83	3.69	3	22.84	3.71	-.67
3.23	1.22	RD	A(D)	38.40	24.26	26	-6.70	N/A	

SAMPLE NUMBER	% INSOLS	INSOLS. COLOUR	ROCK TYPE	I.S.E. % KCl	I.S.E. % K2O	AA %K2O	% DIFF.
15.1	14.82	RDBRN	D(A)	24.31	15.36	16.543	-7.17
15.2	2.22	RD	A(D)	46.17	29.17	30.471	-4.28
15.3	.80	LT BRN	B	21.66	13.68	14.536	-5.87
15.4	.60	RDBRN	B(A)	49.76	31.44	31.003	1.40
15.5	7.85	RDBRN	A	51.05	32.25	34.309	-6.01
15.6	.73	LT BRN	B	70.77	44.71	47.782	-6.43
15.7	1.64	LT BRN	A	59.62	37.66	45.500	-17.22
15.8	2.76	LT BRN	A	60.31	38.10	42.417	-10.18
15.9	1.30	RDBRN	A	62.61	39.55	41.372	-4.40
15.10	4.41	BRN	A	62.98	39.79	40.738	-2.33
15.11	1.66	RDBRN	A	60.26	38.06	38.578	-1.33
15.12	6.96	BRN	A	66.70	42.14	43.535	-3.21
15.13	2.33	RDBRN	A	75.77	47.86	51.320	-6.73
15.14	.36	LT BRN	B	71.32	45.06	45.647	-1.29
15.15	1.18	RDBRN	A	59.10	37.34	41.316	-9.63
15.16	1.77	RD	A(G)	39.59	25.01	25.242	-.92
15.17	.63	BRN	B	29.24	18.47	19.925	-7.28
15.18	4.13	RDBRN	A	44.25	27.96	28.774	-2.84
15A.19	.95	LT BRN	A(G)	45.42	28.69	30.087	-4.63
15A.20	.50	DK BRN	G	14.57	9.20	10.518	-12.50
15A.21	46.16	GRY	Mclay	5.78	3.65	3.8109	-4.22
15A.22	1.83	RDBRN	A(G)	48.42	30.59	30.483	.36

SAMPLE NUMBER	% INSOLS	INSOLS. COLOUR	ROCK TYPE	I.S.E. % KCl	I.S.E. % K2O	XRD %K2O	% DIFF.
8.1	1.00	RD	A(G)	29.45	18.61	19	-2.07
8.2	30.14	GRY		4.36	2.75	5	-44.93
8.3	1.15	RDBRN	A( )	19.93	12.59	29	-56.59
8.4	32.39	GRY	A,H	32.02	20.23	22	-8.04
8.5	1.45	RDBRN	G	38.50	24.32	25	-2.72
8.6	.91	LT BRN	B	64.69	40.87	38	7.54
8.7	.66	LT BRN	B(C)	73.28	46.29	43	7.66
8.8	2.63	RDBRN	A	69.38	43.83	40	9.57
8.9	3.80	RDBRN	A	75.43	47.65	45	5.90
8.10	3.22	RDBRN	A	60.66	38.32	37	3.57
8.11	3.11	RDBRN	A	61.94	39.13	39	.32
8A.14	33.53	LT BRN	H(A)	13.04	8.23	10	-17.65
8A.15	6.40	RDBRN	D	54.32	34.32	37	-7.25
8A.16	.31	LT BRN	B	55.60	35.12	33	6.44
8A.17	.14	LT BRN	B	34.75	21.95	21	4.54
8A.18	1.05	RDBRN	A(G)	34.71	21.93	22	-.33
8A.19	18.74	GRY,BRN	H	2.41	1.52	4	-62.00
8A.20	1.34	RDBRN	D(A)	55.92	35.33	34	3.90

SAMPLE NUMBER	% INSOLS	INSOLS. COLOUR	ROCK TYPE	I.S.E. % KCl	I.S.E. % K2O	XRD %K2O	% DIFF.
10.1	11.66	RDBRN	C	26.76	16.90	17	-.57
10.2	3.78	RDBRN	C	39.06	24.68	21	17.50
10.3	11.53	GRY	H	3.02	1.91	2	-4.53
10.4	1.63	RDBRN	G(A)	29.21	18.45	18	2.52
10.5	.69	LT BRN	G	4.88	3.09	8	-61.44
10.6	.81	LT BRN	G(B)	16.03	10.13	9	12.54
10.7	.71	LT BRN	B(G)	36.34	22.96	21	9.33
10.8	.42	LT BRN	B	30.65	19.36	18	7.56
10.9	2.65	RDBRN	G(A)	34.87	22.03	21	4.89
10.10	3.73	RDBRN	G(A)	22.87	14.45	20	-27.75
10.11	1.50	RDBRN	C(A)	78.85	49.81	46	8.29
10.12	1.20	RDBRN	C(B)	59.22	37.41	34	10.04
10.13	.57	LT BRN	B	65.03	41.08	39	5.34
10.14	.32	BRN	B	63.23	39.95	38	5.12
10.15	8.72	RDBRN	A	56.68	35.81	33	8.51
10.16	11.88	RDBRN	A	54.47	34.41	33	4.27
10.17	1.32	BRN	A	75.92	47.96	44	9.00
10.18	5.16	RDBRN	A	56.69	35.81	35	2.32
10.19	7.66	RDBRN	A	64.87	40.98	37	10.76
10.20	.48	BRN	B	78.29	49.46	45	9.90
10.21	.79	LT BRN	A(B)	59.36	37.50	33	13.63
10.22	2.11	BRN	A(D)	57.42	36.27	30	20.91
10.23	1.37	LT BRN	A	69.85	44.13	41	7.62
10.24	3.21	RDBRN	D	30.07	19.00	18	5.54
10.25	33.15	RDBRN	H	2.79	1.76	N/A	

SAMPLE NUMBER	% INSOLS.	ROCK COLOUR	TYPE	I.S.E. % KCl	I.S.E. % K2O	XRD %K2O	% DIFF.
5.1	1.07	RDBRN		22.08	13.95	12	16.24
5.2	4.07	RDBRN	A	63.95	40.40	36	12.22
5.3	.58	RD,GRY	H	.60	.38	<1	
5.4	7.92	GRY	H	1.02	.65	<1	
5.5	13.05	GRY	H	1.28	.81	<1	
5.6	1.95	RDBRN	H	.28	.18	0	
5.7	5.51	DK BRN	H	.75	.47	<1	
5.8	5.57	DK BRN	H	.58	.36	<1	
5.9	33.87	BRN		1.22	.77	N/A	
5.10	1.80	RD	A	61.04	38.56	40	-3.60
5.11	1.85	RD	A	66.57	42.05	35	20.15
5.12	37.66	GRYSclay		9.01	5.69	7	-18.71
5.13	4.92	RDBRN	A	43.31	27.36	28	-2.30
5.14	.95	RDBRN	B	33.42	21.11	22	-4.05
5.15	1.68	RDBRN	G(A)	14.31	9.04	10	-9.61
5.16	1.95	RDBRN	A	48.88	30.88	26	18.77
5.17	6.15	RDBRN	A	24.90	15.73	15	4.86
5.18	.71	RDBRN	B	59.17	37.38	35	6.80
5.19	12.56	RDBRN	A	58.73	37.10	36	3.06
5.20	6.07	RDBRN	A	66.20	41.82	38	10.06
5.21	2.16	RDBRN	A	59.57	37.63	36	4.53
5.22	.86	BRN	H	.49	.31	<1	
5.23	46.82	DK BRNMclay		3.61	2.28	3	-23.90
5.24	5.95	GRY	H	.30	.19	<1	

SAMPLE NUMBER	% INSOLS	XRD % K2O
1A.1	2.10	33
1A.2	1.90	35
1A.3	.60	38
1A.4	1.30	35
1A.5	3.20	26
1A.6	4.80	31
1A.7	1.80	38
1A.8	2.40	39
1A.9	2.40	42
1A.10	3.10	33
1A.11	4.60	24
1A.12	6.40	30
1A.13	4.20	39
1A.14	4.70	43
1A.15	10.00	34
1A.16	.60	29
1A.17	.50	39
1A.18	.60	32
1A.19	.30	32
1A.20	.30	28
1A.21	.40	21
1A.22	1.10	21
1A.23	14.00	7
1A.24	6.30	30
1A.25	5.40	8

1B.1	1.30	29
1B.2	.70	21
1B.3	.30	21
1B.4	.20	18
1B.5	.60	11
1B.6	2.50	21
1B.7	9.20	29
1B.8	3.50	30
1B.9	28.70	4
1B.10	.50	37

SAMPLE NUMBER	XRD % K2O
7.1	64
7.2	50
7.3	66
7.4	47
7.5	75
7.6	57
7.7	51
7.8	70
7.9	42
7.10	62
7.11	57
7.12	27
7.13	37
7.14	2

SAMPLE NUMBER	% INSOLS	XRD % K2O
9.1	2.10	19
9.2	16.10	4
9.3	1.70	24
9.4	1.00	6
9.5	.50	16
9.6	1.20	34
9.7	5.60	29
9.8	17.00	28
9.9	6.10	40
9.10	1.70	42
9.11	10.80	35
9.12	.30	32
9.13	2.50	44
9.14	1.90	39
9.15	4.00	39

APPENDIX 3

SAMPLE PREPARATION METHOD FOR X-RAY DIFFRACTION. The following is the method used to prepare the samples for determination of % insolubles, % dolomite+anhydrite (soluble in weak HCl), the relative proportions of the three main clay minerals (illite:chlorite:septechlorite), and the presence of other minerals (quartz, hematite, goethite, and swelling chlorite).

1.	Break and sieve sample through 1.7 mm (10 mesh) collect representative portion.	
2.	dissolve in water	retain water to analyze for K_2O using ion specific electrodes
3.	dry and weigh insolubles	calculate weight % insolubles
4.	grind to 0.074 mm (200 mesh) and prepare ethanol slurry mount for XRD	analyze from 54 to 17 °2θ at 1 deg/min
5.	dissolve insolubles in 1N HCl for >15 hours	
6.	dry and weigh HCl-insolubles	test filtrate for SO_4^- using $BaCl_2$
7.	grind to 0.074 mm (200 mesh)	
8.	extract clays (<2 micron fraction) by centrifuging prepare 2 water slurry mounts for XRD	analyze clays from 34 to 2.5 °2θ at 2 deg/min
9.	add ethylene glycol to clay slides*	analyze from 34 to 2.5 °2θ while still wet.

Table A3. Flow chart for sample preparation. HCl-insolubles are all those minerals which did not dissolve in HCl. * A sheet of filter paper was soaked in ethylene glycol. A dry sheet of filter paper was placed between this and the clay on the slides. The ethylene glycol was allowed to soak through the filter paper into the clay for 24 hours. See text for further details.

Dissolving the sample in weak HCl to obtain the percentage of dolomite + anhydrite did not affect the chlorite minerals. The reproducibility of ethanol and water slurry mounts was quite good when compared with other methods, i.e. acetone, water, and ethanol smears. A rock colour chart was used to determine the colour of the ethanol slurry samples (total insols).

Appendix 4: Detailed descriptions of rock types.

Detailed descriptions of sylvinite rock types (A, B, D, G).

The A-type rock (red sylvinite) predominates in the main part of the mining zone and is prominent wherever potash contents are high. The rock is characteristically brick red, ranging from dark to medium shades. Plate 1a is a photograph of the type sample, and Plate 1b,c shows other typical A-type rocks. Generally A-type is opaque and massive, with an interlocking mosaic texture. The rock is porphyroblastic and granoblastic, and grain sizes range from 1 to 5mm in the latter to 10mm in the former. The largest grains, 15-18mm, are mainly halite. In the porphyroblastic varieties, which are the most common, the matrix to the porphyroblasts consists mostly of granular sylvite. The variations of A-type sylvinite are shown in Plate 1c. A decrease in the amount of iron oxides and insolubles would approach the characteristics of B-type potash. A decrease in sylvite content (KCl) brings it closer to being G-type.

The A-type sylvinite is dominated by sylvite that forms orange-red to red grains, both as porphyroblasts up to 1 cm in size, and as fine-grained matrix. The KCl (sylvite) content ranges from 19 to 81%, and averages 54% (Fig. A1a). Some of the large grains are milky and some are colourless (although most of the colourless grains in the rock are halite). The sylvite grains are commonly separated from each other by a very thin film (<1mm) of halite (Plates 1a, 10a). The thin films lead to the conclusion that sylvite formed by precipitating in a halite matrix "mush". Interstitial clots and films of green clay are common. There is a progressive change from sylvite grains that are a fairly uniform brick red to those that have milky or colourless centres and brick red margins. Grains lacking the red colouration, and the grains with the red colour limited to the margins, tend to be the largest. Detailed examination of the coloured rims confirms Holter's (1969) observations that they are due to accumulations of hematite and goethite. Most of the hematite probably originated as goethite or hydrogoethite that was recrystallized during the conversion of carnallite to sylvite (McIntosh and Wardlaw, 1968, Wardlaw, 1968, Fuzesy, 1983).

The largest halite grains are usually clear and colourless, and the smaller ones more milky. Most are subhedral and appear as single grains or clusters isolated in a red sylvite matrix. In some samples, most grains are between 1 and 10mm, and in others they are between 2 and 18mm in size. Greenish-grey insolubles are interstitial, and where amounts are small they form discontinuous films around some grains, especially halite grains. As insoluble amounts

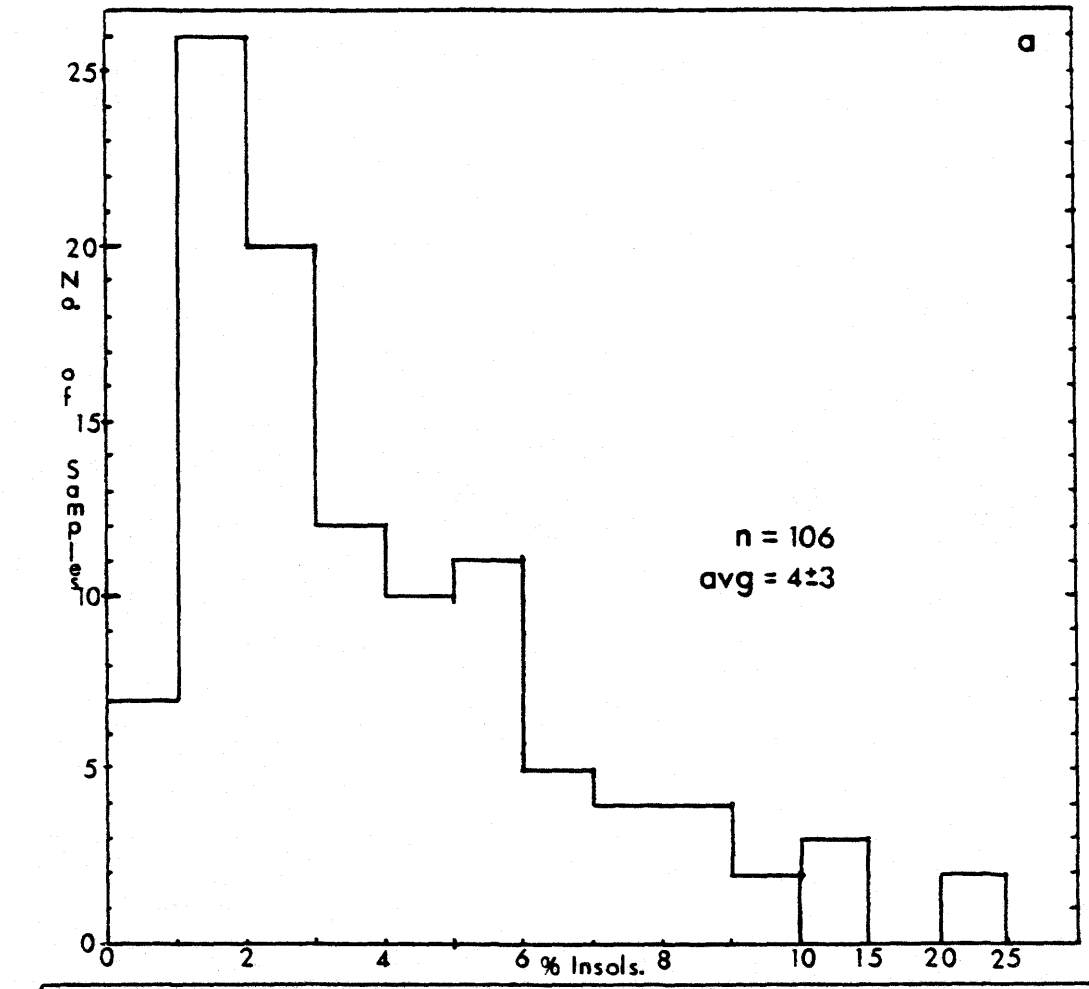

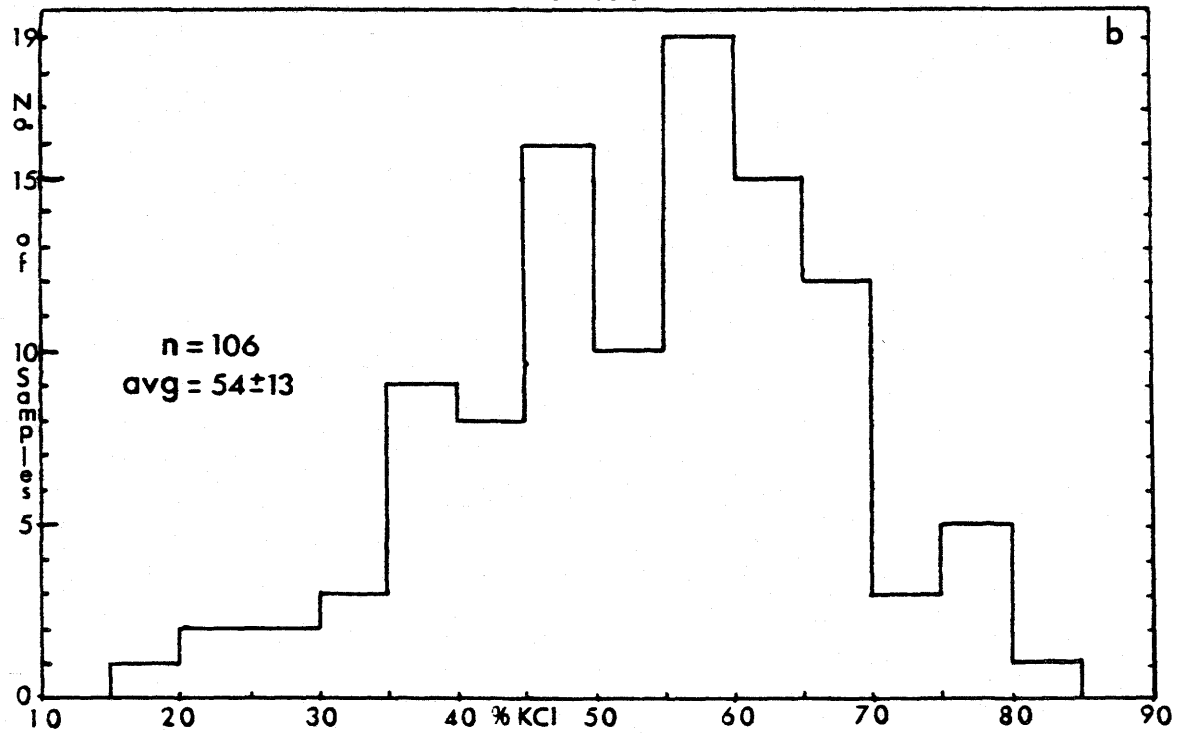

Fig. A1 Histograms of a) % insolubles, and b) % KCl for A-type potash. The average (avg) is given ±1 standard deviation.

increase, they form interstitial clots up to 10mm in size. Fig. A1b shows that the insoluble content of A-type sylvinite is commonly between 1 and 6%, but may be as high as 25 percent. The average amount is about 4%. The greenish-grey insolubles are interstitial, and where amounts are small, they form discontinuous films around grains. Insolubles are common along the boundaries of, and as inclusions in halite grains.

The second major potash-bearing rock type (B-type, pale or pale orange sylvinite), is generally medium orange to pale orange with some local variation in colour. The type sample is shown in Plate 2a, and variations in Plate 2b. The rock differs from the "A" type in being paler, medium orange, and equigranular rather than porphyroblastic. It is generally moderately translucent, and insolubles are sparse. The texture is mainly granoblastic and grain sizes are from 5 to 15mm.

Generally the sylvite ranges from medium orange to milky, with wisps of darker orange prevalent near the grain margins. Dark red rims are rare, indeed the pale colour of the sylvite makes it difficult to distinguish B-type from a pale G-type or some types of halite. The amount of sylvite in B-type sylvinite varies from 19 to 83%, and averages 51% (Fig. A2a). Grains are anhedral, interlocking, and sizes range from 1 to 10mm, and exceptionally from 1 to 20. In some areas, the smaller sylvite grains may be elongated and impart a foliation.

The halite is colourless or milky, and only rarely has orange tints. Cloudiness is more common in small grains, but some of the large ones may have cloudy patches. The grain sizes are similar to the sylvite, but somewhat less variable. The grains are subhedral and interlocking. The amount of insolubles is characteristically low, commonly less than 1%, as high as only 3%, and averages 0.7% (Fig. A2b). Commonly forming small grey-green interstitial masses and films, the insolubles are more abundant where the rock is strongly coloured.

The rock characterized by having large (5 to 10mm) grains of milky sylvite with distinct, dark red rims has been labelled D-type sylvinite. The matrix is limited to small interstitial areas, which gives the rock a coarse-grained granoblastic appearance. Plate 2c shows the type sample of D-type sylvinite, and Plate 3a shows variations to A and G-types. The presence of the dark red colouration keeps the translucence low.

Most of the sylvite grains are milky, but some are colourless. The dark brick-red rims are restricted to the

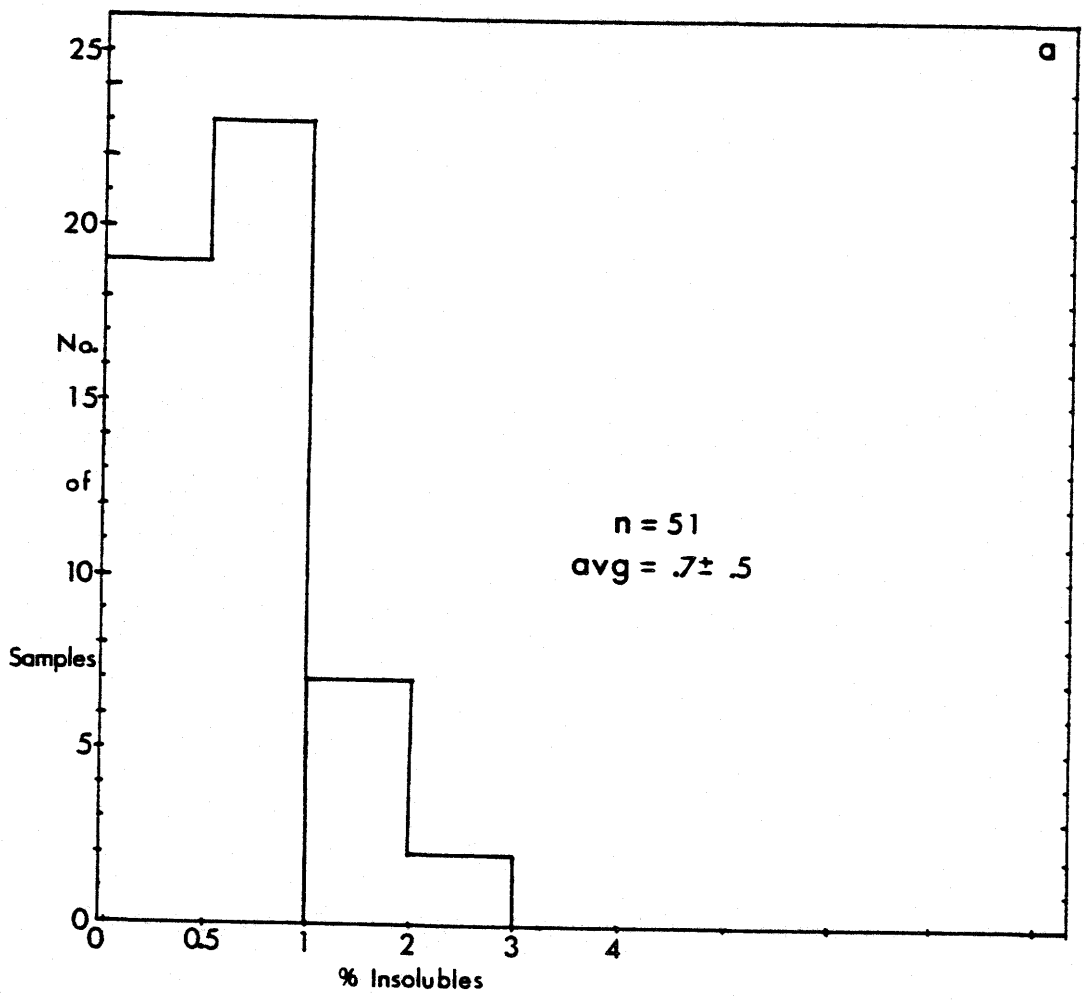

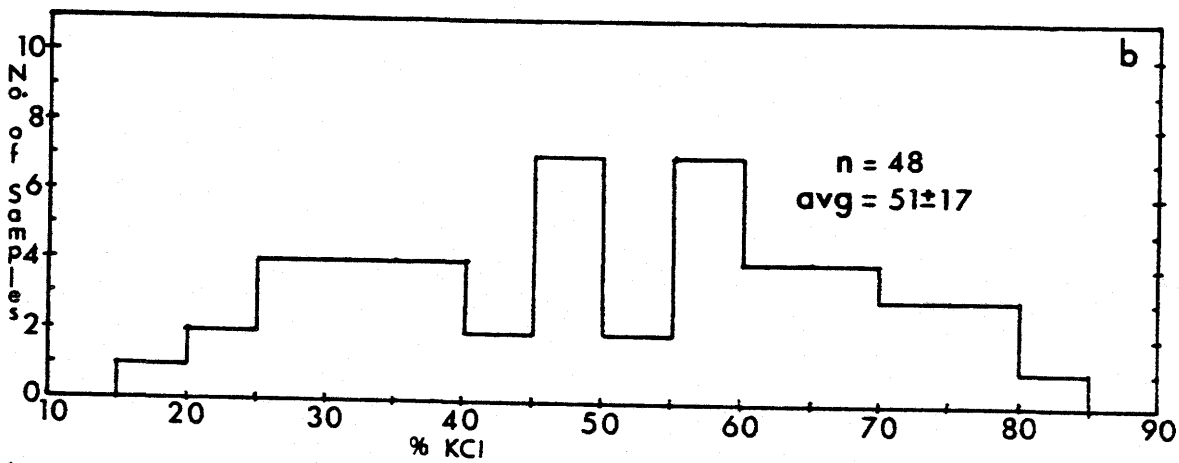

Fig. A2 Histograms of a) % insolubles, and b) % KCl for B-type potash. The average (avg) is given ±1 standard deviation.

outer 1.5mm borders of the grains. Small grains may be coloured throughout, but the colour is mainly patchy. Large grains are subhedral and anhedral, and most are equant.

Most halite grains are clear, and the rest are milky to various degrees. The size distribution is similar to the sylvite, and there is a tendency to form clusters of a few grains, some of which may enclose some red sylvite. Greenish-grey insolubles are the most common, but in some halite clusters they may be brown. The insolubles occur as interstitial inclusions and clots: generally associated with halite. There may also be small, 1 to 5mm thick, discontinuous seamlets of insolubles. The D-type rock is most commonly found just below clay seams. A high average amount of insolubles, about 8%, is probably due to the close association of D-type potash with clay seams, and reflects conditions of increasing deposition or formation of insolubles.

The G-type sylvinite has a patchy appearance. It is characterized by clusters of pale orange to orangey-red sylvite grains interspersed in colourless and white halite grains. Plate 3b shows the type sample and variations of G-type sylvinite. If the sylvite (KCl) content is less than 5% the rock is usually considered to be halite. The sylvite grain sizes are generally less than 6 to 8mm, whereas the halite sizes are up to 20mm. Because of the clustering, sylvite grains appear to be larger than they really are. This is typical of G-type rock.

The sylvite has various shades of orange, which may be uniform, patchy, or confined to the rims of grains. The grains are anhedral, and interlocking. The KCl amounts range from 5 to 45%, for an average of 17% (Fig. A3a). Small orange grains in the halite may be sylvite remnants. Halite films occur between many sylvite grains. In rocks with pale orange sylvite it is commonly difficult to tell apart G and B-types, and this gives rise to G(B)-type.

The colour of the halite is somewhat variable. Colourless grains are the most common, but a few areas are dominated by milky grains. The grain size varies between locations but the range 5 to 15mm is prevalent. Most grains are anhedral although a few subhedral grains occur. The insolubles are commonly greenish-grey and vary in amount from <1 to 15%, for an average of 3% (Fig. A3b). They are interstitial and most commonly associated with halite.

Detailed descriptions of halite rock types.

Red halite resembles G-, D-, or A-type potash rocks in the mine. It is a product of leaching of sylvite

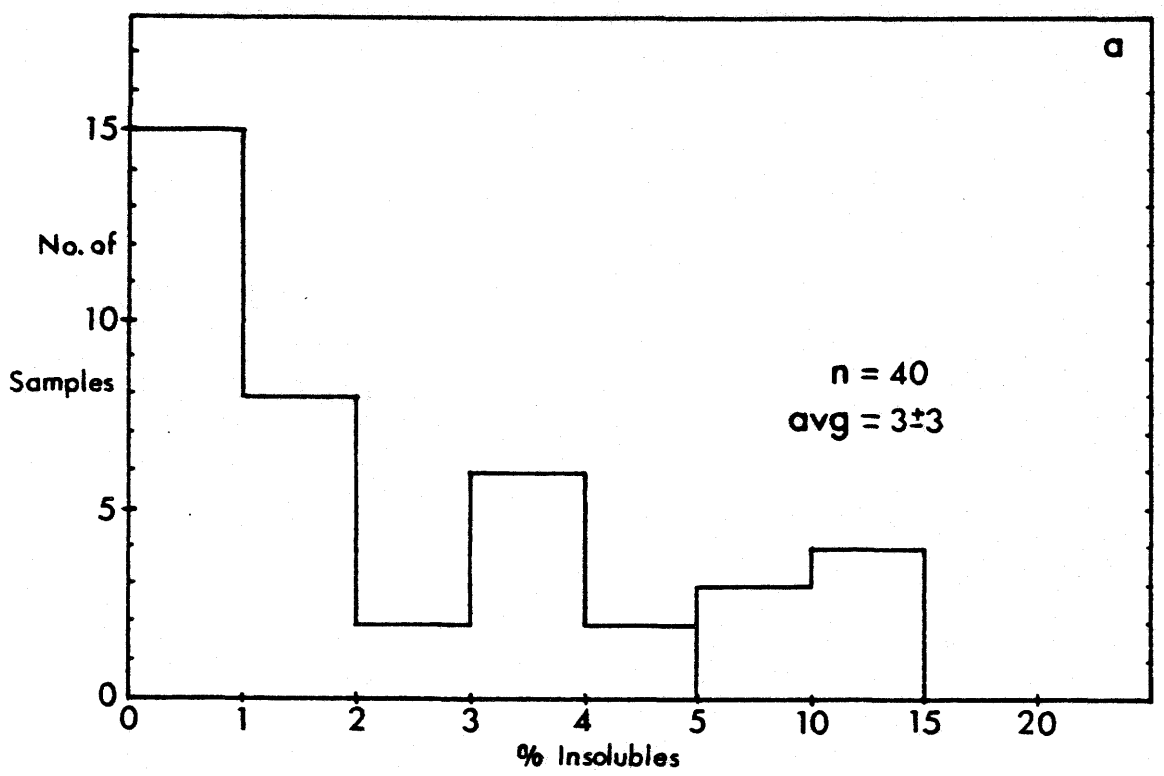

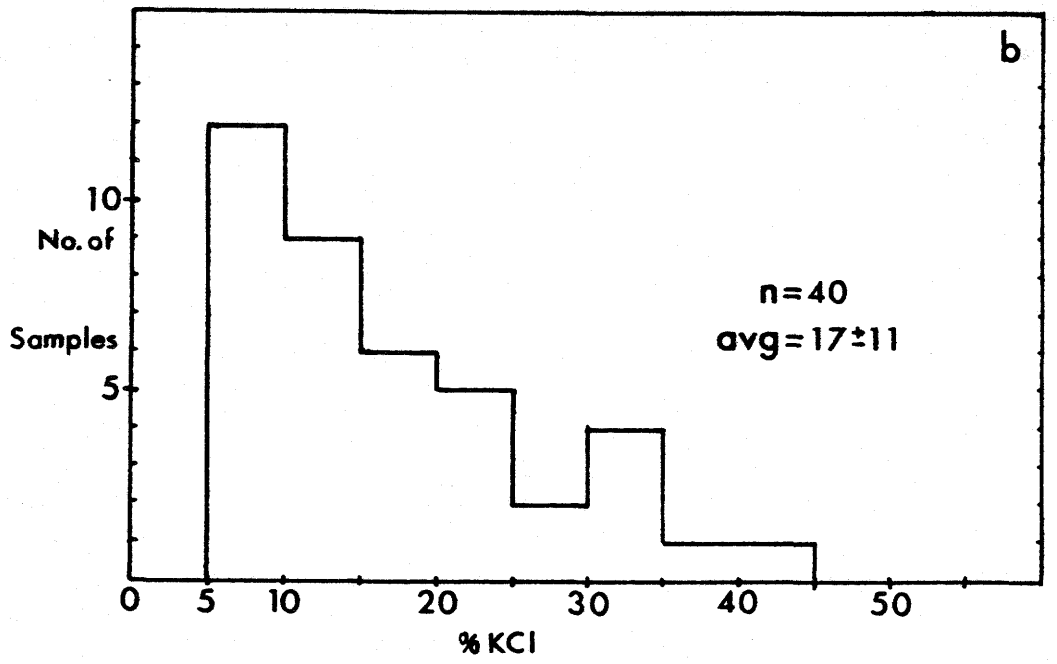

Fig. A3 Histograms of a) % insolubles, and b) % KCl for G-type potash. The average (avg) is given ±1 standard deviation.

from sylvinite and is present in the northern anomaly at Cory Division (Fig. 5.5), and in the anomalies of other mines. The red, which may be anything from maroon to orangey-brown, most commonly coats the smaller 'matrix' grains (<1-6mm) of halite in a very thin film of red colour (Plate 4a,b). Some tiny fibers and plates may be extending inwards, perpendicular to this coat. Some of the larger halite grains (<15mm) may have minor red films around them. Fractures may also be lined with a thin red coat. The red is most likely very fine hematite. The red-coated grains may be in clumps and interstitial between large relatively clear halite grains. The insolubles, mostly greenish-grey, are commonly interstitial. Overall the red coloration is denser, occupies less space, is more broken up, and perhaps larger grained than when it is in the sylvite.

Orange halite that has the colour evenly distributed and that has virtually no sylvite is common in salt anomalies. When it is low in insoluble content it resembles B-type potash. The type samples of orange halite, on each from anomalous and bedded halite, are shown, along with the other types of halite, in Plate 4a. It is commonly found in the halite above the halite-sylvinite contact of salt anomalies (Plate 12b). As in red halite the hematite insolubles of orange halite are most likely residual products after dissolution of sylvite. On first appearance the orange seems to be evenly distributed. A closer look reveals that very small amounts of red to pale orange insolubles (hematite) are scattered along grain boundaries, especially the boundaries of the smaller grains.

Orange halite of a normal salt sequence commonly has up to 5% sylvite (Plate 4a). It is found in the middle of, between seams 406 and 407, and below, the Patience Lake Member (Fig. 4.1). The orange is due to small grains of sylvite and to minor scattered iron oxides; it has a more patchy appearance than the orange halite of salt anomalies.

Brown halite (Plate 4a) is common in the normal bedded sequence such as that between seams 413-414, 408-410, 406-407, and below the Patience Lake Member (Fig. 4.1). It is also common in salt anomalies. The colour is caused by fairly abundant disseminated brown insolubles, which are mostly dolomite and clays. Orange to red hematite insolubles that may be present, also add to the overall brown colour. Sylvite, which has only been found in brown halite of a normal salt sequence, is small (<1-5cm), red, and anhedral.

Grey halite is similar to brown halite except the colour is due to greenish-grey, rather than brown, insolubles (Plate 4a). It is common in both normal and anomalous salt but only the normal salt tends to have

sylvite. White halite could be considered a low-insoluble end-member of brown or grey halite (Plate 4a). It is found in normal and anomalous salt. Where it is in the normal salt, eg. between seams 406 and 407 (Fig. 4.1), sylvite is commonly present up to a few per cent.